INVESTIGATION OF THE MAINTENANCE OF ACTIVATED $CD8^+$ T CELL RESPONSES INDUCED BY PERSISTENT ADENOVIRUS VECTORS

Juliana Carpenter Small

A DISSERTATION

in

Cell and Molecular Biology

Presented to the Faculties of the University of Pennsylvania

in

Partial Fulfillment of the Requirements for the

Degree of Doctor of Philosophy

2014

Supervisor of Dissertation

_____

Dr. Hildegund C.J. Ertl, M.D.

Caspar Wistar Professor in Vaccine Research

Graduate Group Chairperson

_____

Dr. Daniel S. Kessler, Ph.D.

Associate Professor, Cell and Molecular Biology

Dissertation Committee

Dr. Michael R. Betts Ph.D., Associate Professor of Microbiology
Dr. Jean D. Boyer Ph.D., Research Associate Professor of Pathology and Laboratory Medicine
Dr. Phillip Scott Ph.D., Professor of Microbiology and Immunology
Dr. Guido Silvestri M.D., Professor of Pathology and Laboratory Medicine, Emory University

DEDICATION

Dedicated in loving memory to:

My father, Mr. Edward Anthony Small

You have always inspired me, and will continue to do so for the remainder of my life.

ACKNOWLEDGEMENTS

This has been a very long journey and I have many people to thank for seeing me through. First and foremost, I would like to thank my advisor, Dr. Hildegund Ertl. Your lab was the first I rotated through when I started at Penn in 2007. I did not know what a T cell was back then but you helped me to learn that and countless other things over the years. There were plenty of times where I thought I would not make it through but every time you helped me find the motivation to keep plugging away. I cannot thank you enough.

I would also like to thank the Ertl lab, both current members and those who have since moved on. We have put countless hours into helping and supporting each other and it feels like you are as much a part of this thesis as I am. I know for a fact that without the people I have met through this lab I could not have survived this process. I can safely say that you guys are the best. To the grad students and post-docs: I wish you all the very best of luck in all your future endeavors. I'm excited to see what becomes of you!

A big thank you to my committee members, Dr. Michael Betts, Dr. Jean Boyer, Dr. Phillip Scott, and Dr. Guido Silvestri. The time and insight you have given me on this project is invaluable.

I have been more than fortunate to have made many friends throughout my life who have helped me become the person I am today and have helped me negotiate the overwhelming process of earning a Ph.D. Alexis, you have watched me nerd out for as long I can remember. And when dinosaurs are involved, you've been a nerd right by my side. Though distance has separated physically separated us, I'll always love you. Liz, I never knew a deep and amazing friendship could begin over a mutual love of a certain cereal. Having a lab best friend was easily one factor that kept me going through the struggles of this project. I'm so happy you became one of my best friends outside of work because there is so much that wouldn't be the same without you. To the friends I've made in grad school, having a solid group of people around me who happened to be jumping through the same flaming hula-hoops at the same time as I was made this process much more bearable. Even better, no one got burned! You're all so brilliant and

talented and I'm so proud to call each of you my friend. I love you guys and can't wait to see what you all get up to.

My wonderful boyfriend, Roody, deserves a major award for being there for me during this whole process. You are my rock and I would have imploded had you not been there. Thank you for listening to my endless rants and whining about everything related to Science. Even though it's all just lasers and witchcraft to you, you still did your best to give me advice and support. I love you more than I can say.

Most importantly, I'd like to thank my family – my mom, Jeanie, my dad, Edward, and my sister, Elizabeth. You most of all understand the depth of my love of science. You not only tolerated my endless curiosity but also you always encouraged it, even though it could get intensely boring at the dinner table when dad and I got really into a topic. There have been several times on this path when I threatened to quit but you reminded me that the most difficult things in life are often the most rewarding, and then you reminded me that I have an endless talent for worrying and that it would pass. Because of you I have stayed this course throughout my life and now have finished the hardest endeavor I have ever pursed. I love you all and carry you with me in my heart and soul every day.

ABSTRACT

INVESTIGATION OF THE MAINTENANCE OF CD8$^+$ T CELL RESPONSES INDUCED BY PERSISTENT ADENOVIRUS VECTORS

Juliana Small

Dr. Hildegund C.J. Ertl

Vaccines against some of the most pervasive pathogens, including HIV, TB, and malaria, are desperately needed. Available evidence suggests that both central memory and effector CD8$^+$ T cells play a role in mediating protective immunity against many pathogens. Recombinant adenoviruses currently under development as vaccine carriers induce potent and sustained transgene product-specific CD8$^+$ T cell responses. The transgene product-specific CD8$^+$ T cell response remains activated and is delayed in transitioning to central memory. Here we investigate how this response is maintained.

Adenoviral vectors persist and remain transcriptionally active *in vivo.* We investigated the role that continuous transgene expression plays in maintaining the effector memory-biased transgene product-specific CD8$^+$ T cell response. Dual expression vectors based on AdC7 expressing transgenes that could be regulated temporally were generated. Vectors were unexpectedly unstable *in vivo*. Alternatively we inhibited the mTOR pathway, which is downstream of the T cell receptor and has recently been implicated in memory development, using a low dose of rapamycin. Rapamycin failed to enhance the quality of the transgene-product specific CD8$^+$ T cells.

Persisting transgene product could maintain the transgene product-specific CD8$^+$ T cell response by continual recruitment of naïve CD8$^+$ T cells, similar to some other persistent viruses. However, in an adoptive transfer model, we demonstrate that the response is primarily maintained by antigen-experienced cells that do not lose function over time.

Pre-existing anti-adenovirus immunity is common, particularly for the human adenoviruses currently in development as vaccine carriers. Here we demonstrate that pre-existing anti-adenovirus neutralizing antibodies accelerate and enhance transgene product-

specific $CD8^+$ T cell differentiation into central memory. These cells were highly functional and responded robustly to booster immunization. Importantly, this may be due in part to a reduction the vector's reservoir in T cells.

These data suggest that further study of transgene product expression and its functional impact on immune responses is necessary. Further understanding this impact will allow manipulation of immune responses induced by the adenovirus vaccine platform such that they can be tailored to specific pathogens.

TABLE OF CONTENTS

LIST OF FIGURES

CHAPTER 1

INTRODUCTION

ADENOVIRUS PHYLOGENY

In 1953, culture of human adenoid tissues led to the isolation and identification of a distinct virus that was subsequently named after the tissue from which it was isolated: adenovirus (Ad) [1,2]. After more than half a century since they were first identified, adenoviruses have been divided into four genera containing species isolated from many classes of the animal kingdom, including fish, amphibians, reptiles, birds, and other mammals. Human adenoviruses belong to the genus *Mastadenovirus,* which contains all other mammalian adenoviruses, and are further grouped into seven subgroups: A-G. Individual human adenoviruses are identified and assigned a species typically on the basis of neutralization by homologous sera. This has led to the identification of 57 distinct human serotypes.

Historically, hemagglutination properties and neutralization criteria were used to classify the various human adenoviruses. However, advances in genomics and bioinformatics have given us great insight into adenovirus phylogeny. The evolutionary relationships previously designated on the basis of immunological criteria have been confirmed owing to the availability of sequenced Ad genome reference strains. These data have also enabled the investigation of the source of adenovirus genome diversity. Adenoviruses exhibit potential for recombination in experimental co-infection models [3,4]. Recently, whole genome analysis of the completed Ad genome sequences has confirmed that naturally occurring homologous recombination, particularly in the capsid proteins' hypervariable regions [5], is a source of the wide diversity of adenoviruses [6-8]. Additionally, such advances have allowed us to investigate the possibility of interspecies transmission as an additional source of adenoviral genetic diversity. High-resolution X-ray crystal structures and amino acid alignment of hexon suggested that a member of subgroup E, HAdV-4, is closely related to chimpanzee adenovirus 68 [9]. The close phylogenetic relationship of human and simian adenoviruses has lead to the simian adenoviruses' classification within the human subgroups B, C, and E [6,10,11].

ADENOVIRUS STRUCTURE AND GENOME

Adenoviruses have a ~30-36 kilobase (kb) double-stranded DNA (dsDNA) genome surrounded by a non-enveloped icosahedral protein capsid [12]. Each of the twenty faces of the adenovirus capsid contains twelve hexon trimers; thereby making hexon the most abundant capsid structural protein. Hexon is highly conserved between serotypes [9]. However, the outer surface, which is subject to more intense selective pressures, is comprised of amino acid loops with a high degree of sequence diversity, termed hypervariable loops [9]. Most serotype specific neutralizing antibodies are directed against these loops within hexon [13]. Two other major proteins comprise the capsid: penton and fiber. At each vertex where three hexon facets meet, fiber trimers form a spike that protrudes from the penton complex. Fiber has three domains: the highly conserved N-terminus that binds to the penton base, a flexible shaft whose length varies between serotypes and influences virus internalization [14,15], and a globular head responsible for binding to cellular receptors [16,17]. Five minor capsid proteins function to stabilize the capsid.

The adenoviral genome is organized based on the temporal expression of viral transcription units. There are four early transcription units (E1, E2, E3, and E4) each of which have multiple open reading frames or are alternatively spliced into several mRNAs throughout the course of infection [12]. The four early transcription units encode non-structural proteins. E1A proteins are the first to be transcribed as soon as the viral DNA enters the nucleus. These proteins have the critical job of serving as transcription factors to stimulate transcription of the other viral transcription units [18-20] and promoting cell cycle progression such that the cellular replication machinery can be hijacked to replicate the virus [21-23]. E1B proteins largely function to prevent apoptosis of infected cells. The E2 transcription unit encodes proteins necessary for viral DNA replication, including the viral DNA polymerase. Proteins encoded in the E3 transcription unit are responsible for subversion of the host immune response and promoting longevity of the infected cell through prevention of apoptosis. E4 proteins have a wide variety of regulatory functions, including modulation of DNA repair and cell signaling, and promoting synthesis of the late viral proteins. There are five late transcription units (L1-L5) that encode the virus' structural

proteins.

ENTRY AND LIFECYCLE

Early studies of adenovirus revealed that the virus is capable of attaching to HeLa cells [16,24], an immortalized epithelial cell line derived from the cervix. Armed with the knowledge that Coxsackie B virus competes with adenovirus for binding to these cells [25], Bergelson et al. isolated the common receptor used by both viruses for attachment to target cells [26]. Coxsackie and adenovirus receptor (CAR) is a 365 amino acid transmembrane protein [26,27] that functions in cell adhesion [27]. It has since been confirmed that CAR is the receptor for virtually all adenoviruses, with the notable exception of subgroup B viruses [28].

Additionally, CAR is also thought to facilitate dissemination of adenovirus *in vivo*. The studies that identified CAR as the receptor were performed *in vitro* on non-polarized cells. However, *in vivo*, CAR expression is limited to the basolateral side of polarized epithelial cells [27,29] below the tight junctions binding them to one another, ultimately restricting the virion's access. Late in the viral life cycle fiber is produced in excess and has been demonstrated to open tight junctions by disrupting CAR-CAR interactions [30], thus promoting the spread of infection.

The studies demonstrating that fiber mediated attachment to the then unidentified receptor did so using the common subgroup C viruses, HAdV-2 and HAdV-5, on cell lines that were permissive to adenovirus infection [16]. Attempts to determine if subgroup B viruses interacted similarly with target cells permissive to subgroup C viruses revealed that subgroup B viruses did not share a common receptor with subgroup C viruses [28,31]. It has since been revealed that CD46, a ubiquitously expressed regulator of complement, serves as a receptor for subgroup B viruses [32]. Notably, HAdV-3, HAdV-7, and HAdV-14 do not use CD46 [32,33] as their primary receptor but instead use desmoglein 2, a calcium-binding transmembrane glycoprotein involved in cell adhesion of epithelial cells.

As adenoviruses can bind independently of CAR and CD46 to a wide variety of cells, a number of alternative receptors have been proposed. CD80 and CD86 have been proposed as

alternate receptors for some subgroup B viruses [34]. Subgroup C viruses have been proposed to utilize a number of alternative receptors, including glycosaminoglycans in the extracellular matrix [35] and major histocompatibility complex (MHC) class I α2 subunit [36] but this was not confirmed [37]. Finally, subgroup D viruses are proposed to bind sialic acid at the very tip of the fiber knob [38]. The extent to which these are used as receptors *in vivo* has yet to be confirmed.

High affinity binding of fiber with the receptor allows the virion to be held close enough to the cell surface to facilitate entry into the cell. However, entry is not mediated solely through attachment to CAR but requires binding to the integrins αvβ3 or αvβ5 [39,40]. Adenoviruses bind to these integrins using a conserved Arg-Gly-Asp (RGD) motif located on the penton base [40,41]. This interaction triggers internalization of the virion into clathrin-coated pits [42,43]. Once internalized, adenoviruses rapidly escape the endosome in a pH-dependent manner. As the pH drops during endosomal trafficking inward, the capsid undergoes a conformational change that triggers lysis of the endosome, thereby allowing the virus to escape [44,45]. The virion then traffics to the nucleus via microtubules by binding the molecular motor, dynein [46]. The capsid forms a stable interaction with the nuclear pore and the genome is then transported into the nucleus [47], where it can begin transcription of the gene products described earlier.

CLINICAL FEATURES

Adenoviruses are a significant cause of global morbidity in humans and typically cause mild infections of the respiratory and gastrointestinal tracts during the first few years of life [48]. Indeed most children will have evidence of prior exposure by the time they are five years old [48,49]. Although infection is often asymptomatic, adenoviruses are responsible for approximately 5% of symptomatic upper respiratory tract and 10-15% of lower respiratory infections in children [50] and about 17% of gastroenteritis disease in infants [51]. While not all human adenoviruses are associated with disease, certain species are responsible for the vast majority of adenovirus morbidity. Subgroup C viruses are most associated with respiratory tract infections; while viruses belonging to subgroups B and D more commonly cause enteral infections.

Healthy adults are normally not at risk of infection with adenovirus. However, certain populations are at risk for serious adenoviral infection. Military recruits are disproportionately infected with HAdV-4 and HAdV-7, which are responsible for between 60-80% of acute respiratory illness in this population [52]. Ad infection is an even greater issue for those that are immunosuppressed either for transplants or due to HIV. Indeed, disseminated infection occurs in 40% of hematopoietic stem cell transplant patients [53] and is common among HIV patients [54-56]. In these cases, disease is most often severe and life threatening.

ADENOVIRUS AS A PERSISTENT INFECTION

Early clinical evidence suggests that adenovirus establishes a persistent infection. Longitudinal analysis of adenoviral infection in families demonstrated that even after resolution of primary infection when adenovirus could no longer be detected in the upper respiratory tract, virus could be intermittently shed in stool [48,50]. As adenoviruses often cause subclinical infections [49], it was unclear that this shedding represented a new infection or reactivation of a persistent infection. Using serologic evidence, these longitudinal analyses demonstrated that shedding could be due to either scenario: in some patients reinfection was clearly the cause, but in others shedding was due to reactivation [50]. What distinguished the two scenarios though was the duration of shedding. Short-term shedding was observed in individuals who were re-infected, whereas shedding was detected for months to years in individuals who were shedding persistent virus. These results were later confirmed using restriction analysis of viral isolates from infants persistently shedding adenovirus for over a year. The analysis revealed that viruses isolated throughout the study period were always identical to each other [57].

Experimental evidence suggested that this persistent virus was establishing a latent infection as opposed to a chronic infection. The first evidence of this came with the initial identification of adenovirus. When tonsils and adenoids isolated in the absence of adenovirus infection were cultured long-term small amounts of infectious adenovirus could be isolated [2,58]. However, culture did not always result in production of infectious virus, and yet adenoviral DNA

could be isolated from the tissue [59]. Together this suggested that while the virus was there, it was not replicating. In support of this, the addition of phytohaemagglutinin (PHA), a mitogen commonly used to stimulate lymphocytes [60], to cultures that failed to produce replication competent virus resulted in the successful production of infectious virus [61]. These data suggested that adenovirus establishes a persistent but latent infection in these tissues. Since these early studies, adenoviruses have been isolated in the absence of productive infection from an array of tissues, including the gastrointestinal tract, urinary tract, circulating peripheral blood mononuclear cells, the central nervous system, and the conjunctiva of the eye.

Decades of study have been devoted to the determination of the cell type that harbors persistently infecting adenovirus. Initial attempts suggested that fibroblasts within the tonsils and adenoids were responsible [62,63]. In a study to model persistent adenoviral infection of the tonsils and adenoids using suspensions of such tissues, Strohl and Schlesinger estimated the frequency of infected cells in these tissues to be 1 in 10^7 cells. This frequency was then correlated to the frequency of fibroblasts in uninfected tissue, which led to the conclusion that these cells were the primary source of persistent virus [63]. However, evidence began to accumulate that implicated lymphocytes instead. First, it was demonstrated using fluorescent antibodies that lymphocytes isolated from oral ulcers carried adenoviral antigens [64]. Additionally, infectious adenovirus could be cultured from a small fraction of lymphocytes purified from tonsil and adenoid explants, most notably when PHA was added during culture to stimulate lymphocytes [61]. Finally, even when infectious virus could not be isolated, lymphocytes were commonly found to harbor adenoviral DNA [59].

A study to quantify the amount of adenoviral DNA in purified lymphocytes residing in tonsils and adenoids provided definitive evidence that adenovirus persists in lymphocytes [65]. Garnett et al. additionally demonstrated that adenovirus DNA was enriched in a particular subset of lymphocytes, T cells. Subgroup C viruses are exclusively isolated from lymphocytes residing in tonsils and adenoids [49,65], but adenoviruses belonging to additional subgroups have since been isolated from lymphocytes in the gut mucosa [56,66].

It is of particular interest that T cells are the source of latent adenovirus as it remains unclear exactly how adenovirus infects them. T cells poorly express CAR, and αvβ3 and αvβ5 are only upregulated during T cell activation [67]. As such, T cells should be refractory to adenovirus infection. Indeed, experimental infection of T cells with adenovirus is difficult, often requiring ectopic CAR expression [39,68], immortalized lymphocyte lines with high CAR expression [69], or fiber-modified virus [70]. This may suggest that CAR isn't the primary receptor on T cells *in vivo.*

MECHANISMS OF PERSISTENCE OF NATURALLY ACQUIRED ADENOVIRUS

In order for adenovirus to establish a latent infection in lymphocytes the genome would have to be stably maintained in these cells. Common strategies to accomplish this include integration into the host genome and formation of stable DNA structures that are maintained extrachromasomally, such as episomes. Early work suggested that the former strategy is employed. HAdV-12 infection of neonate hamsters leads to integration of at least the E1A and E1B domains, ultimately resulting in tumorigenesis [71]. Studies of human tumors occasionally find evidence of adenoviral DNA within the tumor [72-74]. However, there is a dearth of evidence that suggests that the virus' presence in the tumor is due to integration [73,74], suggesting that adenovirus likely does not integrate into the human genome as a means of persistence. Integration machinery is not encoded in the adenoviral genome; therefore, the frequency of integration would be expected to be low and would have to occur randomly through recombination of the viral genome with the host genome. *In vitro* studies suggest that this occurs with a relatively high frequency, ranging from approximately $5x10^{-3}$ – $1 x10^{-4}$ integrations per cell [75]. In contrast, a recent study examining the integration frequency in the liver following gene transfer instead suggested that the frequency of integration was significantly less, ranging from about 10^{-6} to 10^{-7} integrations per cell. Alternatively, experimental infection of human T cell lines provided evidence that the adenovirus genome instead persists extrachromosomally as an episome. Southern blot analysis revealed that following restriction digest the resulting DNA fragments were the correct size, as predicted from virus alone [69].

In addition to stable maintenance of the genome, the virus would also have to subvert the host's immune responses in order to persist *in vivo*. Indeed, a number of proteins are encoded in the genome that specifically function to this end. Evasion of the host innate response begins as early as expression of the E1 transcription unit. Proteins encoded in this unit prevent interferon-mediated gene expression [76]. The majority of adenoviruses' immune evasion proteins are encoded in the E3 domain, which has long been implicated in adenovirus's persistence. The E3 transcription unit's expression is induced in response to inflammation. Indeed, the E3 promoter contains NF-κB binding sites, which when mutated prevent expression of the E3 unit in response to tumor necrosis factor α (TNF-α) [77]. The E3 transcription unit is alternatively spliced into a number of proteins that prevent CTL-mediated killing of infected cells. One such protein, E3-19K, is responsible for preventing MHC class I transport to the cell surface by sequestering the complex in the endoplasmic reticulum [78,79], thus preventing CTL-mediated lysis. While the function of E3-19K is conserved within adenovirus subgroups [80], there is genetic variation between subgroups [5,81]. This is thought to influence the avidity with which E3-19K from the different species binds HLA alleles [81]. It has been suggested this could indicate that an individual's haplotype may determine if they are more susceptible or resistant to persistent adenoviral infection [82]. Other E3 proteins function to prevent cell-mediated killing by blocking the infected cell's apoptosis cascade. The RID complex, E3-14.7K, and E3-19K all function to this end, interfering with Fas and TRAIL-R1 [83], thus preventing FasL- and TRAIL-mediated apoptosis.

VECTORED ADENOVIRUS

Adenoviruses have long been explored as vectors for gene delivery, at first in order to correct inherited genetic disorders but more recently for vaccination. Such intense exploration has largely been fueled by their tropism for numerous tissues, ability to transduce both dividing and non-dividing cells, and their relatively low pathogenicity. Further, adenoviruses have proven easy to manipulate genetically and to grow in culture [84].

The first generation of Ad vectors was deleted in the E1 domain, a modification that not only allowed for the inclusion of a transgene-expression cassette but also rendered the vector replication defective. As such, the E1 domain must be provided *in trans* in order for the vector to be grown in culture. These first generation vectors could also be deleted in the E3 domain in order to increase their packaging capacity. Gene products from the E3 domain are not necessary for replication and as such do not need to be provided *in trans.*

These first generation vectors could achieve stable transgene expression in immunodeficient mice [85]. However, transgene expression was transient in immune competent animals due to the robust anti-adenovirus immune response. Indeed, these responses were in part directed against viral gene products that continued to be expressed at low levels even though the vector genome was deleted in the E1 domain [86]. This precipitated the development of vectors with fewer encoded viral genes in an effort to reduce the anti-vector response. Later generations of vectors are sometimes deleted in E2, E4, or are completely gutted but for the LTRs and packaging sequence. While these deletions reduce the number of viral antigens and weaken the anti-adenovirus immune response, the vectors are still capable of eliciting transgene product-specific responses [87]. It is this characteristic induction of potent immune responses to encoded transgenes that has prompted the development of adenoviruses as vaccine carriers.

ADENOVIRUS AS A VACCINE CARRIER

Extensive development of vaccines based on adenovirus is under way. This platform is currently being tested for numerous and diverse targets, including viruses, bacteria, parasites, and cancers. Pre-clinically, these vectors induce potent and sustained immune responses directed against the transgene product that can be protective in an appropriate challenge model. Several of these vaccine candidates, including those against malaria [88], Ebola [89], and HCV [90], have performed so well in preclinical models that they are now in various stages of clinical testing.

The most widely studied Ad vector is based on HAdV-5. However, pre-existing immunity to this virus is common globally. Pre-existing immunity poses a serious issue because it limits transduction of target cells [91,92], thereby reducing transgene expression and ultimately the vector's immunogenicity [93]. To overcome this problem, alternative serotypes have also been developed as vectors. These include human serotypes that circulate less frequently in populations, including HAdV-26 and HAdV-35 [94,95], and novel non-human primate serotypes such as those that circulate in chimpanzees [11,96,97]. These alternative species also induce potent B and T cell responses against both the encoded transgene product and the Ad capsid. The $CD8^+$ T cell response is particularly robust.

While the gold standard for vaccine-mediated protection is considered to be induction of neutralizing antibodies directed against a pathogen [98], $CD8^+$ T cells are also important in vaccine-induced immunity. The $CD8^+$ T cell response induced by a vaccine or in response to a natural infection has the potential to be broad as it is not limited to antigens on the surface of a pathogen but can also be directed against both internal epitopes and highly conserved elements.

During a primary immune response, naïve $CD8^+$ T cells are activated in lymphatic tissues following engagement with an antigen presenting cell (APC) displaying the T cell's cognate antigen in the context of MHC class I. The APC provides additional signals in the form of costimulation and cytokines to fully activate these cells. Once activated, $CD8^+$ T cells undergo a period of vast proliferation, during which time effector functions are acquired, including the ability to produce antiviral cytokines such as interferon-γ (IFNγ) and the cytotoxic granules perforin and granzyme needed to eliminate target cells. Fully activated effector $CD8^+$ T cells exit the lymph nodes and traffic to inflamed tissues in the periphery to carry out their effector function and kill infected cells. Once the pathogen is cleared, the overwhelming majority of effector cells, up to 90-95%, will undergo apoptosis. The remaining cells differentiate into memory $CD8^+$ T cells that can endure for life [99]. T cell vaccines specifically seek to take advantage of this natural process in order to generate high numbers of memory cells, which is correlated to protection [100-102].

The $CD8^+$ T cell memory population is highly heterogeneous and can be broadly classified based on the expression of L-selectin (CD62L), a cell adhesion molecule required to

gain entry into the lymph nodes through the high endothelial venules, and CCR7, a chemokine receptor that promotes migration to the T cell areas of the lymph nodes. Central memory T cells (T_{CM}) express both CD62L and CCR7, which allow them to enter and reside in lymphoid tissues [103]. In contrast, effector memory T cells (T_{EM}) express neither CD62L nor CCR7 [103]. This promotes their circulation through the periphery [104]. These two subsets are also functionally distinct. T_{CM} are less differentiated and metabolically quiescent [105]. As such, they are slower to reacquire effector abilities following secondary antigen stimulation [106]. However, they will robustly proliferate, and secrete IL-2, in response to stimulation. On the other hand, T_{EM} are more activated and differentiated, which poises them to rapidly execute effector functions following reencounter with their cognate antigen. Additionally, they are armed with a large amount of cytotoxic molecules, including perforin [106] and can secrete IFN-γ and TNF-α upon restimulation [107]. However, while they will rapidly kill target cells, they have a reduced proliferative capacity compared to T_{CM} cells. The number of effector memory cells declines over time while central memory cells are maintained at very stable frequencies through homeostatic proliferation primarily driven by IL-7 and IL-15 [99,108].

A single cell is capable of giving rise to the diverse subsets of memory $CD8^+$ T cells [109]. There exist two models to explain how memory T cell populations arise. The first model, the linear differentiation model, suggests that an effector T cell will either die during the contraction phase or progressively transition and dedifferentiate from effector to effector memory to central memory over time [110-112]. Alternatively, the second model, the decreasing potential model, suggests that the fate of a $CD8^+$ T cell is determined early in the response by the summation of the signals it receives during priming [113,114]. The fate decisions that give rise to these populations are thus influenced by several factors, including the number of naïve precursors [115,116], strength and duration of the signal from the T cell receptor upon engagement with the peptide-MHC complex [117], the type of costimulation the $CD8^+$ T cell receives [118,119], and the degree of inflammation at priming [114]. As such, the fate of a $CD8^+$ T cell may, potentially be determined as soon as the first cell division after TCR engagement [120].

At the peak of the expansion phase, $CD8^+$ T cells can already be divided into the subset of cells that will eventually die off, i.e. short-lived effector cells (SLEC), and those that will survive contraction and differentiate into memory cells, i.e. memory precursor effector cells (MPEC) [114,121]. The heterogeneity of the memory response is also established at this time; the MPEC population can be further divided into those cells that will become T_{CM} and those that will become T_{EM} [122].

PERSISTING VACCINES

Immunization with a recombinant Ad-based vaccine induces a transgene product-specific $CD8^+$ T cell response that is robust and fails to contract following its peak. Moreover, the population of cells that fails to contract is primarily composed of cells with effector and T_{EM} phenotypes. T_{CM} differentiation is delayed, often taking months to years to accumulate in the lymph nodes because the $CD8^+$ T cells are slow to regain CD62L expression [123].

Reacquisition of CD62L expression on memory cells is slower with subsequent antigen encounters [124,125]. As such, bias toward induction of a memory population primarily composed of more activated, effector memory cells with low CD62L expression is a function of repeated antigen exposure and viral persistence [125-127] and not the transgene itself [126]. Indeed, adenoviral vectors persist *in vivo* following administration [123], despite deletion of the gene products responsible for immune evasion. As expected from the study of wild type virus, the genome is also enriched in T cells, where it can be detected for years following immunization of mice and non-human primates [123]. Strong, constitutively active promoters, e.g. cytomegalovirus (CMV) promoter, are often used to drive expression of the encoded transgene. As such, the encoded transgene is continuously transcribed, presumably intermittently at low levels [123].

A persistent vaccine vector that maintains an effector memory pathogen-specific $CD8^+$ T cell response may be highly advantageous, particularly in the development of vaccines against other persisting pathogens. These pathogens are not only quick to spread but also to put in place immune evasion mechanisms thereby preventing their clearance and allowing them to live in a

balance with the host [128]. Many vaccine strategies that aim to mimic natural infection employ non-persistent vectors that primarily induce central memory. However, because T_{CM} need time in order to respond to re-infection, they may not be able to catch up to the pathogen once its immune evasion strategies are in place. Therefore, a front line of defense made up of activated Tem could be advantageous against both persisting and non-persisting pathogens. Indeed, many infection models have supported this concept. For example, intravenous transfer of $CD8^+$ OT-1-specific T cells, which recognize the immunodominant epitope of ovalbumin, with a more activated, effector memory phenotype conferred more rapid protection against challenge with virulent *Listeria moncytogenes* expressing ovalbumin than their central memory counterpart [125]. Persistent and protective $CD8^+$ T_{EM} responses have also been described for other infections including, *Plasmodium berghei* [129,130], influenza virus [131], and *Salmonella enterica* [132].

Other persistent vectors are also being explored as HIV vaccine platforms and have supplied encouraging results. It is generally believed that a T cell vaccine against HIV will not completely protect from or eliminate HIV infection but would instead lower the viral load and delay progression to AIDS [133]. However, recent studies of vaccines based on CMV have suggested that a strong T cell response biased toward effector memory may be able to control infection before HIV can disseminate and avoid control by the immune system [134,135]. A series of rhesus macaque CMV vectors were engineered to express SIV proteins and used to immunize rhesus macaques. The vaccine induced very robust, persistent effector memory responses that localized to the periphery. More than year after their final immunization, the monkeys were repeatedly challenged intrarectally with a lose dose of SIVmac239, a highly pathogenic, neutralization-resistant clone of a rhesus macaque SIV isolate [136]. Not only did the vaccine delay the onset of progressive infection, it also prevented disseminated infection in 4 of 12 animals [134]. $CD8^+$ T cell depletion of the 4 animals did not result in SIV viremia. The presence of *de novo* $CD8^+$ T cell responses to SIV antigens not encoded in the vaccine suggested that these animals were able to control early replication. A follow up study directly compared the CMV platform to others [135]. Monkeys were immunized with the CMV vector platform alone, the CMV vectors followed by an AdHu5 boost, or a DNA prime followed by AdHu5 boost. Over a year after the final immunization, the monkeys

were challenged as described above. The results were largely consistent with the previous study. 13 of 24 animals that received the CMV vaccines were able to rapidly control SIV infection, while the DNA prime/Ad5 boost platform only lowered the viral load setpoint. Control in both studies was mediated by effector memory $CD8^+$ T cells; whereas, the DNA prime/Ad5 boost induced a more central memory-biased response. This may suggest that there is a window of opportunity in which T_{EM} can mediate control. These results are encouraging for the design of vaccines that induce effector memory T cell responses.

CONCERNS WITH A PERSISTING VACCINE

The persistence of adenoviral vectors may have important consequences on the function of the induced $CD8^+$ T cell memory response. Studies of other persistent infections, including LCMV clone 13, have revealed that chronic antigen exposure can dramatically impair the induced $CD8^+$ T cell response and, in the most severe scenarios, cause deletion of the induced $CD8^+$ T cells [137-139]. This can be measured by hierarchal loss of the ability to secrete IL-2, followed by tumor necrosis factor-α (TNF-α), and IFN-γ. Additionally, the $CD8^+$ T cells lose their cytotoxic capabilities. Some groups have reported that the $CD8^+$ T cell population induced following immunization with recombinant adenovirus primarily consists of effector memory cells that bear a partially exhausted phenotype and fail to produce IL-2 upon restimulation [140]. However, it is important to note that these "partially exhausted" cells were protective when immunized animals were challenged [140]. Indeed, this phenotype is more consistent with highly activated effector cells than exhausted cells that cannot mediate protection upon challenge. The progressive loss of function as cells become exhausted as described above is directly related to the amount of persisting antigen [137]. High amounts of antigen are sufficient to drive responding $CD8^+$ T cells to exhaustion. However, adenoviral vectors persist latently and presumably only produce transgene product intermittently [123]. Therefore, levels of persisting antigen are not high enough to drive the transgene product-specific $CD8^+$ T cell response to exhaustion.

Even though adenoviral vectors are unlikely to drive a $CD8^+$ T cell response to exhaustion, it is worth considering that T_{EM} cells are more terminally differentiated than T_{CM}. They have shorter teleomeres [141] and express less telomerase than T_{CM} [142]. While this is in agreement with their limited proliferative potential, this may also suggest the extent to which they can divide is limited. In support of this, T_{EM} also express higher levels of killer cell lectin-like receptor G1 (KLRG1) [143], a marker of replicative senescence [144]. KLRG1 binds members of the cadherin family, thereby preventing IL-2 production [145] and proliferation following TCR stimulation [146]. KLRG1 accumulates on these cells with successive rounds of antigen stimulation and is considered a reliable marker of antigen experience [124,147]. Additionally, repetitive antigen stimulation drives permanent changes to the cell's transcriptome, including increasing expression of genes associated with senescence [148]. As such, the first line of defense generated in the context of a persisting vaccine could potentially be pushed to a point after which it may no longer mediate protection.

THE ROLE OF CENTRAL MEMORY T CELLS

$CD8^+$ central memory T cells play a role in maintaining the T_{EM} population. Repetitive antigen stimulation skews the memory response in favor of increased numbers of T_{EM} [124]. However, in situations in which antigen does not persist, the T_{EM} population gradually declines over time [132], as residual antigen is cleared from depots located in the draining lymph nodes of peripheral tissues [149]. Once the depot is cleared, the numbers of T_{EM} stabilize [150] and are replenished through homeostatic proliferation of T_{CM} [132,149,151]. It may be beneficial in vaccine design to induce a population of T_{CM} that can maintain a first line of defense.

However, there exists controversy on the role that central memory cells play in controlling infection. Studies in which equal numbers of effector memory or central memory $CD8^+$ T cells are adoptively transferred into mice prior to infection generally support the concept that effector memory cells confer more rapid control. However, in these models the use of mouse lymphocytic choriomeningitis virus clone 13 (LCMV), which rapidly establishes a chronic infection,

demonstrated that central memory cells were better able to control disseminated infection. This was largely attributed to their increased proliferative capacity that resulted in large numbers of effector cells during the anamnestic response that likely compensated for an overwhelmed T_{EM} response at the periphery [107,152]. Other lines of evidence also support a role for T_{CM}. In the context of the HIV vaccine model described earlier, a DNA prime following by an Ad5 boost generates a more central memory T cell population [135,153]. While this response does not protect against infection, it serves to ameliorate the course of disease by reducing the SIV viral load [135,153]. Interestingly, while the CMV-based SIV vaccine described above protected more than 50% of the animals from SIV challenge, those that were unable to control the initial infection also had high viral load setpoints. This was attributed to the lack of expansion in the memory $CD8^+$ T cell response after challenge. These studies highlight the importance of T_{CM} as a second line of defense.

GOALS OF THE STUDY

Available evidence thus suggests that both subsets of memory $CD8^+$ T cells play important roles in control of infection. The contribution of each subset into control of infection will likely depend on several factors, including the pathogen's route of entry, how quickly it can replicate and disseminate, and where the pathogen may localize in the host. In designing vaccine platforms it will be important to assess these factors in order to optimize the vaccine. The studies presented in this thesis were designed to investigate strategies to balance the $CD8^+$ T cell response induced following immunization with adenoviral-based vaccines. More specifically, as vectors based on adenovirus induce robust $CD8^+$ T cell responses that are biased toward effector memory, we explored methods to create a $CD8^+$ T cell memory response with a better balance between central and effector memory cells.

AIM 1

Adenoviral vectors persist and remain transcriptionally active in activated T cells *in vivo.* This correlates with two features of the transgene product-specific $CD8^+$ T cell response induced by immunization with adenoviral vectors. First, the transgene product-specific $CD8^+$ T cell response fails to contract following immunization. Second, there is a marked delay of more than a year in the accumulation of transgene product-specific $CD8^+$ T cells with a central memory phenotype. As levels of persistent antigen are known to influence anti-viral $CD8^+$ T cell responses, we hypothesized that continued production of transgene product from the adenoviral vector genome prevents the contraction of the transgene product-specific $CD8^+$ T cell pool, thereby maintaining them in an activated effector and effector memory state. In chapters 2 and 3 of this dissertation we address this hypothesis in two ways. In the first approach, we aimed to generate vectors with transgenes whose expression could be temporally regulated. We hypothesized that discontinuing transgene expression would allow the transgene product-specific $CD8^+$ T cell response to contract and differentiate into the central memory compartment. In a second approach, we aimed to manipulate the mTOR pathway that is downstream of T cell receptor signaling and recently has been implicated in memory development [154]. We hypothesized that inhibition of mTOR activity following adenoviral immunization would accelerate the formation of a pool of central memory transgene product-specific $CD8^+$ T cells. To this end, we inhibited mTOR activity in a mouse model using a low dose of rapamycin at different phases of the $CD8^+$ T cell response following immunization with an adenoviral vector. Mice were assayed for $CD8^+$ T cell numbers and memory phenotypes in several tissues.

AIM 2

The $CD8^+$ T cell pool that fails to contract following induction with an adenoviral vaccine bears some resemblance to those induced by other persistent viruses. The $CD8^+$ T cell pool is phenotypically heterogeneous, composed primarily of effector and effector memory cells, but is

highly functional and protective. A common strategy for maintaining such activated and functional responses necessary for combating ongoing, low-level viral replication is to continuously prime *de novo* CD8+ T cells. However, adenoviral vectors are replication-defective, although transgene product continues to be expressed at low levels during persistence, which may give responding transgene product-specific $CD8^+$ T cells an opportunity to rest from antigenic stimulation and transition to central memory. Therefore we hypothesized that the transgene product-specific $CD8^+$ T cell pool is maintained by recall of antigen-experienced $CD8^+$ T cells instead of asynchronously primed $CD8^+$ T cells. The hypothesis was explored in chapter 4 by adoptively transferring naïve or antigen-experienced $CD8^+$ T cells into adenovirus-immunized mice and following the transferred cells' responses over time.

CHAPTER 2

OPTIMIZATION OF ADENOVIRAL VECTORS TO INVESTIGATE THE INFLUENCE OF PERSISTENT TRANSGENE EXPRESSION ON $CD8^+$ T CELL RESPONSES INDUCED FOLLOWING IMMUNIZATION

ABSTRACT

Adenoviral vectors persist and remain transcriptionally active *in vivo.* This persistent transgene expression is correlated to the failure of the transgene product-specific $CD8^+$ T cell response to contract and transition to central memory following immunization. In order to directly investigate these correlations, we utilized a well-characterized recombination system that would allow us to temporally regulate expression of the encoded transgene. This required the construction of adenoviral vectors capable of expressing two transgenes at once. In the first part of this chapter, we describe the optimization of a series of replication-defective adenovirus vectors designed to express transgene products from two expression cassettes placed into the deleted E1 and E3 domains. Vectors with fewer shared elements in E1 and E3 expression cassettes optimally expressed transgenes and induced B and T cell responses to encoded transgenes. In the second the part of this chapter, we constructed vectors based on the optimal design from part 1 to generate vectors encoding a transgene that could be temporally regulated. However, these vectors were unexpectedly unstable. Alternative approaches to regulating transgene expression from an adenoviral vector will have to be utilized.

First part adapted from:

Construction and Characterization of E1- and E3-Deleted Adenovirus Vectors Expressing Two Antigens from Two Separate Expression Cassettes. Small JC*, Kurupati RK*, Zhou X*, Bian A, Chi E, Li Y, Xiang Z, and Ertl HCJ. *Human Gene Therapy*. **25**, 328-338 (2013).
*These authors contributed equally

INTRODUCTION

Ad vectors persist in a transcriptionally active state at low levels in mice and non-human primates [123] and naturally acquired adenoviruses persist in human lymphatic tissues, particularly in tonsils and adenoids [65]. Additionally, Ad vectors induce a robust population of activated transgene product-specific $CD8^+$ T cells that fails to contract over time and is delayed in differentiating into the central memory compartment. Studies of other pathogens suggest that persisting antigen is sufficient to maintain this type of response. Therefore, we aimed to investigate the influence of persistent transgene expression on the differentiation of transgene product-specific $CD8^+$ T cell responses following immunization with adenoviral vectors. This necessitated the development of Ad vectors carrying transgenes whose expression could be regulated *in vivo.* The first part of this chapter concerns the optimization of vectors encoding multiple transgenes, the results of which were applied in the second part in the construction of vectors generated to explore the question described above.

Ad vectors are deleted in the E1 to limit their replication *in vivo*. Deletion of the E1 domain allows exogenous DNA sequences up to 4.7 kilobases (kb) to be inserted into the vector genome [155]. Insertion of foreign DNA enables us to direct an immune response to an antigen from a particular pathogen. However, protection against many pathogens may require vaccines that express multiple antigens. Historically, several approaches to achieve this goal have been explored. One approach is to mix vectors expressing different target antigens [156]; however, this approach requires generation of multiple vectors, which is both cumbersome and costly, especially for large-scale, clinical applications. Alternatively, multiple transgenes, either in the form of a single fusion gene or separated by an internal ribosomal entry site (IRES), whose expression is driven by a single promoter, can be inserted into the E1 domain. This approach is not without limitations, as insertion of long coding sequences into the E1 domain results in diminished transgene expression that ultimately reduces induction of transgene product-specific immune responses [157]. A third approach that has been explored is to insert independent expression cassettes with identical promoters into the deleted E1 domain [158], but this often results

in homologous recombination between the promoters and, consequently, the removal of one expression cassette from the Ad genome.

To avoid these complications, a different approach is necessary. Secondary generations of Ad vectors are deleted in multiple domains, including the E3 domain, which encodes genes that are unnecessary for viral replication. Deletion of the E3 domain increases the packaging capacity of Ad vectors to 7.5 kb [159]. This was taken advantage of in the study presented here. A series of vectors based on chimpanzee Ad serotype 7 (AdC7), also called SAdV-24, were generated that carried one expression cassette in the deleted E1 domain and a second different expression cassette in the deleted E3 domain. Each expression cassette carried a different promoter to drive their respective transgene's expression. Additionally, combinations of various regulatory elements, including introns and enhancers, and expression cassette orientation were tested for their impact on transgene expression and subsequent induction of immune responses.

The results indicate that the orientation of the E3 expression cassette dramatically affects vector fitness and transgene expression. Vectors with E3 expression cassettes inserted parallel to E3 transcription (5' to 3', or forward oriented) could commonly not be rescued whereas insertion in the opposite orientation resulted in fitter vectors, although this was influenced by the choice of the promoter in the E3 cassette. Additionally, the presence of shared sequences, such as introns and enhancers, between the E1 and E3 expression cassettes impacted transcription of each transgene and thereby induction of transgene product-specific immune responses.

In the second part of this chapter, the above results were applied to generate AdC7 vectors encoding a transgene whose expression could be temporally controlled. Vectors were designed such that the E1 expression cassette contained a transgene flanked by loxP sites (floxed) and the E3 expression cassette contained CreERT2, a fusion protein of Cre recombinase, which recombines loxP sites, and a mutated version of the ligand-binding domain of the human estrogen receptor (ER). The mutation makes CreERT2 activity inducible as only the synthetic ligand and estrogen antagonist, 4-hydroxytamoxifen (4-OHT), can bind to the ER [160]. Administration of 4-OHT would therefore provide conditional and temporal control over expression of the floxed transgene and thus enable studies into its role in maintaining the

elevated and prolonged transgene product-specific effector/effector memory $CD8^+$ T cell response. Floxed dual expression vectors were constructed and results indicated that transgene expression could be regulated *in vitro.* However, upon further inspection it was discovered that the vectors recombined at the loxP sites during viral expansion.

RESULTS A. OPTIMAL DESIGN OF ADENOVIRAL VECTORS EXPRESSING DUAL TRANSGENES

Vector construction and quality control

In order to optimize vectors expressing transgenes from both the E1 and E3 loci, a series of shuttle vectors was designed to insert expression cassettes encoding transgenes and various regulatory elements into the E1- and E3-deleted AdC7 vector genome. Expression cassettes designed for insertion into the deleted E1 domain used the cytomegalovirus (CMV) promoter to drive expression of the inserted transgene and the bovine growth hormone (BGH) poly(A) tail. The expression cassette was further modified by deletion of the CMV enhancer, intron, or both. Shuttle vectors designed to insert expression cassettes into the deleted E3 domain contained expression cassettes whose transgene's expression was driven either by the Rous Sarcoma Virus (RSV) promoter or by the chicken β-actin (CB) promoter. All expression cassettes encoded the rabbit globin poly(A) tail. E3 expression cassettes were further modified by deletion of the CMV enhancer sequence, the intron, or both. Additionally, E3 shuttle vectors were designed to insert the E3 expression cassette in the same direction as E3 transcription, 5' to 3' (forward), or the opposite orientation, 3' to 5' (reverse). Once constructed, the E1 and E3 shuttle vectors were used to construct pAdC7 molecular clones. Completed pAdC7 clones were linearized and transfected into HEK 293 cells in order to rescue AdC7 virus. Rescued viruses were further expanded on 293 cells. A list of the different vectors generated and their qualities is shown in **Figure 2.1**.

If three attempts failed to rescue virus that could be further expanded, the virus was considered unfit. Most recombinant AdC7 molecular clones bearing an E3 cassette with the RSV

promoter were unfit. When this cassette was forward-oriented, all viruses failed to rescue, regardless of whether or not an E1 expression cassette was included. One viral clone with only a reverse-oriented E3 expression cassette was also unable to be rescued. However, when an E1 expression cassette was included in that construction, the virus was successfully rescued. Use of the CB promoter in the E3 cassette yielded more promising vectors. Two of four molecular clones yielded infectious viral particles when this cassette was in the forward-orientation; all viruses containing this cassette in the reverse-orientation were rescued.

All rescued viruses were quality controlled following expansion by assessing genetic integrity, viral particle yields, and infectivity. Genetic integrity was confirmed by restriction digest of isolated viral DNA from expanded virus; enzymes were chosen to specifically identify the unique expression cassettes. All viruses showed expected banding patterns for their expression cassettes. Viral particle yield was determined following expansion on 10^9 HEK 293 cells. Expansion of traditional AdC7 vectors encoding a single transgene in E1 typically yield between 0.1 to $2x10^{14}$ viral particles (vp) (**Figure 2.2A**). All viruses capable of being rescued, regardless of E3 promoter and orientation, yielded similar numbers of virus particles and were comparable to the traditional vector. However, removal of sequences (intron, enhancer, or both) shared between the E1 and E3 cassettes tended to result in superior yields. Infectivity, or the number of viral particles needed to productively infect a single cell, is determined by the ratio between the number of viral particles isolated and the multiplicity of infection (MOI), which is assessed by titrating vector on HEK 293 cells. Traditional AdC7 vectors typically have an infectivity ratio of <1:500 (**Figure 2.2B)**. All rescued dual expression vectors had infectivity ratios that were comparable to that of the single expression AdC7 vector. The pattern of variation observed between groups followed that observed in the differences in viral particle yields. The infectivity ratio was highly variable within each construct family but this appeared to be dependent on the type of transgene encoded in each expression cassette.

FIGURE 2.1. Diagrams of dual expression vectors' expression cassettes and their qualities

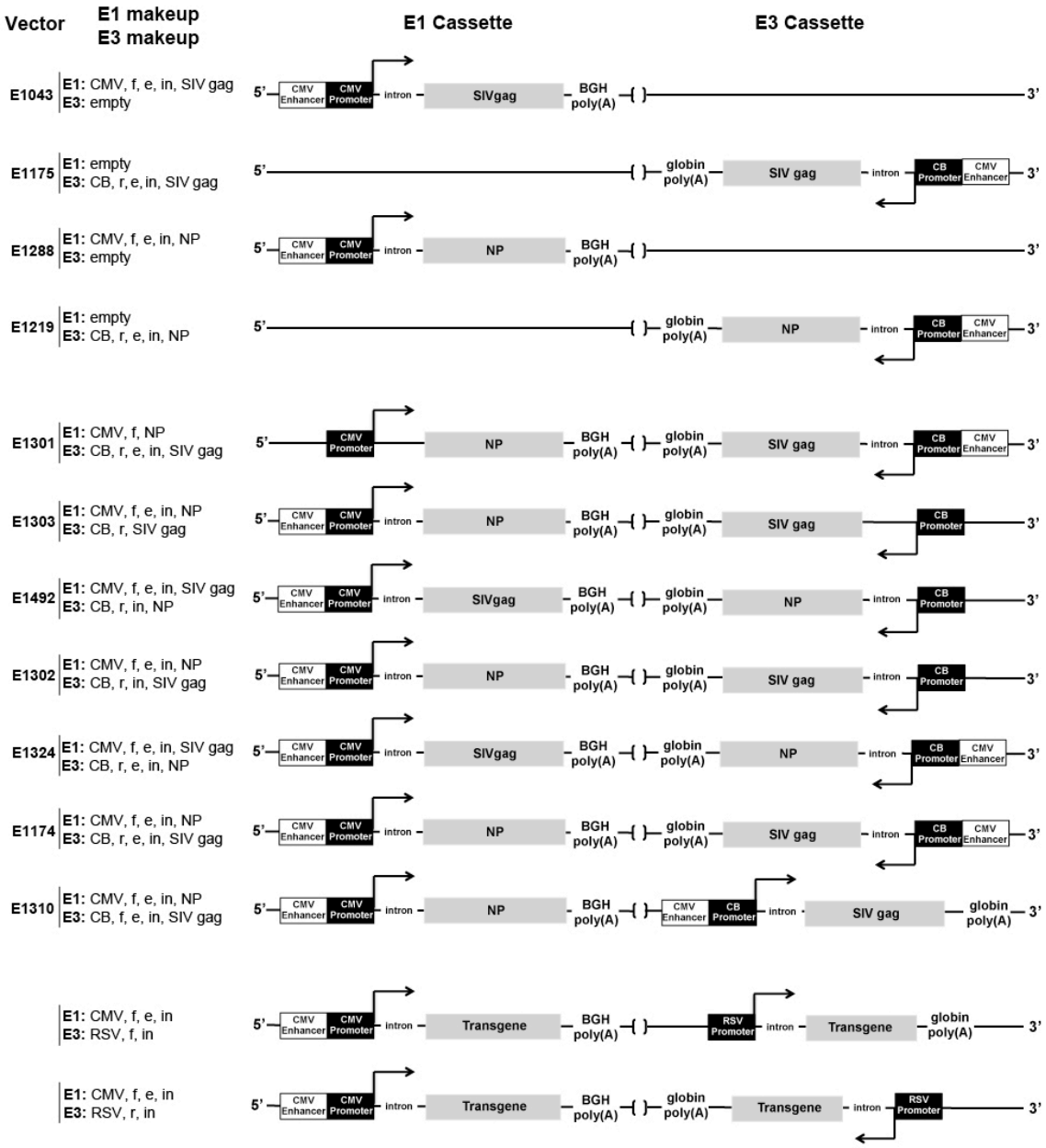

For each vector discussed in Figures 5.2 - 5.7, a schematic of the expression cassettes inserted into the E1 and E3 domains are shown with the vector number and the long form list of E1 and E3 characteristics is included. The first four vectors described are the control vectors, the following six are the experimental vectors presented in all figures, and the final two vectors are the two that carried the RSV promoter and are discussed only in Figure 2. The a key for list of characteristics provided in the E1 makeup/E3 makeup column is included: **Domain into which the cassette was inserted:** promoter (cytomegalovirus (CMV), chicken β-actin (CB), or rous sarcoma virus (RSV)), cassette orientation (forward (f) or reverse (r)), enhancer (e), intron (i), transgene (influenza nucleoprotein (NP) or gag of simian immunodeficiency virus (SIV gag)). If the list does not contain an "e" or "i", then the cassette does not contain them. If there is no expression cassette in one domain that domain is listed as "empty".

FIGURE 2.2. Dual expression vectors' growth characteristics and infectivity

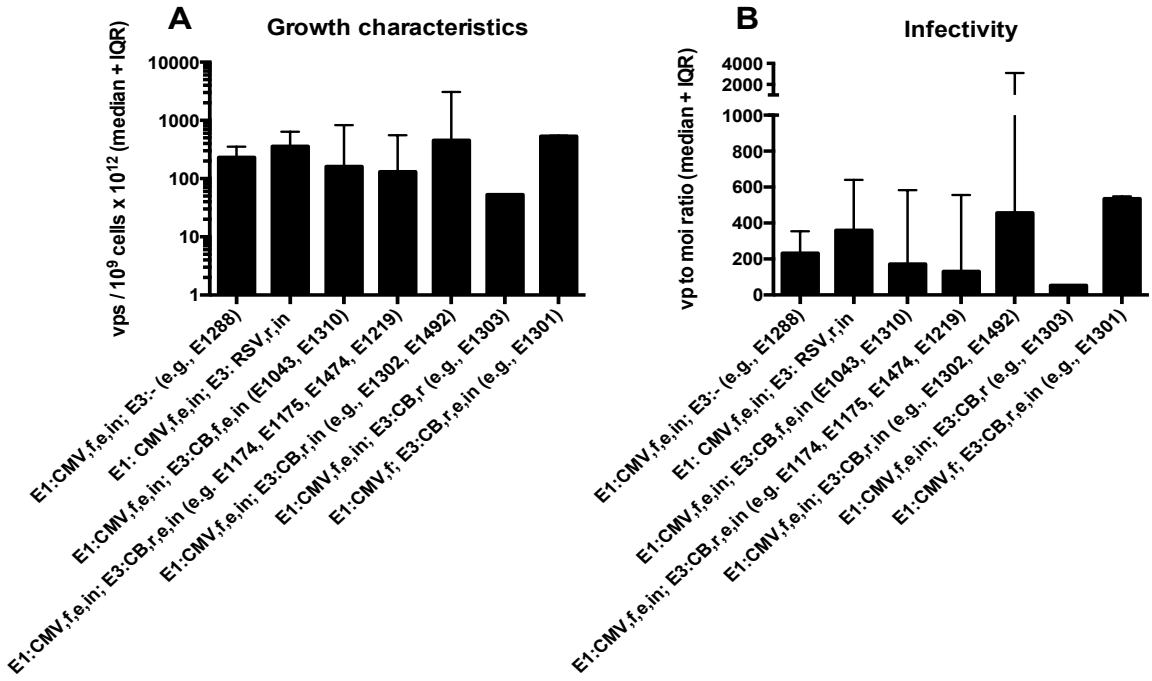

[A] Shows the virus particle yield per 10^9 HEK 293 cells as medians + interquartile range (IQR). Each bar represents the growth characteristics for pooled lots of viruses with the same basic vector design described on the X-axis. Vectors that conform to the appropriate design are listed in parentheses. Their characteristics are described in Figure 5.1.

[B] Graph shows the vp to MOI ratios as a representation of infectivity for the same types of vectors shown in **[A]** as median + IQR.

Transgene product expression

We specifically focused on vectors that carried *gag* of Simian Immunodeficiency Virus (SIV) and nucleoprotein (NP) of influenza A/PR8 as transgenes in either E1 or E3. These vectors drove expression from the E1 domain using the CMV promoter and used the CB promoter in E3. Controls for the remaining experiments included AdC7 vectors that encoded *gag* or NP in either E1 or E3. Transgene expression from each cassette was measured using reverse transcription real-time PCR (qRT-PCR). HEK 293 cells were infected with 1000 vp per cell and total RNA was isolated and reverse transcribed 24 hours later. Real time PCR analysis showed that transcription of each transgene varied between vector types. This variation was only partially explained by differences in vector infectivity (vp to MOI ratio shown in **Figure 2.2**).

As expected, NP was not expressed in cells infected with vectors that did not encode NP (E1175, E1043, Ad-GFP) (**Figure 2.3A**). Single expression control vectors encoded with NP in E1 (E1288) or in E3 (E1219) demonstrate that moving the position of the NP expression cassette from E1 to E3 reduces its transcription. This phenomenon was largely recapitulated in the dual expression vectors. Those vectors that carried NP in the E3 domain (E1492, E1324) expressed NP at levels comparable to E1219. However, the reduced NP expression in cells infected with E1492 was likely due to its high vp to MOI ratio, implying that there were fewer infectious viral particles available to infect the 293 cells. Dual expression vectors with NP encoded in the E1 domain tended to express higher levels of NP. The highest NP expression level was observed when the NP expression cassette was accompanied by the forward-oriented E3 expression cassette (E1310). Reversing the orientation of the E3 expression cassette dampened NP expression (E1174). Further modification of the two expression cassettes gave mixed results. As expected, removal of the regulatory elements from the E1 NP expression cassette (E1301) resulted in decreased in NP expression. Interestingly, removal of regulatory elements from the E3 cassette (E1303, E1302) enhanced NP transcription.

Different patterns of gag expression were observed. While moving NP to E3 expression cassettes resulted in lowered expression, encoding gag in E3 resulted in overall higher gag expression (**Figure 2.3B**). This phenomenon was observed for both the control vectors (E1175,

E1043) and for the dual expression vectors. Orientation of the E3 cassette affected *gag* transcription in the opposite manner it affected expression of NP in the E1 cassette – *gag* expression was lowest when the E3 cassette was in the forward orientation (E1310). Reversal of the E3 expression cassette resulted in higher levels of *gag* transcription. Removal of the regulatory elements from the E1 domain had little effect on *gag* transcription from the E3 domain. We expected that removal of the regulatory elements from the E3 *gag* expression cassette would reduce *gag* expression, similar to what was observed for NP expression (E1301, **Figure 2.3A**). Instead, *gag* expression was the highest in cells infected with the vectors from which the enhancer element was removed (E1303) or both the enhancer and intron were removed from the E3 expression cassette (E1302).

Protein expression was measured by western blot on protein lysates harvested 24 hours after infection with the dual expression vectors. NP protein expression was measured in 293 cells infected with either 1000 or 10,000 vp per cell of the dual expression vectors that carried NP in E1 (E1174, E1303, E1302, E1301) and the two control vectors encoding only NP in E1 or in E3 (E1219, E1228). As shown in **Figure 2.4A,** NP expression was comparable between all vectors at each dose. More vectors were included (E1175, E1310, E1324, E1492) and tested for Gag expression by infecting cells with 10,000 vp per cell (**Figure 2.4B**). Gag expression was more variable than that of NP protein but the results largely mirrored those seen for gag RNA transcripts. As expected, if *gag* was not encoded in the vector, Gag protein was not detected. The lowest amount of Gag was detected in lysates from cells infected with E1310, the vector carrying NP in E1 and gag in the forward-oriented E3 expression cassette. Gag was most highly expressed in cells infected with the vector that encoded NP in the standard E1 expression cassette and encoded gag in E3 in the reverse-orientated expression cassette that lacked the enhancer element (E1302). Both of these results were consistent with those observed for RNA transcription (**Figure 2.3**).

FIGURE 2.3. Levels of NP and *gag* transcript expression

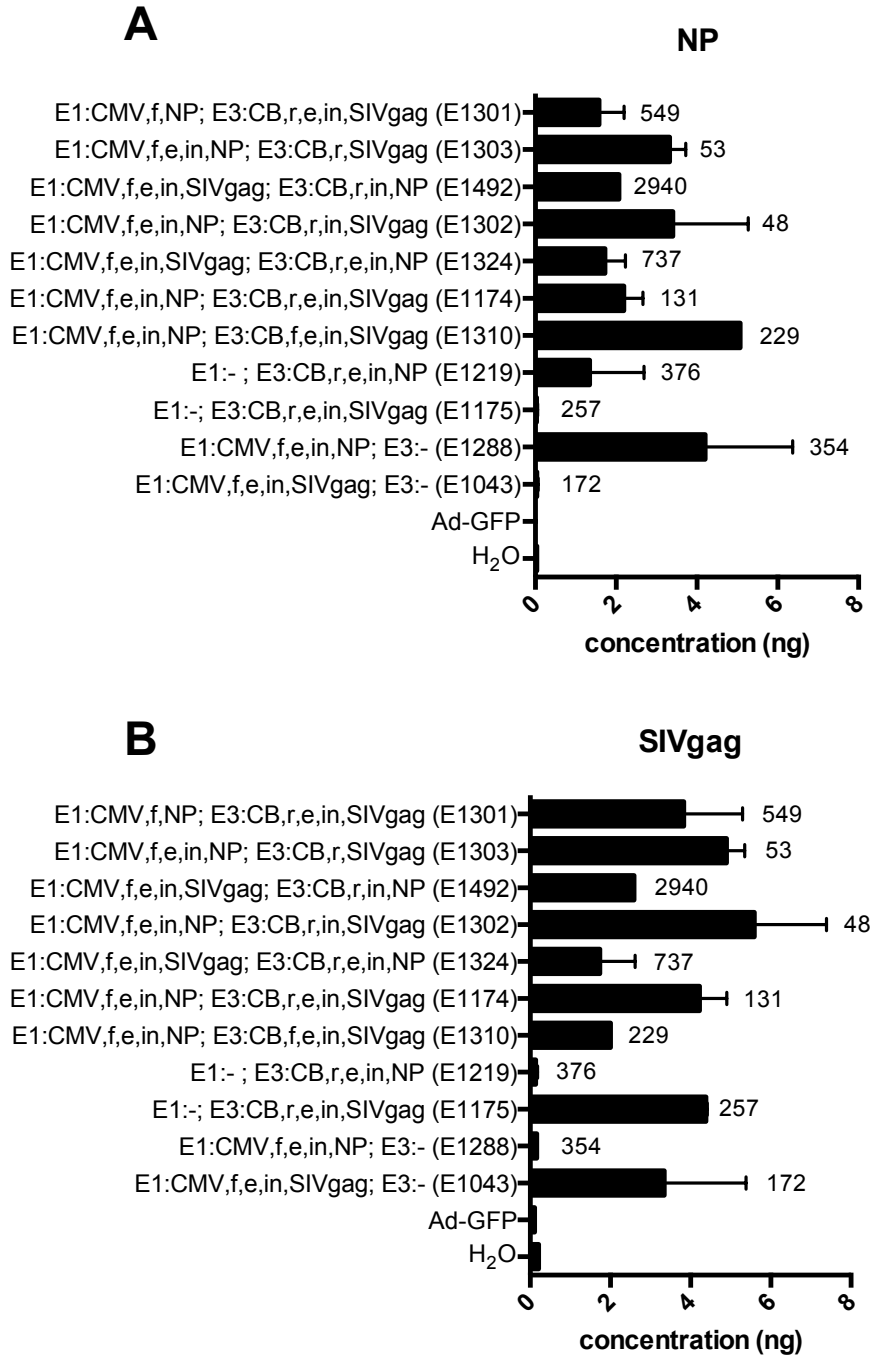

Graphs show quantitative reverse transcriptase PCR results indicating levels of transcript expression achieved within 24 hours by 10^6 HEK 293 cells infected with 10^{10} vp of the indicated vector. Experiments were conducted twice for most vectors and bars show median levels + IQR range. [**A]** shows results for NP transcripts, [**B]** shows results for gag transcripts as median + range. Numbers above the bar show the vp to MOI ratio of the indicated vector. H_2O and an Ad vector expressing green fluorescent protein (GFP) were used as negative controls.

FIGURE 2.4. NP and Gag protein expression

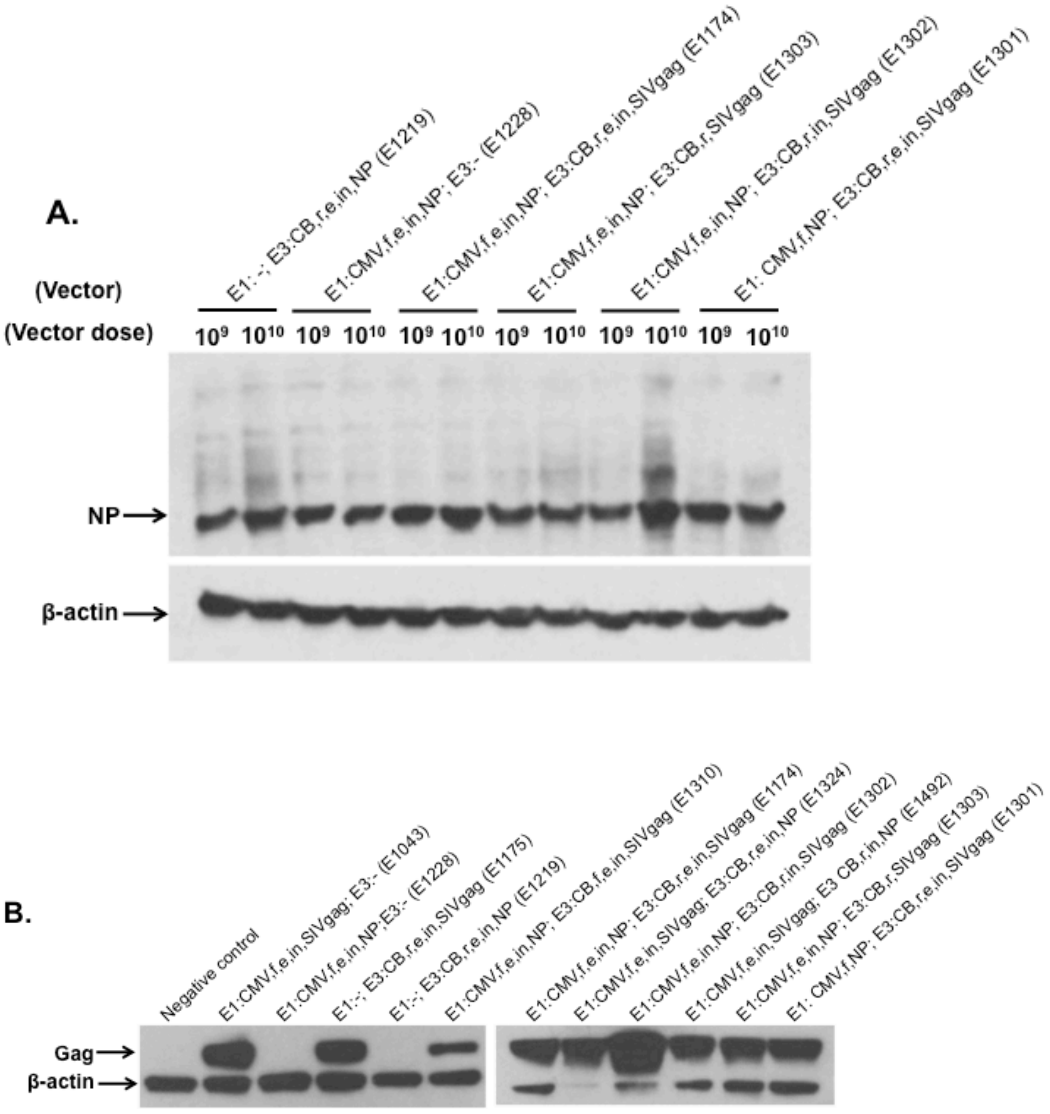

Graphs show Western Blots for NP **[A]** and Gag **[B]**. To determine expression levels of NP, 10^6 HEK 293 cells were infected with 10^9 or 10^{10} vp of indicated vector. Gag expression was tested in 10^6 HEK 293 cells infected with 10^{10} vp of indicated vector. Cell lysates were collected 24 hours after infection for both **[A]** and **[B].** Blots were probed for β-actin as a loading control.

Vector Immunogenicity

As the vectors were demonstrated to express well *in* vitro, their immunogenicity was next measured. Outbred ICR mice were immunized intramuscularly (IM) with 10^{10} vp of the more promising vectors that express NP and Gag. As controls, groups of mice were immunized with vectors expressing NP or Gag from E1 or E3. Mice were bled six weeks after immunization and serum was tested for NP- and Gag-specific antibodies by ELISA. Each dual expression vector induced detectable antibody responses to both the NP and Gag antigens (**Figure 2.5**). E1303, which lacked both the intron and enhancer elements in the E3 expression cassette, induced a NP-specific antibody titer of approximately 200 μg/mL, the highest of all the dual expression vectors (**Figure 2.5A**). The lowest anti-NP antibody titer (less than 100 μg/mL) was induced by E1302, which did not carry an enhancer in the E3 expression cassette, despite a similar expression pattern *in vitro* to that of E1303. Two other dual expression vectors were tested for induction of NP-specific antibody responses: E1301, which lacked the intron and enhancer in the E1 expression cassette, and E1174, which contained both the enhancer and intron in both the E1 and E3 expression cassettes. Both vectors induced NP antibody titers comparable to those induced by the two NP-only control vectors, approximately 125-150 μg/mL (E1288, E1219). Immunization with the dual expression vectors induced higher titers of Gag-specific antibodies than NP-specific antibodies (**Figure 2.5B**). The E1303 vector induced a Gag-specific antibody titer of ~800 μg/mL, which was the highest titer induced. The other vectors tested induced titers of approximately 500 μg/mL, which was comparable to titers induced by the control vectors, E1043 and E1175.

Induction of $CD8^+$ T cell responses specific to each transgene was also measured as a test of vector immunogenicity. Groups of C57Bl/6 mice were immunized IM with 10^{10} vp of the indicated vectors; a group of naïve mice was included as a control. Two and six weeks following immunization, peripheral blood mononuclear cells (PBMCs) were isolated and tested for $CD8^+$ T cell responses specific to NP and Gag by intracellular cytokine staining (ICS) for IFN-γ, TNF-α, and IL-2 following *in vitro* stimulation with corresponding peptides. Boolean gating was used to determine the sum of all possible cytokine responses and background was subtracted. All vectors

with the exception of E1174 and E1301 induced NP-specific $CD8^+$ T cell responses (**Figure 2.6A**). The control vector only carrying NP in E1 (E1288) induced, as expected, a robust NP-specific $CD8^+$ T cell frequency of about 6% at two weeks after immunization that contracted to 1% at six weeks post-immunization. The vector in which the E3 cassette was in the forward orientation, E1310, induced an equally potent NP-specific $CD8^+$ T cell response that contracted less than that of the control vector at six weeks. This corresponded well with its expression data, which demonstrated that NP was most highly expressed from this vector (**Figure 2.3)**. Complete removal of the regulatory elements that were shared between E1 and E3 resulted in a vector that induced a more modest NP-specific $CD8^+$ T cell frequency of 2% at two weeks following immunization. However, the response contracted less than that of the other dual expression vectors. The similar vector, E1302, which has the intron in the E3 cassette, induced a response at two weeks comparable to that induced by the control vector and E1310. The NP-specific $CD8^+$ T cell response contracted and was maintained at a frequency similar to that of E1302. Gag-specific $CD8^+$ T cell responses were overall lower and more delayed than the NP-specific $CD8^+$ T cell response (**Figure 2.6B**). E1310 induced a very robust NP-specific $CD8^+$ T cell response but failed to induce a Gag-specific response at either timepoint; whereas, E1174 failed to induce an NP-specific response but did induce a very modest Gag-specific $CD8^+$ T cell response of less than 1% that was sustained throughout the experiment. E1301, which also did not induce a detectable NP-specific $CD8^+$ T cell response, induced a modest Gag-specific $CD8^+$ T cell response at 2 weeks that did not peak until 6 weeks after immunization. E1302 and E1303 both induced robust Gag-specific $CD8^+$ T cell responses. While E1302's peak response was more delayed than that of E1303, it was maintained at a higher level.

FIGURE 2.5. NP- and Gag-specific antibody responses

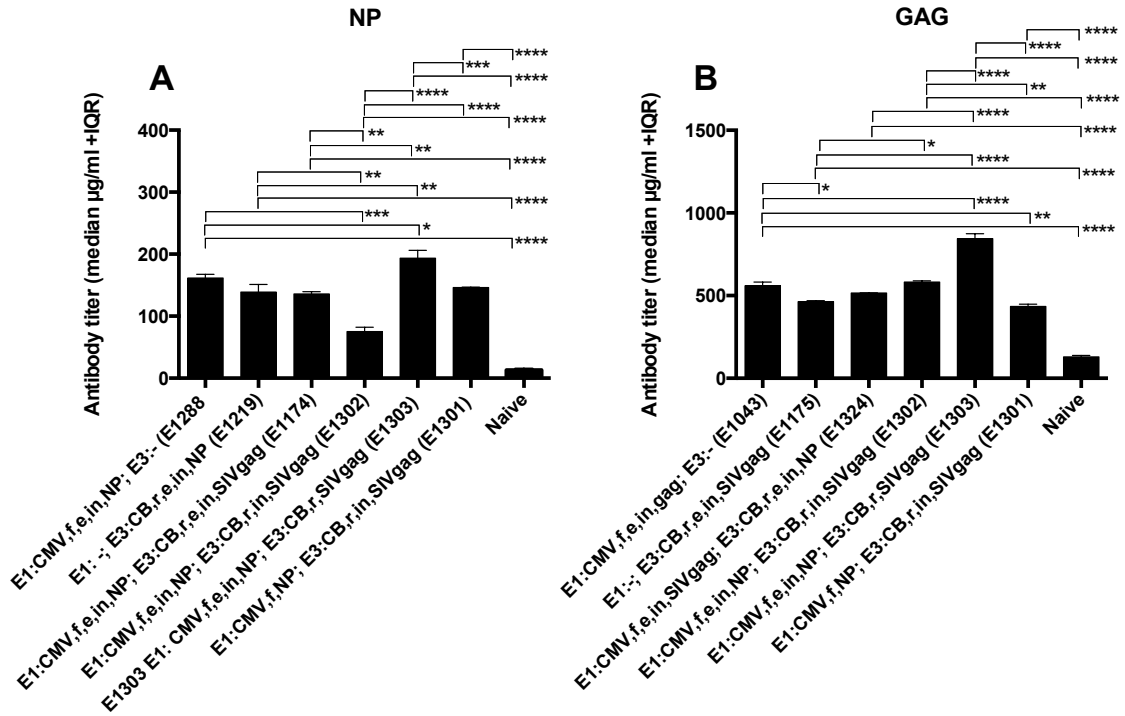

Pooled sera from mice immunized with the indicated vectors were tested for antibodies to NP **[A]** or Gag **[B]** by ELISA four weeks after vaccination. The graphs show area under the curve for two replicates of serially diluted sera. Lines indicate significant differences between the samples determined for by one-way ANOVA with Tukey correction.

* indicates level of significance as follows: * p >0.05-0.01, ** p < 0.01 – 0.001, *** p < 0.001-0.0001, **** p < 0.0001.

FIGURE 2.6. Kinetics of NP- and Gag-specific $CD8^+$ T cell responses

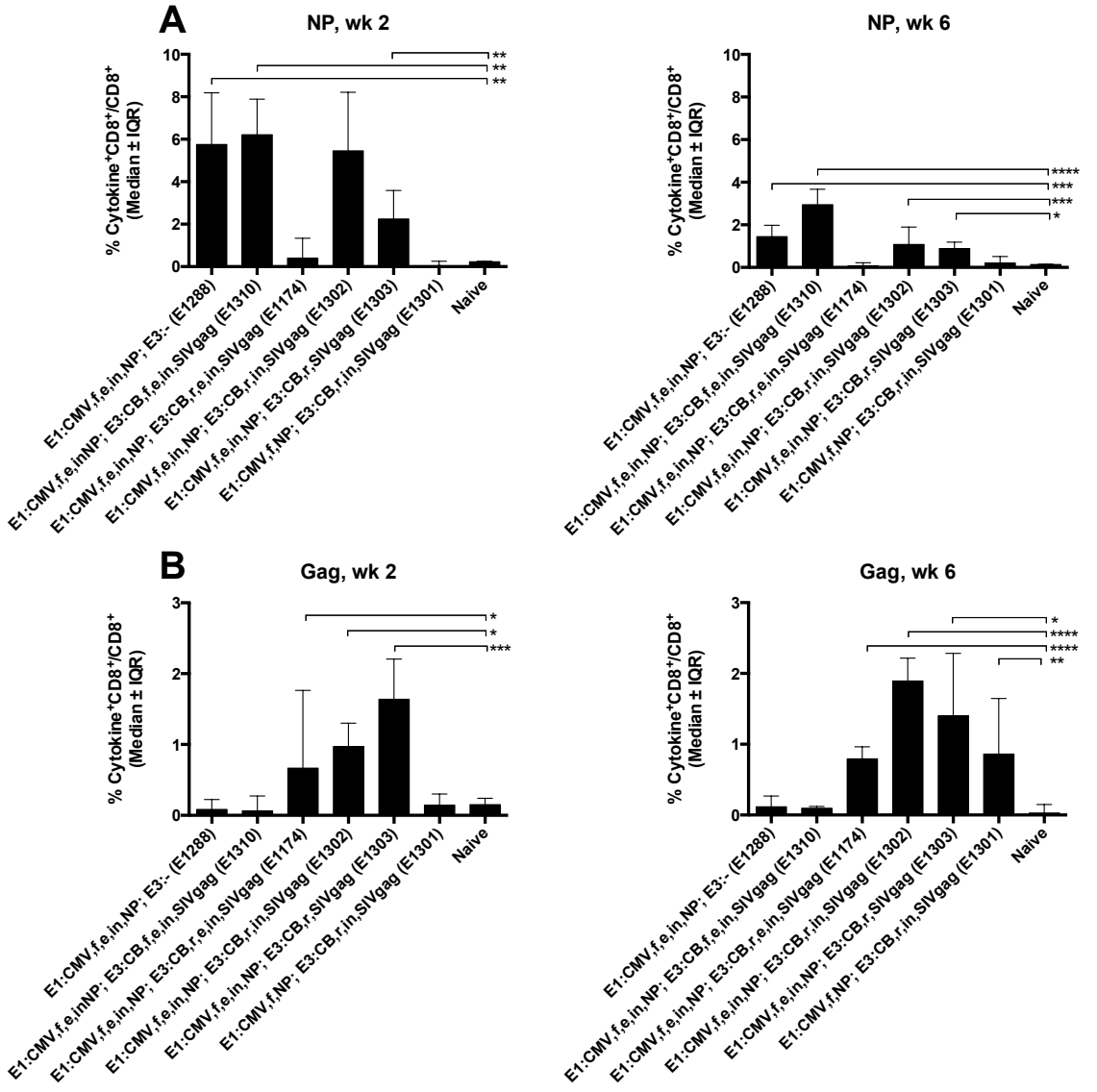

PBMCs from individual mice were tested 2 and 6 weeks after immunization for NP- **[A]** and Gag- **[B]** specific $CD8^+$ T cell responses by ICS. Graphs show the % of $CD8^+$ T cells over total $CD8^+$ T cells that produced cytokines after stimulation with the specific peptides after subtraction of background data obtained with cultures stimulated with an irrelevant peptide. Differences from results obtained with PBMCs from naïve mice were assessed with one-way ANOVA and uncorrected Fischer's LSD.

* indicated level of significance as follows: * p >0.05-0.01, ** p < 0.01 – 0.001, *** p < 0.001-0.0001, **** p < 0.0001.

RESULTS B. DEVELOPMENT OF NOVEL ADENOVIRAL VECTORS WITH CONDITIONAL TRANSGENE PRODUCT EXPRESSION

Test of concept with single expression vectors

A primary goal of this thesis was to directly investigate the role of persistent transgene expression from the Ad vector genome on the maintenance of the transgene product-specific $CD8^+$ T cell response. This necessitated the generation of Ad vectors whose transgene expression could be temporally regulated. One system often used to this end is the Cre/lox system that conditionally induces site-specific recombination [160]. As a test of concept, Ad vectors based on chimpanzee serotype 7 were generated that carried green fluorescent protein (GFP) flanked by loxP sites (5'-ATA ACT TCG TAT AGC ATA CAT TAT ACG AAG TTA T-3') in an expression cassette inserted into the E1 domain (AdC7-GFP^{loxP}) (**Figure 2.7A**). In order to determine if the expression of the transgene could be regulated using this method, HEK 293 cells were engineered to stably express CreERT2 (293-CreERT2. 10^6 293-CreERT2 cells were infected with 10^7 or 10^8 vp AdC7-GFP^{loxP}. At the time of infection, cells were treated with either 0.2 μM, 2 μM 4-OHT, or the equivalent volume of vehicle. Flow cytometry was used to measure GFP expression 24 hours after infection. Results indicated that even a low dose of 4-OHT was capable of inducing Cre activity in the cell line and thereby excision of the floxed GFP from the Ad genome (**Figure 2.7B**). This experiment suggested that transgene expression from the Ad genome could be regulated using the Cre/lox site-specific recombination system.

FIGURE 2.7. Test of concept – Ad vectors can have inducible transgene expression.

A.

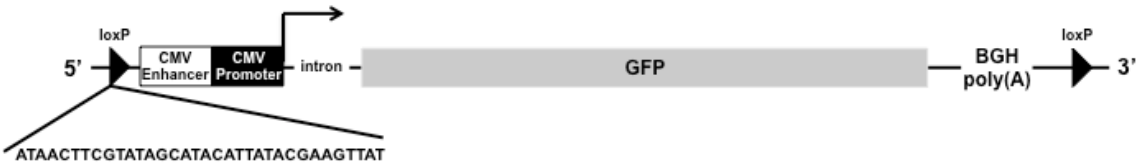

B.

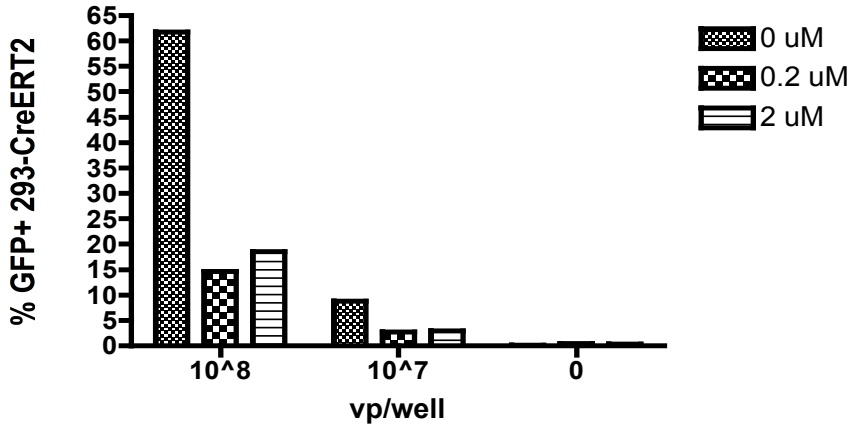

Transgene expression can be regulated from the Ad genome using Cre/lox recombination. **[A]** Shows a schematic of the E1 cassette carried by AdC7-GFP^{loxP}, which was used to infect cells for **[B]**. The E1 cassette used the cytomegalovirus (CMV) promoter to control expression of GFP. Additionally, the CMV enhancer and an intron were used to enhance expression. The Bovine Growth Hormone (BGH) polyadenylation signal was inserted 3' to the GFP coding sequence. LoxP sites (5'-ATA-ACT-TCG-TAT-AGC-ATA-CAT-TAT-ACG-AAG-TTA-T-3') were inserted 5' to the CMV enhancer and 3' to the poly(A) tail in parallel orientation, so that the flanked sequence is excised from the genome upon Cre-mediated recombination. LoxP sites and directionality are indicated by black triangles. This expression cassette was inserted 5' to 3' (forward orientation) into the genome of an E1- and E3-deleted AdC7 molecuar clone.

[B] 10^8 and 10^7 viral particles (vp) of AdC7-GFP^{loxP} were used to infect HEK 293 cells stably expressing inducible Cre recombinase (293-CreERT2 cells). 1 hour prior to infection, 293-CreERT2 cells were treated with 9.5 µL 2 µM or 0.2 µM 4-hydroxytamoxifen (4-OHT) to activate Cre-ERT2 activity. To demonstrate that Cre activity is inducible, cells were treated with the equivalent volume of vehicle (95% EtOH). As a negative control for expression, groups of uninfected cells were treated with both doses of tamoxifen and vehicle. 24 hours after infection, cells were assayed for GFP expression by flow cytometry. Graph shows percentage of GFP positive 293-CreERT2 cells over all cells.

Dual expression vector construction

Use of Ad vectors carrying only a floxed transgene would limit the use of these vectors to a transgenic mouse model that ubiquitously expressed CreERT2, vectors were engineered to carry CreERT2 as a transgene in the deleted E3 domain. The previous set of experiments demonstrated that vectors containing fewer shared sequences between the E1 and E3 expression cassettes had more optimal, balanced expression of both transgenes. As such new series of dual expression vectors was constructed following the design of the best performing vector (E1302) described above. Their design is shown in **Figure 2.8A**. The E1 expression cassette was constructed such that the CMV promoter controlled expression of the inserted transgene, which, in the following studies, was either *gag* of HIV-1 or GFP. Removal of the CMV enhancer and the intron from the E1 expression cassette was shown to dampen expression of the E1 transgene without having much effect on expression from E3; therefore, we included both elements in the cassette. Finally, the expression cassette was floxed. The E3 expression cassette encoded CreERT2 under the control of the CB promoter. It was demonstrated earlier that the orientation of the E3 expression cassette dramatically influences the expression of both encoded transgenes. Although placing the E3 cassette in the forward (5' to 3') orientation lead to very robust E1 transgene expression, expression from the E3 cassette was not optimal. Optimal expression of CreERT2 needed to be achieved to ensure excision of all floxed sequences; therefore, as vectors carrying the E3 cassette in the reverse orientation tended to have better expression of the E3 transgene, the CreERT2 expression cassette was inserted into E3 in the reverse orientation. Additionally, only an intron was included in the E3 expression cassette because inclusion of both the intron and enhancer, which were shared between both expression cassettes, reduced expression of the E3 transgene.

***In vitro* transgene expression and regulation**

In order to confirm that both the floxed transgene, in this case HIV *gag*, and CreERT2 were expressed and that CreERT2-mediated recombination of loxP sites could be induced, 10^6 Chinese hamster ovary (CHO) cells expressing the coxsackie and adenovirus receptor (CAR)

were infected with 10^9 vp of AdC7-HIVgag^{loxP}-CreERT2 and treated with either 4-OHT or the equivalent volume of vehicle. As a positive control for *gag* expression, a group of cells was infected with 10^9 vp of AdC7-HIVgag^{loxP}. One week later, total RNA and protein lysates were collected. Reverse transcription of total RNA revealed that *gag* was expressed in the absence of CreERT2 activity but following treatment with 4-OHT *gag* RNA was no longer detected (**Figure 2.8B**). Of note*, gag* expression from AdC7-HIVgag^{loxP}-CreERT2 was reduced compared to the positive control vector.

Gag and CreERT2 expression were also confirmed by Western blot of infected cells (**Figure 2.8C**). Doses ranging from 10^8 vp to 10^{10} vp were used to infect 10^6 CHO-CAR cells. 10^9 vp of AdC7-HIVgag^{loxP} was used as a positive control. Groups of cells were again treated either with 4-OHT or vehicle. Protein lysates were collected one week later. In the absence of 4-OHT, the highest expression of Gag was achieved with the 10^{10} vp dose of AdC7-HIVgag^{loxP}-CreERT2, which was slightly greater than that of the positive control. As expected, Gag expression decreased as the vector dose was decreased. The same expression pattern was observed for CreERT2. These results demonstrate that while CreERT2 is expressed, it is not active in the absence of tamoxifen treatment. However, CreERT2 activity was induced following tamoxifen treatment as evidenced by only faint detection of Gag one week after infection. Taken together, these results indicate that both transgenes are expressed *in vitro* and, importantly, CreERT2 activity, and thereby Gag expression, can be regulated with tamoxifen.

***In vivo* transgene expression**

As the transgenes were demonstrated to express well *in vitro*, transgene expression was next determined *in vivo*. BALB/c mice were injected IM with 10^{11} vp of AdC7-GFP^{loxP}-CreERT2 or the equivalent dose of AdHu5-GFP as a positive control for GFP expression. Two days later, the injected muscle was visualized for GFP expression as shown in **Figure 2.9A**. Very robust GFP expression was observed in the legs of mice injected with the positive control vector. Unexpectedly, GFP was unable to be detected in mice injected with AdC7-GFP^{loxP}-CreERT2.

The lack of expression *in vivo* could perhaps be explained if AdC7-GFP^{loxP}-CreERT2 had a very high infectivity ratio (vp to MOI), although this would impact *in vitro* expression as well. However, the ratio was 182:1, which is considered average. Another possible explanation for the lack of expression could be that the integrity of the vector's genome was compromised. To this end, viral DNA was purified from all dual expression vectors carrying a floxed transgene in E1 and CreERT2 in E3. Both the viral DNAs and the corresponding molecular clones used for viral rescue were subjected restriction digest with an enzyme chosen specifically to screen the floxed transgene (**Figure 2.9B**). Some banding pattern differences between the plasmid and viral DNA were expected, because the viral DNA lacks some sequences present in the molecular clone. However, a 2.2 kb band was missing from the isolated viral DNA. This band corresponded to the restriction sites that flanked the E1 cassette that the floxed transgene. Lack of this band indicated that the cassette was no longer present in the genome. The viral DNAs were sequenced to confirm loss of the E1 expression cassette. Sequencing data was in agreement with the restriction digests (schematic in **Figure 2.9C**). Only a single loxP site was detected in each genome and no expression cassette sequences were detected. This indicated that the viral genome recombined at the loxP sites during viral expansion, which most likely gave the mutant a growth advantage over the original recombinant vector. Interestingly, restriction digestion of the vectors that carried a floxed transgene in the E1 domain but did not carry CreERT2 revealed that the genome of these vectors remained intact during rescue and expansion.

FIGURE 2.8. Construction and expression of AdC7 vectors dually expressing a floxed transgene and CreERT2.

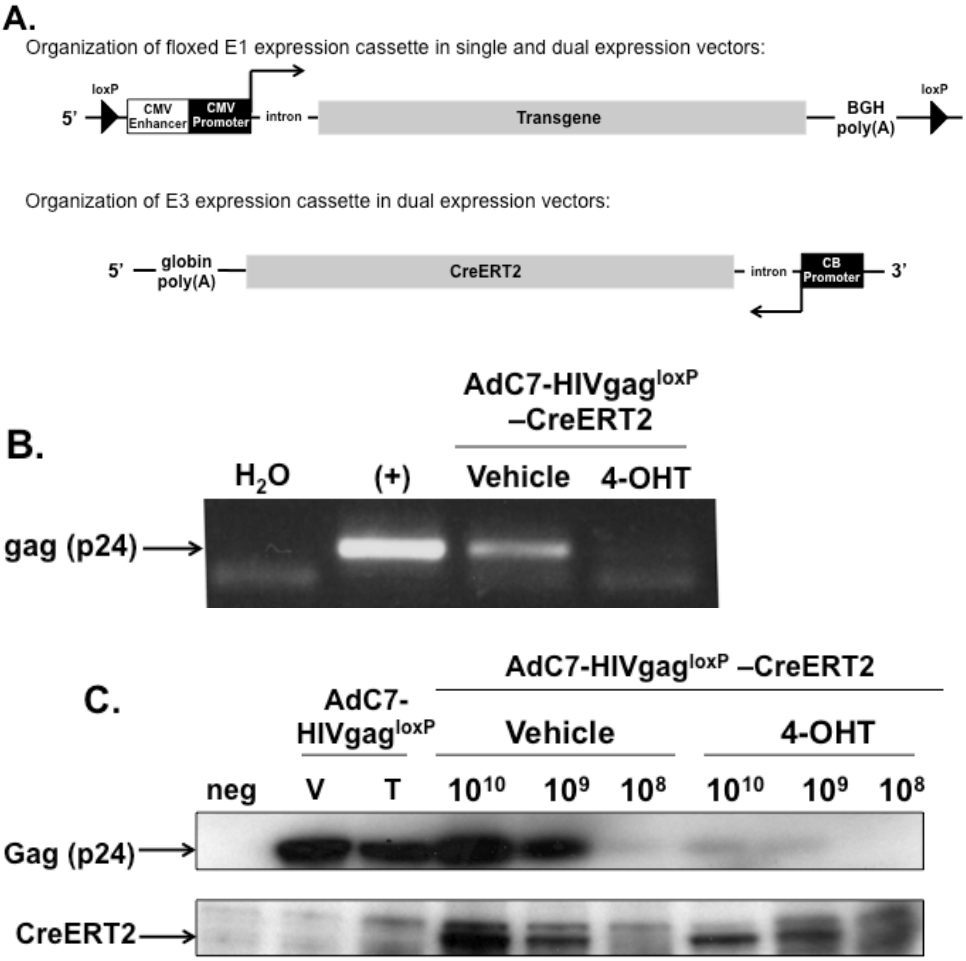

[A] Shows a schematic of the E1 and E3 expression cassettes. The E1 cassette was identical to that described in **Figure 2.7. A**. The transgenes used for the following experiments were gag of HIV-1 (shown in **[B]** and **[C]**) and GFP (shown in **Figure 2.9A and B**). The E3 expression cassette was modeled after that carried in E1302 (described in **Figure 2.1**). The vectors will be referred to as AdC7-HIVgag^{loxP}-CreERT2 or AdC7-GFP^{loxP}-CreERT2.

[B] Expression of HIV gag (p24) as measured by reverse transcriptase PCR. 10^6 CHO-CAR cells were infected 10^9 vp AdC7-HIVgag^{loxP}-CreERT2. 1 hour prior to infection cells were treated with either 2 μM 4-OHT or the same volume of vehicle. Cells were infected with 10^9 vp AdC7-HIVgag^{loxP} as a positive control for gag expression. As a negative control cells were infected with 10^9 vp AdC7 expressing rabies virus glycoprotein. Total RNA was isolated 1 week following infection and 2 μg was reverse transcribed. Gag was then amplified in a regular PCR from 1 μL of cDNA template. The resulting PCR fragments were visualized on a 1% TAE agarose gel stained with EtBr.

[C] Protein expression of HIV gag (p24) and CreERT2 as measured by Western Blot. . $1x10^6$ CHO-CAR cells were infected 10^{10},10^9, or 10^8 vp AdC7-HIVgag^{loxP}-CreERT2. 1 hour prior to infection cells were treated with either 2 μM 4-OHT or the same volume of vehicle. Cells were infected with 10^9 vp AdC7-HIVgag^{loxP} as a positive control for gag expression. They were also treated either with vehicle (V) or 2 μM 4-OHT (T). Uninfected cells were used as a negative control.

FIGURE 2.9. Dual expression vectors carrying floxed transgene and inducible Cre recombinase fail to express *in vivo.*

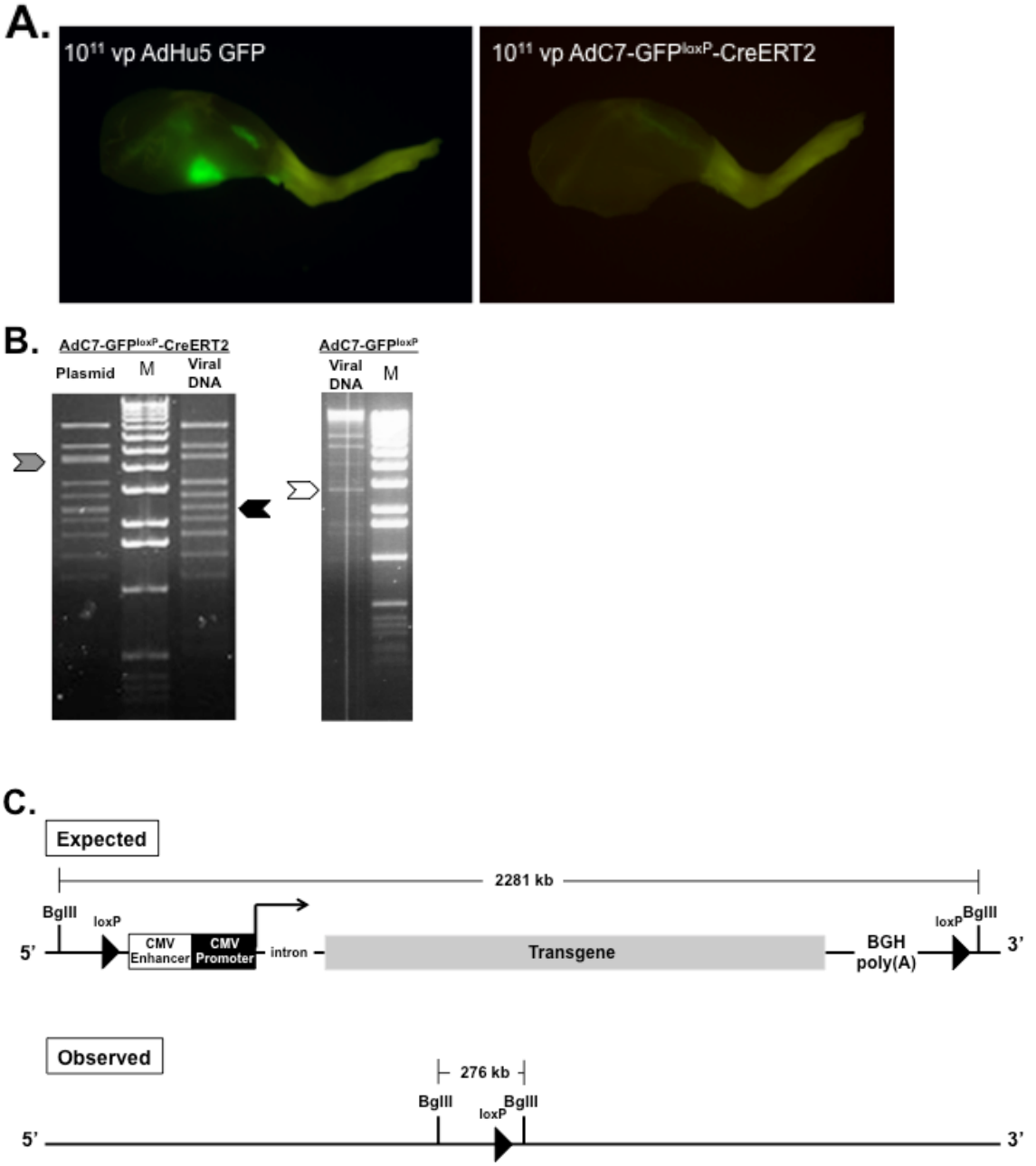

[A] Shows GFP expression in hind limbs following immunization with GFP-expressing Ad vectors. BALB/c mice were immunized with 10^{11} vp AdC7-GFP^{loxP}-CreERT2 or, as a positive control from GFP expression, 10^{11} vp AdHu5-GFP. 48 hours later, mice were sacrificed and legs were removed and visualized for GFP expression using Illumatool Lighting System. A Kodak DCS14N digital SLR camera with a 60-mm Micro Nikkor lens at f3.5 using 1:2.2 magnification was used to take photographs.

FIGURE LEGEND CONTINUED ON PAGE 43

[B] The molecular clone (plasmid) DNA of all dual expression vectors carrying floxed transgenes and the corresponding viral DNA isolated from expanded viruses were subjected to restriction digestion with BglII enzyme for 1 hour at 37°C. Additionally, AdC7-GFP^{loxP} viral DNA was subjected to restriction digest with SphI for 1 hour at 37°C Digests were visualized on a 1% TAE agarose gel stained with EtBr. “M” indicates the 1 kb plus ladder. For the dual expression vector digests: the grey arrow indicates an expected band because the plasmid DNA is circular while the viral DNA is linear. The black arrow indicates an unexpected missing band at 2.2 kb corresponding to the floxed E1 expression cassette. For the sing expression vector: the white arrow indicates the expected 2.7 kb band corresponding to the floxed E1 expression cassette. Shown here are digestions for AdC7-GFP^{loxP}-CreERT2 plasmid and viral DNA. Identical results were obtained for all other vectors tested.

[C] Shows a schematic of results. The missing band corresponded to a 2281 kb fragment that encompassed the floxed expression cassette in the E1 domain. The viral DNA was additionally sequenced (not shown) and the sequencing data corresponded with the restriction digestion. It revealed that the two BglII sites now encompassed a fragment that no longer contained the E1 expression cassette but contained only a single loxP site and the remaining base pairs between each BglII and loxP site.

DISCUSSION

Ad vectors elicit potent immune responses not only to their viral antigens but also to the products of encoded transgenes. Their consistently potent induction of transgene product-specific B and $CD8^+$ T cell responses has made them ideal vaccine platform candidates. As such, Ad vectors derived from a variety of serotypes have been extensively developed as vaccine carriers and are currently being tested in clinical trials.

For some pathogens it may be necessary to direct a broader immune response that is not limited to a single antigen. To this end, multiple Ad vectors, each expressing a different antigen of interest, could be used for immunization. This approach has been used with success [156] but it is both cumbersome and costly. Therefore, several strategies have been employed to express multiple transgenes from a single Ad vector. Two of the most commonly used strategies are to encode a long fusion protein of the genes of interest or to separate two transgenes by an internal ribosomal entry site (IRES). The former strategy may interfere with folding of the resultant fusion protein, which may alter protein functionality and immunogenicity. Dual expression Ad vectors have been designed using the latter method [161,162]. While both transgenes separated by an IRES are expressed, very often the downstream transgene is expressed at lower levels than the upstream transgene. This would be problematic if stoichiometric amounts of each transgene are required. It is worth noting that long transgenes inserted into the Ad genome are not expressed as well as shorter transgenes, leading to dampened immune responses [157]. Therefore, this would be problematic for all the strategies described above.

Insertion of tandem expression cassettes into the deleted E1 domain has also been used to design dual expression Ad vectors. The earliest vectors encoded two identical expression cassettes that only differed in the transgene each cassette carried [158]. However, serial passaging of vectors carrying identical expression cassettes often reveals that vectors with large regions of homology, e.g. identical promoters or other shared sequences, are genetically unstable and often recombine, resulting in excision of one expression cassette [163]. Others have designed vectors

using different promoters alone [164,165] or in combination with different regulatory elements, such as the polyA tail [163], to drive expression of the transgenes inserted into the E1 domain.

Ad vectors are often deleted in multiple gene domains or are fully gutted. These deletions not only reduce immune responses to viral antigens but also increase the carrying capacity of the vector [155]. One group used this approach to design vectors that expressed three transgenes by encoding one in the E1 domain under the CMV promoter and using a bidirectional promoter to drive expression of two other transgenes inserted into the region between the E4 domain and fiber [166].

In the study presented here, we designed a series of AdC7 vectors encoding transgenes in the deleted E1 and E3 domains and systematically tested how the components of each cassette impact transgene expression. As use of identical expression cassettes has been shown to promote homologous recombination in Ad5- and Ad35-based vectors [163,167] and use of heterologous expression cassettes inserted into E1 and E3 have been shown to express well in Ad5-based dual expression vectors [168,169], we chose to control expression of each transgene with heterologous promoters. The CMV promoter is widely used to drive ubiquitous and high levels of gene expression, although it is sensitive to silencing [170,171]. Despite this, we constructed our dual expression vectors such that the CMV promoter always drove E1 transgene expression. Two other widely used promoters, the RSV and chicken beta-actin (CB) promoters, were used to drive expression of the E3 transgene, in most cases *gag* of SIV. Others have used the RSV promoter in dual expression Ad vectors in the E3 domain [172]. However, our attempts to generate Ad vectors with this promoter often yielded unstable vectors that could not be rescued. Vectors' growth characteristics were improved by using the CB promoter in the E3 cassette.

Expression cassette orientation is an important consideration in the construction of adenoviral vectors. Others have demonstrated that orienting transgenes in the same direction as E1 transcription (5' to 3') leads to better growth characteristics [173] and transgene expression [174]. While E1 orientation was not tested in these studies, the findings concerning E3 cassette orientation are in contrast with this, even though E3 transcription also occurs 5' to 3'. When the E3 cassette was inserted in that direction (forward orientation), vectors were often unable to be

rescued. Use of the RSV promoter in this orientation did not yield viable vectors, whereas, some vectors encoding the CB promoter in the forward orientation were able to be rescued and propagated. Interestingly, the vectors that could be rescued (E1310) had the highest level of transcription from the E1 cassette but lower levels of expression from the E3 cassette. Switching the orientation to the opposite of E3 transcription (3' to 5') improved growth characteristics of these vectors and led to more balanced expression of the E1 and E3 transgenes.

The presence of shared introns and enhancer sequences in both E1 and E3 directly affected expression of the E1 transgene. Removal of one or both regulatory elements from the E3 domain tended to increase expression from E1 without having much impact on expression from the E3 domain. This may suggest that the shared elements are competing for limited factors.

In vitro expression data for each transgene suggested that the position of each transgene within the Ad genome influenced expression. NP was more highly expressed from the E1 domain than the E3 domain, while *gag* was more highly expressed from the E3 domain. Therefore, it was important to consider if the position of the transgene within the Ad genome also impacted corresponding B and T cell responses, which could be affected by expression *in vivo*, processing of each transgene, and presentation. *In vitro* expression data did not predict transgene product-specific antibody responses from control vectors. Those expressing NP alone in either the E1 (E1288) or E3 (E1219) domain induced comparable NP-specific antibody titers, despite unequal expression *in vitro*. Whereas, Gag expression was higher from the vector carrying *gag* in the E3 domain (E1175) but induced a slightly lower Gag-specific antibody response than the vector carrying *gag* in the E1 domain (E1043). Taken together these results may indicate that the impact of position on induced immune responses may be dependent on the transgene itself and not on processing and presentation of the transgene.

Immune responses to the transgenes in some dual expression vectors were predicted by their respective expression *in vitro*. E1310, the vector in which NP was encoded in E1 and gag in the forward-oriented E3 cassette, had high levels of NP expression but low levels of Gag expression *in vitro* and accordingly had the highest NP-specific $CD8^+$ T cell responses but failed

to induce Gag-specific $CD8^+$ T cells. Other vectors followed this pattern as well, including E1301 and E1174.

In some cases, immune responses to the dual expression vectors were not predicted by *in vitro* expression patterns. The E1302 and E1303 vectors, which differ only in that E1303 lacked both the enhancer and intron in E3 while E1302 only lacked the enhancer, showed similar levels of NP and Gag expression *in vitro*. However, T cell responses to the two vectors were opposite – E1302 induced a robust NP-specific $CD8^+$ T cell response, while E1303 induced a modest NP-specific $CD8^+$ T cell response. Responses followed the opposite pattern for Gag-specific $CD8^+$ T cell responses – E1302 initially induced a modest response that became more robust later, while E1303 induced a very robust and sustained response. It is possible that E1302 and E1303 expressed NP and Gag differently *in vivo.* While this may be part of the explanation, it is also possible that the immunodominance of each transgene product influenced the resulting $CD8^+$ T cell responses. In a similar study of an AdHu35-based dual expression vector encoding HIV Env gp-160 and malaria antigens, the $CD8^+$ T cell responses to the malaria antigen encoded in the E3 domain were very low, while the Env-specific response was robust [167]. This observation was attributed to Env's immunodominance over the malaria antigen and was overcome by increasing the vector dose. The dual expression vectors designed this study would be expected to express NP and Gag in the same cells. It is therefore possible that NP is more immunodominant than Gag. As such, the E1302 vector appears to induce NP- and Gag-specific $CD8^+$ T cell responses that suggest this – the NP-specific $CD8^+$ T cell response is rapid and robust and the Gag-specific $CD8^+$ T cell response is initially very modest but peaks following contraction of the NP-response. Perhaps removal of all regulatory elements from the E3 domain resulted in increased Gag expression that could overcome the immunodominance of the NP antigens to induce a more robust Gag-specific $CD8^+$ T cell response sooner after immunization.

An additional goal of this study was to generate a dual expression vector encoding a transgene whose expression could be regulated temporally. This vector was designed to give insight into how continued transgene expression from the adenoviral genome during its persistence alters the corresponding $CD8^+$ T cell responses against the transgene. To this end,

we chose the Cre/lox system of recombination to regulate transgene expression from AdC7-derived vectors. In a preliminary study, we demonstrated that inducible CreERT2 recombinase stably expressed in HEK 293 cells could be used to recombine loxP sites in the adenoviral genome. In order to make the system more translatable to animal models, floxed transgenes and CreERT2 were cloned into an AdC7 dual expression vector modeled after the E1302 vector described above. The E1302 vector was chosen as the model for the floxed dual expression vectors because it was shown to express both transgenes well *in vitro* and it induced a robust $CD8^+$ T cell response against the transgene product from the E1 domain. Therefore, a cassette carrying a floxed transgene was inserted into the E1 domain and a cassette carrying CreERT2 was inserted into the E3 domain. While expression of both the floxed transgene and CreERT2 could be detected *in vitro*, expression could not be measured *in vivo*. Analysis of genome stability revealed that the floxed transgene had unexpectedly been deleted from the genome during viral rescue. One potential explanation for this is that adenoviruses are known to recombine homologous sequences between two genomes during replication [175]. However, if this were the case, we would expect to see similar deletion of transgenes in vectors that carry the floxed expression cassette only. However, we only observed this deletion in the dual expression vectors carrying both the floxed expression cassette and CreERT2, suggesting that the observed deletion is Cre-mediated recombination. It is important to note that CreERT2 is constitutively expressed in infected cells but is sequestered in the cytoplasm by Hsp90 [160]. Only when tamoxifen is introduced can the recombinase translocate into the nucleus to recombine loxP sites. Alternatively, the size of the vector genome can directly influence the genome's stability. Larger genomes generated by inserting overly long transgenes into a deleted E3 domain tend to be slightly less stable than if no transgene was inserted [159]. The E3 deletion provides space for an expression cassette 3.5 kb in length. While the CreERT2 expression cassette was shorter than this (3.3 kb), it is possible that its inclusion in the dual expression vector made the vector less stable than the matched single expression vectors, which ultimately promoted rearrangement of the genome at the homologous loxP sites.

In order to continue to investigate the question the floxed dual expression vectors were designed to answer, alternative approaches must be used. Future studies could be undertaken in CreERT2 transgenic mice that are available to us using the AdC7 vectors encoding only the floxed transgene. Alternatively, vectors could be designed using inducible promoters to temporally control transgene expression. This may be a more ideal approach, as it would avoid the homologous recombination that potentially could occur between the loxP sites.

In conclusion, the studies presented here demonstrate that genetically stable dual expression vectors based on AdC7 can be generated. These vectors express both transgenes well and induce potent B and T cell responses. These studies also highlight that factors other than the strength of the promoters used in each expression cassette influence gene expression and the corresponding immune responses raised against each transgene. Careful consideration of the choice of transgenes and elements to enhance expression must be made. These studies will aid in the development of future Ad-based vaccines.

MATERIALS AND METHODS A.

OPTIMAL DESIGN OF ADENOVIRAL VECTORS EXPRESSING DUAL TRANSGENES

Adenovirus vector construction

Ad vectors were deleted in the E1 and E3 domains. Shuttle plasmids were used to sub-clone transgenes together with regulatory elements into these deleted domains. Shuttle plasmids designed to insert transgenes into the deleted E1 domain contained an expression cassette composed of the transgene of interest and regulatory elements to control the transgene's expression, including the cytomegalovirus promoter and enhancer, an intron, and a poly(A) tail. In some cases, a second transgene was inserted into the deleted E3 domain. The shuttle plasmids facilitating this contained an expression cassette comprised of the transgene and its regulatory elements, including the chicken beta-actin promoter or the RSV promoter and the rabbit beta-globin poly(A) tail. Transgenes were inserted into the Ad molecular clone using rare-cutting restriction enzymes. Insertion into the E1 domain was facilitated by digestion with I-CeuI and PI-SceI followed by ligation. The resulting expression cassette was oriented 5' to 3'. Insertion into the E3 domain was achieved by digestion with SceI followed by ligation. The resulting expression cassette was oriented 3' to 5' or 5' to 3'.

Viruses were rescued following successful cloning, as follows. 5 µg of the molecular clone were linearized by digestion with PacI for 1 hour at 37°C in a final volume of 50 µL. Linearized DNA was then transfected into HEK 293 cells (at 50% confluency) using $CaCl_2$ transfection kit (Invitrogen, Grand Island, NY). The protocol was modified slightly from the manufacturer's protocol. The digested DNA was added to 37 µL of 2M $CaCl_2$ and the final volume was brought to 300 µL with sterile H_2O. The DNA-$CaCl_2$ solution was then slowly dripped into 300 µL of HEPES-buffered saline solution while gently vortexing. After 30 minutes of incubation at room temperature, the precipitate was added to the cells. Transfected cells were then returned to a 37°C incubator and monitored for 7-10 days for cytopathic effect (CPE), which would be indicative of replicating virus. When CPE was extensive, the cells and media were collected. Three consecutive rounds of rapid freezing and thawing were performed to release virus

contained in cells. Rescued virus was then expanded by serially passaging on HEK 293 cells. The final product was purified on a $CsCl_2$ gradient and concentration of virus particles (vp) was measured by spectrophotometry.

RT-PCR Analysis

Total RNA from HEK 293 cells transduced with AdC7 vectors 24 hours earlier was isolated using RNeasy Mini prep kit (Qiagen, Valencia, CA). The quantity of RNA was determined by spectrometry. RNA samples were stored at -80 °C till use. For each sample, 2 µg of RNA were reversed transcribed using the High Capacity cDNA Reverse Transcription kit (Life Technologies, Carlsbad, CA) following the manufacturer's protocol. The real-time PCR reaction was subsequently carried out using Fast SYBR Green Master Mix (Applied Biosystems; Carlsbad, CA) at a final volume of 25 µl. For amplification of NP, the following primers were used at 5 pmol/µl: forward: 5'-AGC-AGG-TAC-TGG-GCC-ATA-AGG-3' and reverse: 5'-ACT-GAG-AAC-GTA-GGT-TGT-ATG-CTG-3'. For amplification of SIV gag, the following primers were used at 5 pmol/µl: forward: 5'-AAG-CCC-ATC-AAG-TGC-TGG-AAC-3' and reverse: 5'-TCT-TGC-CGC-ACT-TC-CAC-3'. The housekeeping gene GAPDH was used as an internal control and was amplified using 5 pmol/µl of the following primers: forward: 5'-TGC-CCC-CAT-GTT-GTG-ATG-G-3' and reverse: 5'-AAT-GCC-AAA-GTT-GTC-ATG-GAT-GAC-C-3'. 1 µL of cDNA was used as template. Quantitative RT-PCR amplification of each gene was performed as follows: initial amplification of primers was performed at 95°C for 20 seconds, followed by 40 cycles of denaturation at 95°C for 3 seconds and amplification at 60°C for 30 seconds. All real-time PCR reactions were carried out on ABI Prism 7500 Fast Sequence Detection System. Reactions were run in triplicate in two separate experiments. Standard curves used to calculate amounts of NP and SIV gag RNA in each sample were determined by serially diluting plasmids encoding NP and SIV gag from 5 ng/well to 0.31625 ng/well. Expression data for NP and SIV gag were normalized to GAPDH to control for variability in samples.

Western Blots

HEK 293 cells plated on 6-well plates were infected with two different doses of viral vectors (10^3 and 10^4 vp/ cell). 24 hours post infection cells were harvested and treated with RIPA buffer containing HALT protease inhibitors (Thermo Fisher Scientific, Pittsburgh, PA). Protein samples were prepared by diluting in a reducing sample buffer and electrophoresed on 4-15% SDS-PAGE gels (Bio-Rad, Hercules, CA) with Tris running buffer (Bio-Rad), transferred to PVDF membrane, and probed with either primary monoclonal antibody anti-NP (Southern Biotech, Birmingham, AL) or primary monoclonal anti-SIV Gag p27 (NIH AIDS Research and Reference Reagent Program, Germantown, MD) at 4 °C overnight. Horseradish peroxidase-conjugated goat anti-mouse secondary antibody (KPL, Gaithersburg, MD) was added and protein expression was detected by autoradiography using ECL substrate kit (Thermo Fisher Scientific). β-actin was used as protein loading control and probed with an anti-mouse β-actin primary antibody (Sigma-Aldrich, St. Louis, MD).

Mice

Thy1.1$^+$ C57BL/6 mice were purchased from Jackson Laboratories (Bar Harbor, ME). ICR mice were purchased from ACE Animals (Boyertown, PA). Mice were housed in the vivarium at the Wistar Institute (Philadelphia, PA). All experiments and procedures were performed in accordance with approved animal protocols.

ELISA

Sera of individual mice were pooled and tested for Gag- or NP-specific antibodies by ELISA. Briefly, 96-well plates were coated overnight at 4°C with Gag protein at 10 μg/ml or A/PR8 virus at 32 HAU/ml. Wells were washed with PBS/0.05% Tween-20, followed by overnight blocking at 4°C with PBS/3% BSA/0.05% Tween-20. Wells were then washed and incubated with serial-diluted samples (in duplicates) for 2 hours at room temperature. Wells were subsequently washed, and bound IgG was detected with a goat anti-mouse IgG alkaline phosphatase conjugate (Sigma-Aldrich). Bound enzyme was detected with DEA substrate (KPL) and read on a microplate reader at 405 nm.

Tetramer and ICS

ICS to detect Gag- and NP-specific $CD8^+$ T cell responses was performed as follows. Lymphocytes were stimulated either with a peptide (2 µg/ml) carrying the immunodominant $H2k^b$-restricted class I epitope of NP (ASNENMETM) or with a peptide pool (3 µg/ml) of 15-mers overlapping by 11 amino acids covering the entire SIVmac239 Gag sequence. A rabies virus glycoprotein peptide or a peptide of the $H2k^b$-restricted class I epitope of ovalbumin, SIINFEKL, were used as a negative stimulation controls; both negative peptides were used at the same concentration ad the positive peptides. After stimulation, lymphocytes were stained with anti-CD8, and anti-CD44 antibodies and with a stain identifying dead cells. Cells were stained for 30 minutes at 4°C then washed twice with PBS. Following permeablization, samples were stained for 30 minutes at 4°C with APC-labeled anti-IFNγ, Alexa700-labeled anti-IL-2, and PE-Cy7-labeled anti-TNFα. All antibodies (Biolegend, San Diego, CA) were diluted at 1:100 in 1X Perm/Wash. After washing, cells were fixed with Fixative Buffer (BD Biosciences, Franklin Lakes, NJ). Cells were run on an LSRII (BD Biosciences) and data were analyzed with FlowJo (TreeStar, Ashland, OR).

Statistical analysis

Experiments were conducted repeatedly using 3-4 mice per group. Results show the median ± IQR. Significances between groups were analyzed by one-way ANOVA.

MATERIALS AND METHODS B.

DEVELOPMENT OF NOVEL ADENOVIRAL VECTORS WITH CONDITIONAL TRANSGENE PRODUCT EXPRESSION

Construction of loxP single and dual expression vectors

Shuttle vectors were constructed to insert transgenes flanked by loxP sequences (floxed) into the deleted E1 domain. LoxP sites (5'- ATA ACT TCG TAT AGC ATA CAT TAT ACG AAG TTA T-3') were cloned into the empty shuttle vector such that they flanked the regulatory

elements of the empty expression cassette. Both loxP sites were oriented in the same direction (5' – 3'). This was achieved by generating forward and reverse primers, each with loxP sites, to amplify the region of the empty expression cassette in the shuttle plasmid. Additionally, each primer contained a restriction site to facilitate cloning the amplified fragment into the shuttle vector. The amplified PCR product was then sub-cloned into the in shuttle plasmid by restriction enzyme digestion and ligation. Successful cloning was confirmed by sequencing over regions containing loxP sites. The transgene, either gag of HIV-1 or GFP, was inserted into the empty loxP shuttle plasmid using the multiple cloning site (MSC) downstream from the intron and upstream of the poly(A) tail. The resulting shuttles were used to sub-clone the floxed expression cassette into the deleted E1 of the AdC7 molecular clone, as described above.

Additionally, dual expression vectors were generated that encoded floxed transgenes in E1 (as described above) and CreERT2 in the deleted E3 domain. CreERT2 is a fusion protein of Cre recombinase and mutated version of the human estrogen receptor that can only bind the synthetic estrogen ligand 4-hydroxytamoxifen. CreERT2 was cloned into the MCS of a shuttle vector used to insert transgenes into the E3 domain. The chicken beta-actin promoter (CB) was used to drive CreERT2 expression. Additionally, the CreERT2 expression cassette lacked an intron and contained the rabbit beta-globin poly(A) tail sequence. CreERT2 was then cloned into the E3 domain as described above. All vectors were rescued and quality controlled as described above.

Cre-293 cell line

For *in vitro* studies of Ad vectors containing a single floxed transgene, generation of a cell line stably expressing the inducible recombinase CreERT2, which identifies and recombines loxP sites, was necessary. 5 µg of a plasmid that expressed CreERT2 under the control of the CMV promoter and encoded the neomycin resistance gene was linearized and transfected into HEK 293 cells with $CaCl_2$ in the method described above. The following day, the antibiotic geneticin (G418) (Sigma-Aldrich) was added to the culture media at a concentration of 0.5 mg/mL to select for cells that were stably transfected with the plasmid that carried a G418-resistance gene. Fresh

media and G418 were added to cultures every 3 days. When individual colonies could be observed, they were harvested and transferred to individual wells of a 24-well plate to continue to be cultured under selective conditions. Ten days later colonies were transferred to T-75 flasks and expanded. When these cultures were confluent, cells were trypsinized and plated on a 6-well plate. 24 hours later, both reverse transcriptase PCR and Western Blot were used to confirm CreERT2 expression.

LoxP Site Functionality

$1x10^6$ 293-CreERT2 cells were infected with doses ranging from 1000 vp/cell to 10 vp/cell of AdC7 encoding floxed GFP (AdC7-GFP^{loxP}). 2 μM or 0.2 μM 4-hydroxytamoxifen (4-OHT or tamoxifen) (Sigma-Aldrich) was added at time of infection. As a negative control, cells were treated with equal volume of vehicle (95% EtOH). Importantly, the volume of vehicle and tamoxifen was less than 10 μL per well, which contained 3 mL of culture media. Cells remained viable through the experiment as they remained attached to the plate. GFP expression was analyzed 48 hours later by flow cytometry.

LoxP site functionality was tested in dual expression vectors by infecting $1x10^6$ chinese hamster ovary (CHO) cells stably transfected with the coxsackie-adenovirus receptor (CHO-CAR) with AdC7 vectors dually expressing floxed Gag from E1 and CreERT2 from E3 (AdC7-gag^{loxP}-CBr-CreERT2). Doses ranged from 10^{10} vp to 10^8 vp. 2 μM 4-OHT and vehicle treatment was started 1 hour prior to infection. 3 and 7 days after infection, Gag and CreERT2 expression were confirmed by Western blot and reverse transcriptase PCR. As a control, groups of cells were infected 10^9 vp of AdC7-$HIVgag^{loxP}$ and treated with either vehicle or 2 μM 4-OHT.

For Western blot, cells were washed 3 times with ice cold PBS without Ca^{2+} or Mg^{2+} then lysed for 1 hour on ice in RIPA Buffer containing Complete protease inhibitors (Roche; Indianapolis, IN). Protein samples were then diluted in loading buffer containing NuPAGE reducing reagent (Life Technologies) and electrophoresed on NuPAGE 4-10% SDS-PAGE gels (Life Technologies) with Tris running buffer. Samples were then transferred to PVDF membrane and probed overnight at 4°C with mouse monoclonal anti-HIV gag p24 or rabbit polyclonal

antibody anti-Cre recombinase (Abcam, Cambridge, MA). After washing with 0.1% PBS-T, HRP-conjugated secondary antibodies (anti-mouse for Gag, anti-rabbit for CreERT2) were diluted in 5% blotto and incubated for 1 hour at room temperature. PBS-T was used to wash the membranes a final time and protein expression was detected on membranes using ECL substrate kit (Thermo Fischer Scientific).

Total RNA was isolated for reverse transcriptase PCR using TRI reagent (Sigma-Aldrich) according to the manufacturer's protocol. RNA was reverse transcribed using SuperScript II Reverse Transcriptase (Life Technologies) according to the manufacturer's protocol. HIV gag and CreERT2 were amplified by regular PCR using Platinum Taq polymerase (Life Technologies), resulting in a 250 bp fragment and a 200 bp fragment, respectively. 5' and 3' primers used for amplification of gag were: 5'-ACC-ACA-TCT-ACC-CTG-CAG-GAA-CAG-3' and 5'-AGG-GTC-TCT-GTC-ATC-CAA-TTC-TTC-3'. The PCR consisted of 30 cycles of 94°C for 30 seconds, 57°C for 30 seconds, and 72°C for 1 minute. The 5' and 3' primers used for amplification of CreERT2 were: 5'-ACG-GCG-CTA-AGG-ATG-ACT-CTG-G-3' and 5'-ATC-CGC-CGC-ATA-ACC-AGT-GAA-AC-3', respectively. The PCR consisted of 30 cycles of 94°C for 30 seconds, 57°C for 30 seconds, and 72°C for 1 minute. Amplicons (5 µL) were visualized on a 1% TAE agarose gel.

Muscle imaging

BALB/c mice were immunized IM in the lower leg with 10^{11} vp of AdC7-GFP^{loxP}-CBr-CreERT2. Legs were removed 48 hours later and GFP expression was visualized using Illumatool Lighting System (Lightools Research, Encinitas, CA). A Kodak DCS14N digital SLR camera (Kodak, Rochester, NY) with a 60-mm Micro Nikkor lens of f3.5 using a 1:2.2 magnification (Nikon, Tokyo, Japan) was used to take photographs. Raw images were converted to TIFF files.

Quality control of isolated viral DNA

Isolated viral DNA from vectors encoding floxed GFP or gag and matched plasmid molecular clones used to rescue the vectors were subjected to restriction digest to determine if

the transgene had been excised from Ad genome during viral rescue and expansion. DNAs were digested with BglII and SphI (both from New England BioLabs, Ipswich, MA) for 1 hour at 37°C. Digestion products were run on a 1% TAE agarose gel.

CHAPTER 3

INHIBITION OF THE MAMMALIAN TARGET OF RAPAMYCIN FAILS TO AUGMENT FORMATION OF CENTRAL MEMORY $CD8^+$ T CELLS IN THE PRESENCE OF PERSISTING ANTIGEN

ABSTRACT

Inhibition of the mammalian target of rapamycin (mTOR) pathway enhances differentiation of anti-viral central memory $CD8^+$ T cells induced during acute viral infections. Recombinant adenovirus (Ad) vectors persist at low levels and remain in a transcriptionally active form. A consequence of this persistence is that Ad vector vaccination induces potent and sustained transgene product-specific $CD8^+$ T cell responses that fail to transition into central memory. Here we tested in mice if treatment with rapamycin, which blocks mTOR activity, could promote formation of central memory transgene product-specific $CD8^+$ T cells following vaccination with Ad vectors. Our results demonstrate that rapamycin given early after Ad vector vaccination transiently increases the magnitude of the transgene product-specific $CD8^+$ T cell response while a delayed treatment has no such effect. Neither regimen improves formation of central memory $CD8^+$ T cells. These results show that transient inhibition of the mTOR pathway does not override the effect of persisting antigen on continuous $CD8^+$ T cell activation.

INTRODUCTION

In recent years, $CD8^+$ T cell metabolism has been extensively studied and it has been revealed that along their path of differentiation, $CD8^+$ T cells undergo two major switches in their metabolism [105]. Mature, naïve $CD8^+$ T cells are actively maintained in a quiescent state. As such, these cells are locked in G_0 and rely on catabolic metabolism for their energy needs. This is mediated by mitochondrial oxidative phosphorylation of glucose, amino acids, and lipids. However, full activation of $CD8^+$ T cells results in vast clonal expansion and upregulation of effector molecules. As such, $CD8^+$ T cells shift to an anabolic metabolism in order to keep up with increased energy demands. Glucose uptake is dramatically increased and effector $CD8^+$ T cells switch from oxidative phosphorylation to primarily aerobic glycolysis, which is unusual as glycolysis is less efficient but enables synthesis of the cells' building materials. Following pathogen clearance the vast majority of effector cells will undergo apoptosis, but those that remain and differentiate into memory will again switch their metabolism and revert back to a catabolic, quiescent state.

Mammalian target of rapamycin (mTOR) is a key regulator of cellular metabolism that tightly controls cellular growth and proliferation. mTOR is a serine/threonine kinase that exists in two distinct complexes: mTORC1 and mTORC2 [176]. A key difference in these two complexes is that mTORC1 is sensitive to inhibition by rapamycin, an immunosuppressant often administered to prevent rejection of organ transplants, while mTORC2 is not. mTORC1 is directly inhibited by the TSC1/TSC2 complex, whose activity is controlled by the PI3K-AKT and AMPK pathways. Given this, mTOR integrates environmental signals to regulate protein synthesis predominantly via S6K1 and 4E-BP1 and to promote glycolysis and lipid biosynthesis.

Emerging evidence has demonstrated that mTOR is intimately involved in shaping $CD8^+$ T cell metabolism and differentiation. In order for naïve T cells to maintain quiescence, mTOR activity must be held in check. T cells that are deficient in the TSC complex, and thus unable to inhibit mTOR, are activated, proliferate, and are prone to apoptosis [177]. In activating naïve $CD8^+$ T cells, TCR engagement and co-stimulation activates a signaling cascade that results in optimal

mTOR activation, the level of which is directly dependent on amount and duration of antigen stimulation [105]. This causes dramatic upregulation of the glucose transporter [105] thus allowing the cell to switch metabolic programs and acquire effector functions. Simultaneously, mTOR activity promotes downregulation of CD62L and CCR7 [178], thereby allowing the activated effector cells to traffic to sites of inflammation. When antigen is cleared and the TCR is no longer engaged, the glucose transporter is downregulated and effector cells are effectively starved. Those cells that survive contraction transition into memory and metabolically switch back to autophagy for energy demands. Sensing glucose deprivation, AMPK blocks mTORC1 activity [179] and promotes autophagy in the form of fatty acid oxidation [180], allowing effector cells to transition to memory. As such, drugs that activate AMPK or block mTOR activity, like rapamycin, promote transition into memory [154,180]. Additionally, mTOR alters transcriptional programs crucial for T cell fate decisions. It has been demonstrated that inhibition of mTOR activity blocks the transcription factor T-bet while promoting Eomesodermin [181], which control differentiation of effector and memory cells, respectively [182].

Manipulation of the mTOR pathway was shown to enhance formation of central memory $CD8^+$ T cells, suggesting the potential of mTOR inhibitors as vaccine adjuvants. Araki et al. demonstrated in mice that treatment with a low dose of rapamycin during the T cell expansion phase following LCMV infection enhanced the quantity of memory $CD8^+$ T cells, while treatment during contraction enhanced the quality of these cells [154]. Similar results were observed in rhesus macaques treated with rapamycin during vaccinia virus infection [183]. These studies suggest that rapamycin could potentially be used as a vaccine adjuvant.

Replication-defective adenoviral (Ad) vectors have garnered much attention as vaccine platforms. An attractive feature of Ad vectors is that they are known to induce very potent and sustained transgene product-specific $CD8^+$ T cell responses following immunization [184]. The failure of this $CD8^+$ T cell response to contract is due to persistent transgene product expression from Ad vectors maintained in activated T cells [123]. Transgene product-specific $CD8^+$ T cells that remain following primary immune responses bear an effector or effector memory phenotype and their differentiation to central memory is markedly delayed [123]. While a large pool of armed

effector-like $CD8^+$ T cells standing guard at a pathogen's port of entry may be beneficial in preventing acquisition of viruses [134,185], a larger pool of long-lived central memory $CD8^+$ T cells, with their vast potential for expansion following antigenic reencounter, could be beneficial to protect against systemic dissemination of reinvading pathogens [185].

Here we tested if inhibition of mTOR through rapamycin could override the continuous stimulation of $CD8^+$ T cells by low levels of transgene product produced by persisting Ad vaccine vectors. To this end mice were treated with a low dose of rapamycin either early during the $CD8^+$ T cell expansion phase following immunization or later after responses had peaked. We demonstrate that early rapamycin treatment transiently increases the magnitude of the transgene product-specific $CD8^+$ T cell responses in blood and, less so, in spleen, but fails to alter frequencies of $CD8^+$ T cells that migrated to lymph nodes. Beginning treatment with rapamycin several days following immunization fails to enhance the magnitude of the $CD8^+$ T cell responses. Neither regimen increases formation of central memory $CD8^+$ T cells. While rapamycin treatment enhances the formation of central memory $CD8^+$ T cells to non-persisting pathogens, our data show that it is not effective in overriding the effect of persisting antigen on continuous $CD8^+$ T cell activation.

RESULTS

The effect of early rapamycin treatment of $CD8^+$ T cell responses to the transgene product of an Ad vector

Low dose rapamycin treatment given to limit mTOR activity during the $CD8^+$ T cell expansion phase was demonstrated to increase the number of $CD8^+$ memory precursors and thus increase the resulting number of memory cells following infection with lymphocytic choriomeningitis virus (LCMV) [154]. To test if rapamycin affected the quantity of transgene product-specific $CD8^+$ T cell responses induced following immunization with an Ad-based vaccine, BALB/c mice were intramuscularly (IM) vaccinated with 10^{10} vp of an E1-deleted adenovirus based on human serotype 5 expressing Gag of HIV-1 (AdHu5-gag). Groups of mice were treated daily for 10 days starting on the day of immunization either with 75 μg/kg of rapamycin or with 10

μL/g of sham as a control. Mice were bled or euthanized periodically and numbers of Gag-specific $CD8^+$ T cells were measured by staining isolated lymphocytes with a tetramer specific to the immunodominant, H-2^d-restricted immunodominant epitope of Gag (AMQMLKETI). As shown in **Figure 3.1A**, Gag-specific $CD8^+$ T cells from both rapamycin-treated and sham-treated groups expanded in all compartments until day 21 post-immunization, after which point modest contraction was observed in the blood and spleen. Gag-specific $CD8^+$ T cells remained fairly stable in the lymph nodes. The most robust expansion of Gag-specific $CD8^+$ T cells was observed in blood. Here, rapamycin treatment significantly increased the absolute number of Gag-specific $CD8^+$ T cells at the peak response as compared to those from mice that had only received sham treatment. Although numbers remained elevated for the duration of the experiment, the difference was only significant at the peak of the response.

Analysis of the $CD8^+$ T cells at the peak of their response has revealed that they are a heterogeneous population consisting of terminally differentiated short-lived effector cells (SLEC) and memory precursor effector cells (MPEC) fated to become memory cells with high proliferative capacity, and cells with more intermediate phenotypes [186]. MPEC and SLEC can be defined by differential expression of the interleukin-7 receptor α chain (CD127), which is required for formation of memory cells [187], and killer cell lectin-like receptor subfamily member G1 (KLRG1), which is a marker of terminally differentiated antigen-experienced $CD8^+$ T cells [143]. As such, MPEC are defined by high CD127 expression and low KLRG1 expression; whereas, the opposite expression pattern is observed on SLEC [186]. Inhibition of mTOR during the $CD8^+$ T cell expansion phase increased the overall magnitude of the response by enhancing the number of memory precursors formed following LCMV infection but did not alter the quality of the induced $CD8^+$ T cells [154]. In order to determine if rapamycin treatment increased memory precursor numbers and altered the memory phenotype of the transgene product-specific $CD8^+$ T cells following Ad vaccination, KLRG1, CD127, and CD62L, which can be used to distinguish between effector memory and central memory T cells based on low or high expression, respectively, were measured over time on Gag-specific $CD8^+$ T cells isolated from blood, spleen, and lymph nodes (**Figure 3.1B**). In both groups, the frequency of Gag-specific $CD8^+$ T cells that had converted to a

CD62L^{hi} phenotype were modest in all tissues tested, with the highest conversion occurring in lymph nodes. Rapamycin treatment did not significantly alter frequencies of CD62L^{hi} Gag-specific CD8^{+} T cells except 10 days after cessation of treatment (day 21) in blood, however this increase was modest and transient. Percentages of CD127^{hi} Gag-specific CD8^{+} T cells were also similar between the two cohorts at most time points in all tissues. Significant differences were measured in blood on day 10 and 49 and in both lymph nodes and the spleen on day 21. Additionally, rapamycin treatment had no effect on the numbers of cells expressing decreased levels of KLRG1. Therefore, rapamycin treatment did not increase the MPEC frequency.

One measure of T cell quality is their capacity to produce multiple cytokines in response to re-stimulation. It is generally considered that an antigen-specific CD8+ T cell population that is capable of producing multiple cytokines, or is more polyfunctional, is more effective. To test if rapamycin treatment affected polyfunctionality of Gag-specific CD8^{+} T cells, we measured production of the cytokines interferon–γ (IFN-γ), tumor necrosis factor-α (TNF-α) and interleukin-2 (IL-2) in blood and spleen. Additionally, the chemotactic cytokine macrophage inflammatory protein-1α (MIP-1 α) was measured in T cells from spleen. As shown in **Figure 3.2A**, rapamycin treatment increased the magnitude of cytokine producing Gag-specific CD8^{+} T cells in blood and spleen, although this reached significance only in cells isolated from the blood. Cytokine profiles were measured following *in vitro* re-stimulation of Gag-specific CD8^{+} T cells isolated from blood and spleen at 12 weeks following immunization (**Figure 3.2B**). Gag-specific CD8^{+} T cell cytokine profiles were largely similar between the two cohorts of mice and consisted of cells producing mainly IFN-γ alone or in combination with TNF-α; in the spleen, these combinations included MIP–1α. Again, although the profiles were largely the same between the two groups, rapamycin treatment preferentially expanded the number of cells producing these combinations of effector cytokines. In some cases, rapamycin treatment also lead to a small increase in polyfunctional cells, although this was not significant.

As an additional measure of the functional quality of the induced Gag-specific CD8^{+} T cell response, both the rapamycin- and sham-treated groups were boosted 12 weeks after

immunization with 10^{10} vp of a heterologous Ad vector based on chimpanzee serotype 7 carrying the HIV-1 Gag transgene (AdC7-HIVgag). A group of mice primed with this virus alone was included as a control. In all compartments, Gag-specific $CD8^+$ T cells from both groups robustly expanded following booster immunization regardless of treatment (**Figure 3.3**). Rapamycin-treated mice developed higher numbers of Gag-specific $CD8^+$ T cells than sham treated mice. Nevertheless the fold of expansion as assessed by the ratio of the numbers of Gag-specific $CD8^+$ T cells before and after the boost was very similar between the rapamycin- and sham-treated groups in the blood, 10.5 and 9, respectively, (**Figure 3.3A**) and lymph nodes, each boosted 1.7-fold (**Figure 3.3C**). In spleen (**Figure 3.3B**), the sham-treated group actually showed a more pronounced expansion of Gag-specific $CD8^+$ T cells compared to rapamycin-treated mice, 2.8-fold compared to 4.2-fold, respectively. Taken together, these results demonstrate that rapamycin treatment did not enhance the ability of the Gag-specific $CD8^+$ T cells to expand following secondary exposure to their cognate antigen and therefore did not enhance the quality of the induced Gag-specific $CD8^+$ T cell response.

FIGURE 3.1. Early rapamycin treatment transiently increases Gag-specific CD8$^+$ T cells without altering memory phenotype.

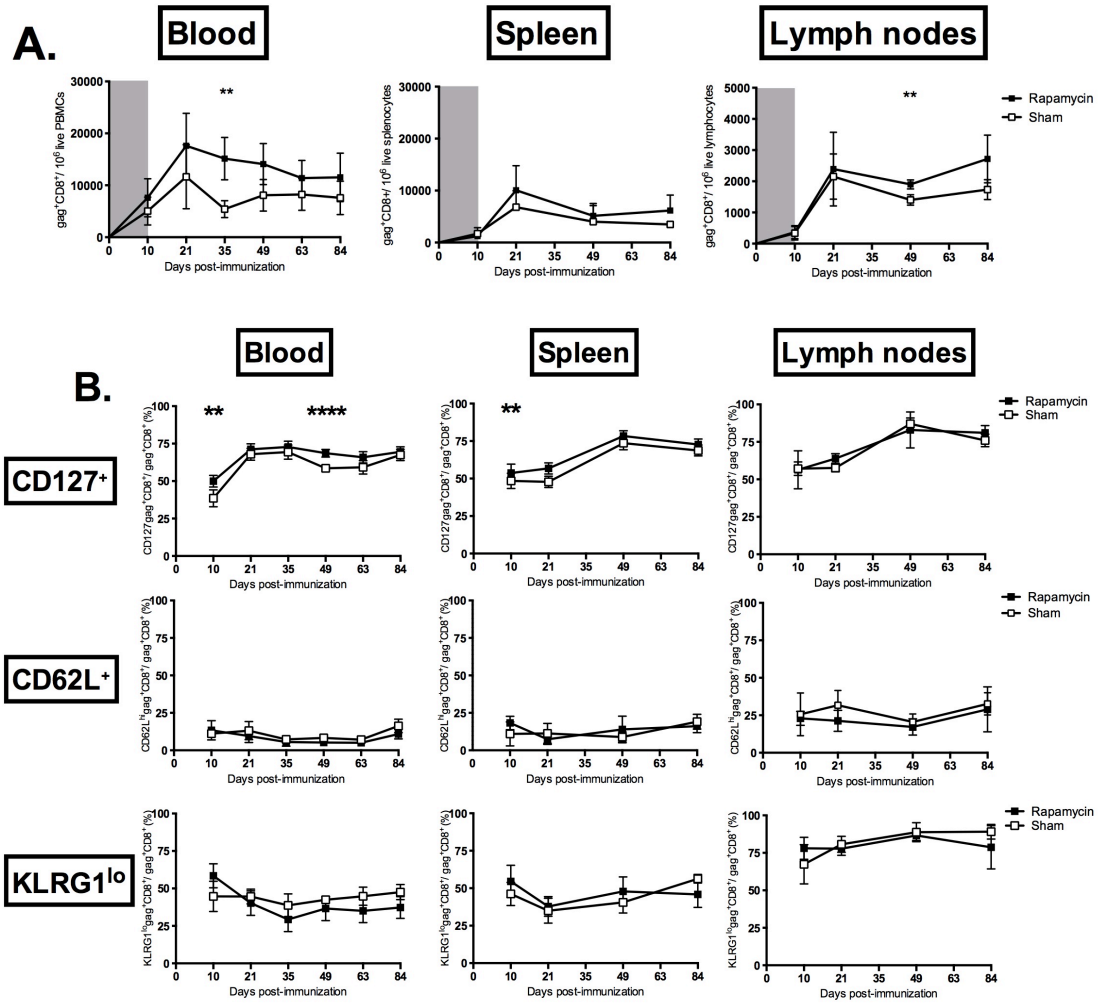

Groups of 5 BALB/c mice were immunized intramuscularly with 10^{10} vp AdHu5-HIVgag. At the time of immunization and continuing until day 10 post-immunization, one group was treated intraperitoneally (IP) with 75 µg/kg/day of rapamycin. As a control, the other group was IP injected with sham (0.1% DMSO in PBS) treatment given at 10 µL/g. Rapamycin-treated group is indicated by black boxes while sham-treated group is indicated by white boxes. The grey area indicates the treatment phase. Significance was determined using multiple t-tests with Holm-Sidak correction for multiple comparisons.

[A] All mice were bled for PBMCs or euthanized for splenocytes and lymphocytes at the indicated time points. Graphs show the mean number of Gag-specific CD8$^+$ T cells over 10^6 live cells ± standard deviations (SD). The following p-values were obtained: Blood: Day 35: p=0.0011; Lymph nodes: Day 49: p=0.0019.

[B] Shows the longitudinal phenotyping of Gag-specific CD8$^+$ T cells from indicated time points and tissues. Graphs show the mean frequency of Gag-specific CD8$^+$ T cells with the indicated phenotype (CD127$^+$, CD62L$^+$, or KLRG1^{lo}) over the total Gag-specific CD8$^+$ T cell response ± SD. The following p-values were obtained: Blood: CD127: Day 10: p=0.0057, Day 49: p<0.0001; Spleen: CD127: Day 10: p=0.0089.

Significant differences are indicated by * for p-values ≤ 0.05-0.01, ** p-values < 0.01-0.001, *** p-values ≤ 0.001-0.0001, **** p-values < 0.0001. Lines show the comparison groups.

FIGURE 3.2. Early rapamycin treatment transiently increases cytokine production.

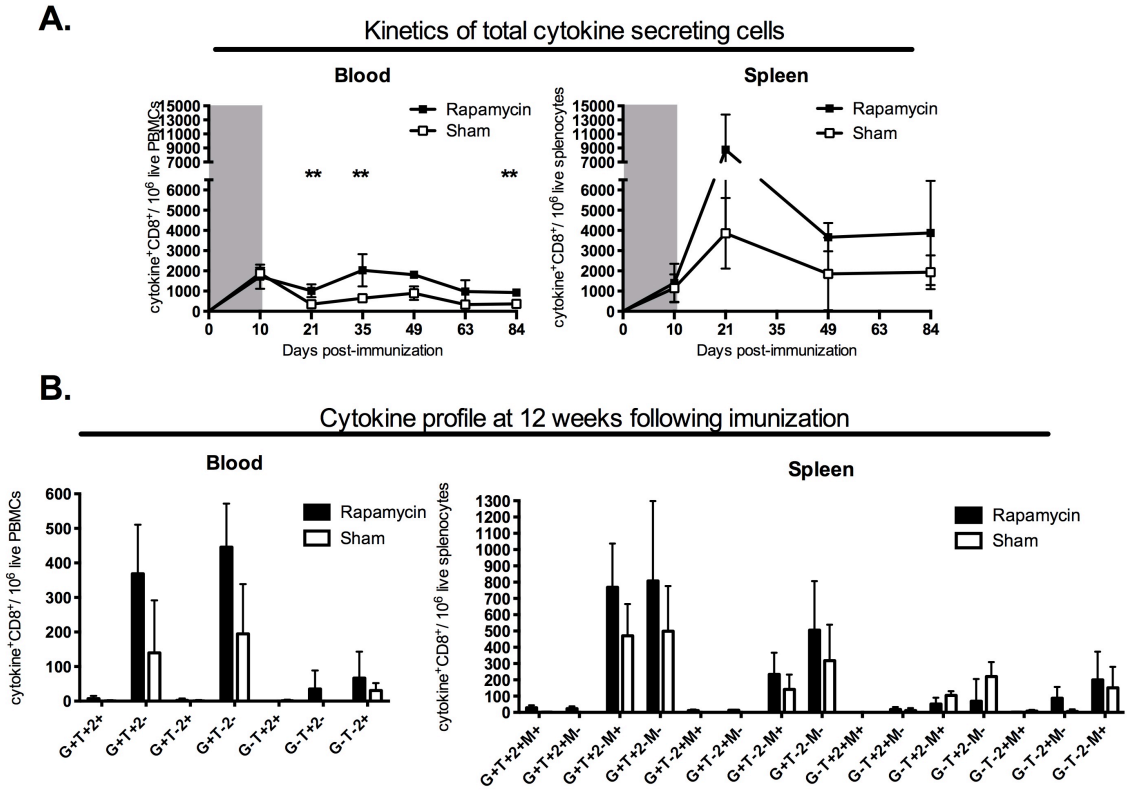

Shows the kinetics of total cytokine-producing cells **[A]** and the cytokine profile 12 weeks following immunization **[B]**. IFN-γ (G), TNF-α (T), and IL-2 (2) production was measured for PBMCs. IFN-γ, TNF-α, IL-2, and MIP-1α (M) production was measured for splenocytes. For determination of the kinetics, mice were bled or euthanized at the indicated time points and PBMCs or splenocytes were isolated, respectively. The lymphocytes were stimulated with either the Gag peptide AMQMLKETI or the equivalent amount of an irrelevant peptide to measure background stimulation. Line graphs show the mean number of cytokine producing cells following the subtraction of background stimulation and summation of Boolean gates used to determine the cytokine profile ± SD. Significance between rapamycin- and sham–treated groups was determined for each time point using multiple t-tests with Holm-Sidak correction for multiple comparisons. The following p-values were obtained: **[A]** Blood: Day 21: p=0.002, Day: 35: p=0.006, Day 84: p=0.0038.

Significant differences are indicated by * for p-values ≤ 0.05-0.01, ** p-values < 0.01-0.001, *** p-values ≤ 0.001-0.0001, **** p-values < 0.0001. Lines show the comparison groups.

FIGURE 3.3. Early rapamycin treatment causes a more robust peak recall response.

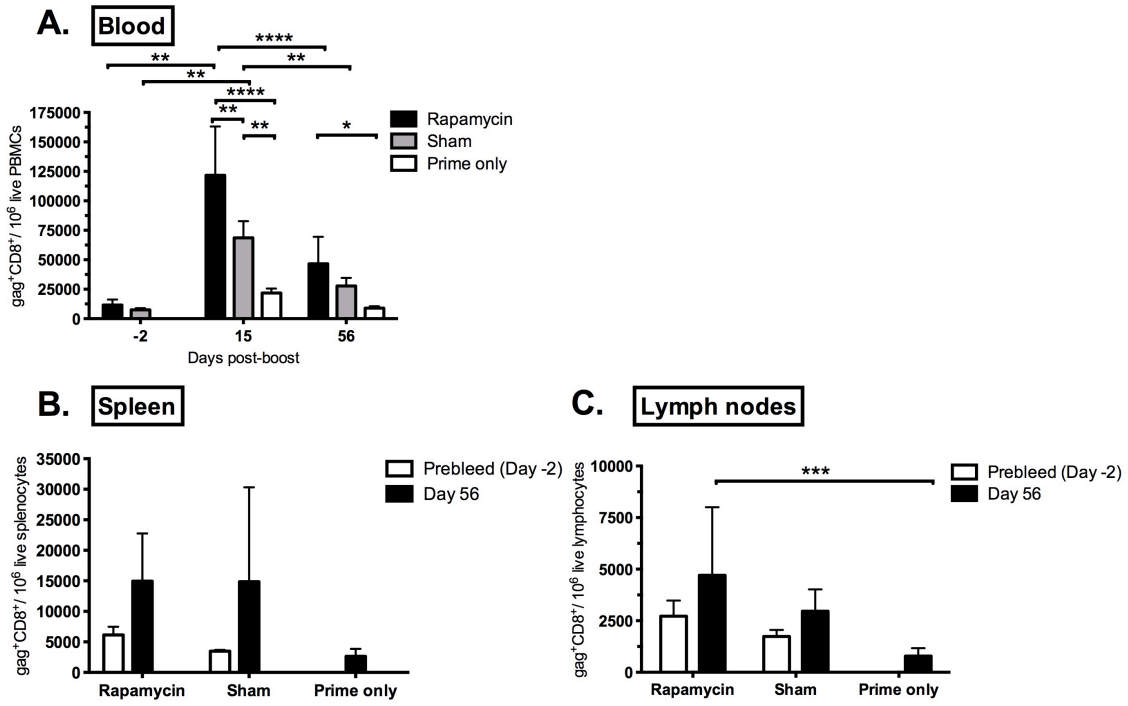

BALB/c mice treated with either rapamycin or sham were boosted with 10^{10} vp AdC7-HIVgag 12 weeks after first vaccination. A group of naïve mice was primed with this vaccine in order to serve as a control. Gag-specific $CD8^+$ T cell responses in blood **[A]** were measured 2 days prior to the boost and again at 15 and 56 days after the boost. In the spleen **[B]** and lymph nodes **[C]**, Gag-specific CD8+ T cell responses were measured 2 days prior to the boost and 56 days after the boost. Graphs show mean number of Gag-specific $CD8^+$ T cells identified by staining with the tetramer over 10^6 live lymphocytes ± SD. In the blood **[A]**, the rapamycin-treated group is indicated by the black bar, the sham-treated group is indicated by the grey bar, and the prime only group is indicated by the white bar. In spleen **[B]** and lymph nodes **[C]**, the white bar indicates the prebleed 2 days prior to boosting and the black bar indicates the day 56 post-boost time point.

Statistical significance was determined by 2-way ANOVA with Holm-Sidak correction for multiple comparisons. The following p-values were obtained: **[A]** Day 15: rapamycin vs. prime only: $p<0.0001$, sham vs. prime only: $p=0.0058$, rapamycin vs. sham: $p=0.0021$; Day 56: rapamycin vs. prime only: $p=0.0446$; Rapamycin: prebleed vs. day 15: $p=0.001$, day 15 vs. day 56: $p<0.0001$; Sham: prebleed vs. day 15: $p=0.002$ day 15 vs. day 56: $p=0.0028$; **[C]** Day 56: rapamycin vs. prime only: $p=0.0006$.

Significant differences are indicated by * for p-values ≤ 0.05-0.01, ** p-values < 0.01-0.001, *** p-values ≤ 0.001-0.0001, **** p-values < 0.0001. Lines show the comparison groups.

The effect of late rapamycin treatment of $CD8^+$ T cell responses to the transgene product of an Ad vector

Araki et al. demonstrated that limiting mTOR activity during the contraction phase accelerated $CD8^+$ T cell differentiation into the central memory compartment. To assess if inhibition of the mTOR pathway at a later stage of T cell activation following Ad immunization affected the transgene product-specific $CD8^+$ T cells' fate decisions, BALB/c mice were immunized IM with 10^{10} vp AdHu5-HIVgag and then treated daily from days 10 to 30 post immunization with either rapamycin or sham. Mice were bled or euthanized and Gag-specific $CD8^+$ T cells were measured at the time points indicated in **Figure 3.4A**. Gag-specific $CD8^+$ T cells from both the rapamycin- and sham-treated groups expanded in the blood, spleen, and lymph nodes, reaching a peak at 3 weeks in the spleen and lymph nodes and at 5 weeks in blood following immunization. Numbers of Gag-specific $CD8^+$ T cells then remained stable in blood but contracted in the spleen and lymph nodes. There was no significant difference in the overall magnitude of the Gag-specific $CD8^+$ T cell response in the two cohorts.

We measured expression of CD62L, CD127 and KLRG1 following immunization to determine if delaying rapamycin in relation to vaccination increased formation of Gag-specific central memory $CD8^+$ T cells. As shown in **Figure 3.4B,** we found that differences between the two groups were subtle and only reached significance for expression of CD127 and KLRG1 at some time points. Specifically $CD127^+$ Gag-specific $CD8^+$ T cells were more frequent in blood on day 21 while KLRG1 was differentially expressed in blood on day 10, in spleen on day 49 and in lymph nodes on days 21 and 49. Taken together, these results indicate that the delayed rapamycin treatment did not enhance memory differentiation.

Ad vector-induced $CD8^+$ T cells were tested following peptide stimulation *in vitro* for production of IFN-γ, TNF-α, and IL-2 in blood and spleen. MIP-1α was again only included for splenocytes. Rapamycin treatment only transiently increased numbers of cytokine-producing Gag-specific $CD8^+$ T cells in the blood on day 21 (**Figure 3.5A**). Otherwise, the delayed drug treatment did not affect the cytokine profile of Ad vector-induced $CD8^+$ T cells (**Figure 3.5B**), similar to **Figure 3.2B**.

At 12 weeks post-immunization both the rapamycin- and sham-treated groups were boosted with 10^{10} vp of AdC7-HIVgag. In all compartments, Gag-specific $CD8^+$ T cells from all groups expanded robustly following immunization (**Figure 3.6**). In the blood (**Figure 3.6A**) rapamycin treatment led to transiently higher numbers of Gag-specific $CD8^+$ T cells than sham treatment. Comparison of the fold increase of Gag-specific $CD8^+$ T cells revealed that Gag-specific $CD8^+$ T cells from rapamycin-treated mice had expanded more robustly (20.5-fold) than those from sham-treated mice (10.7-fold). In the spleen and lymph nodes there were no significant differences in numbers of Gag-specific $CD8^+$ T cells between the rapamycin- and sham-treated groups (**Figures 3.6B and 3.6C**), although each group boosted robustly and similarly. These results further support the notion that later rapamycin treatment did not enhance the quality of the induced the Gag-specific $CD8^+$ T cell response.

FIGURE 3.4. Later rapamycin treatment neither increases numbers nor alters phenotype of Gag-specific CD8$^+$ T cells.

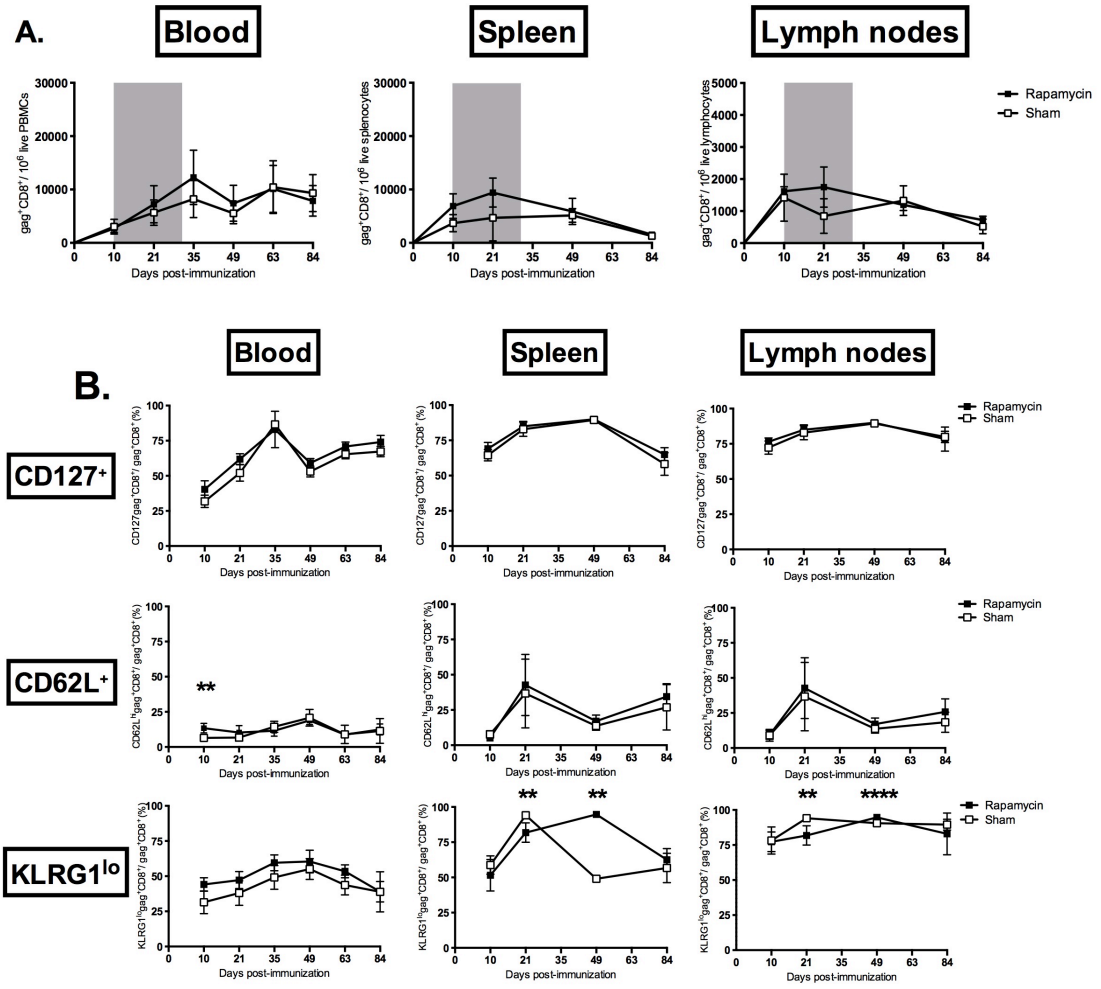

Groups of 5 BALB/c mice were immunized intramuscularly with 10^{10} vp AdHu5-HIVgag. 10 days after immunization and continuing until 30 days after immunization, one group was treated intraperitoneally (IP) with 75 µg/kg/day of rapamycin. As a control, the other group was IP injected with sham (0.1% DMSO in PBS) treatment given at 10 µL/g. Rapamycin-treated group is indicated by black boxes while sham-treated group is indicated by the white boxes. The grey area indicates the treatment phase. Significance between rapamycin- and sham-treated groups was determined using multiple t-tests with Holm-Sidak correction for multiple comparisons.

[A] All mice were bled for PBMCs or euthanized for splenocytes and lymphocytes at the indicated time points. Graphs show the mean number of Gag-specific CD8$^+$ T cells over 10^6 live cells ± SD.

[B] Shows the longitudinal phenotyping of Gag-specific CD8$^+$ T cells from indicated time points and tissues. Graphs show the mean frequency of Gag-specific CD8$^+$ T cells with the indicated phenotype (CD127$^+$, CD62L$^+$, or KLRG1^{lo}) over the total Gag-specific CD8$^+$ T cell response ± SD. The following p-values were obtained: Blood: CD62L$^+$: Day 10: p=0.00372; Spleen: KLRG1^{lo}: Day 21: p=0.0056, Day 49: p<0.0001; Lymph nodes: KLRG1^{lo}: Day 21: p=0.0056, Day 49: p=0.00529.

Significant differences are indicated by * for p-values ≤ 0.05-0.01, ** p-values < 0.01-0.001, *** p-values ≤ 0.001-0.0001, **** p-values < 0.0001. Lines show the comparison groups.

FIGURE 3.5. Later rapamycin treatment transiently increases cytokine production.

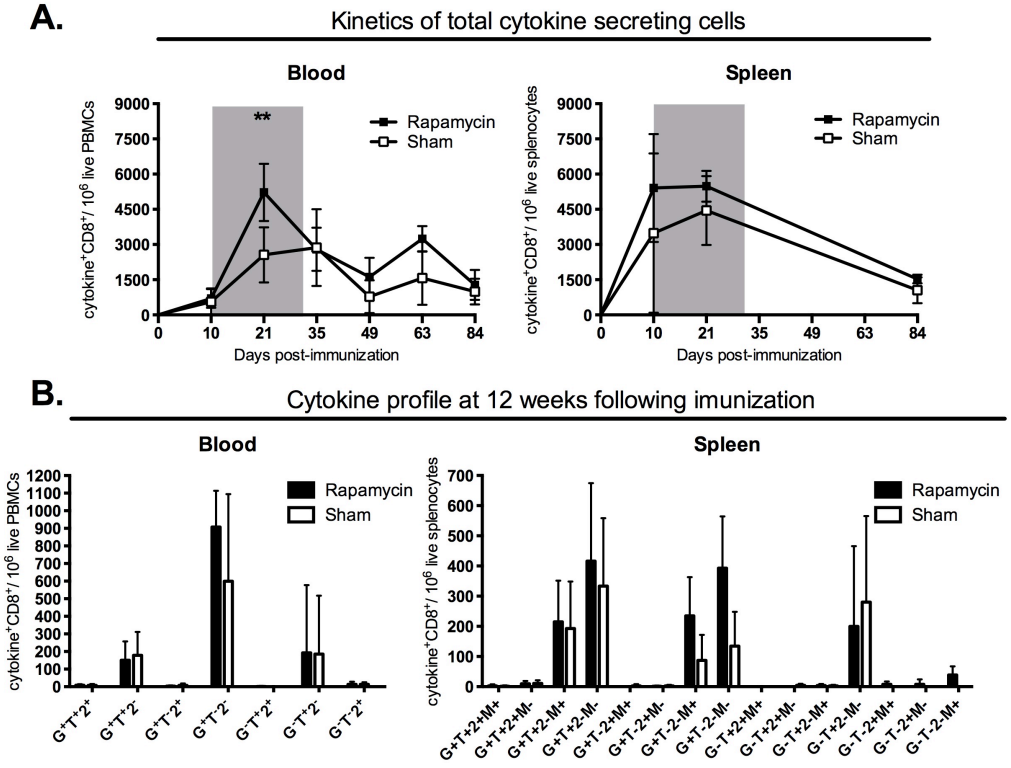

Shows the kinetics of total cytokine-producing cells **[A]** and the cytokine profile 12 weeks following immunization **[B]**. IFN-γ (G), TNF-α (T), and IL-2 (2) production was measured for PBMCs. IFN-γ, TNF-α, IL-2, and MIP-1α (M) production was measured for splenocytes. For determination of the kinetics, mice were bled or euthanized at the indicated time points and PBMCs or splenocytes were isolated, respectively. The lymphocytes were stimulated with either the Gag peptide AMQMLKETI or the equivalent amount of an irrelevant peptide to measure background stimulation. Line graphs show the mean number of cytokine producing cells following the subtraction of background stimulation and summation of Boolean gates used to determine the cytokine profile ± SD. Significance between rapamycin- and sham–treated groups was determined for each time point using multiple t-tests with Holm-Sidak correction for multiple comparisons. The following p-values were obtained: **[A]** Blood: Day 21: p=0.0078.

Significant differences are indicated by * for p-values ≤ 0.05-0.01, ** p-values < 0.01-0.001, *** p-values ≤ 0.001-0.0001, **** p-values < 0.0001. Lines show the comparison groups.

FIGURE 3.6. Later rapamycin treatment transiently improves recall response.

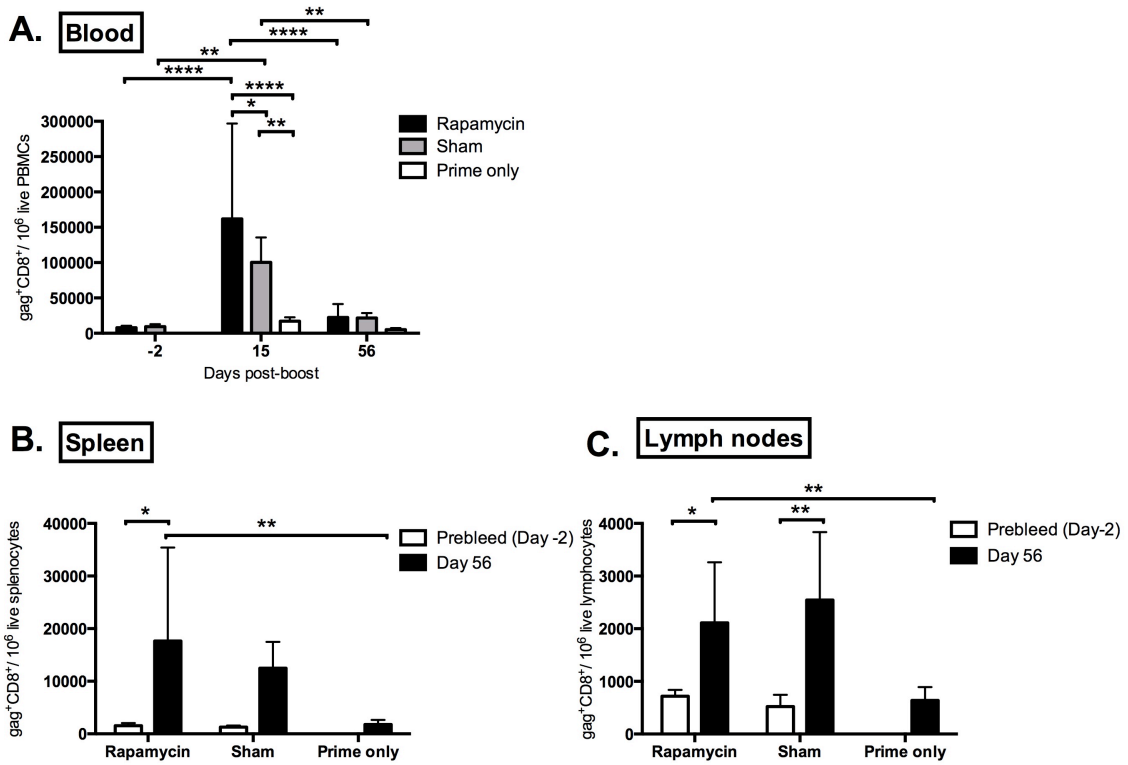

BALB/c mice treated with either rapamycin or sham were boosted with 10^{10} vp AdC7-HIVgag 12 weeks after first vaccination. A group of naïve mice was primed with this vaccine in order to serve as a control. Gag-specific $CD8^+$ T cell responses in blood **[A]** were measured 2 days prior to the boost and again at 15 and 56 days after the boost. In the spleen **[B]** and lymph nodes **[C]**, Gag-specific $CD8^+$ T cell responses were measured 2 days prior to the boost and 56 days after the boost. Graphs show mean number of Gag-specific $CD8^+$ T cells identified by staining with the tetramer over 10^6 live lymphocytes ± SD. In the blood **[A]**, the rapamycin-treated group is indicated by the black bar, the sham-treated group is indicated by the grey bar, and the prime only group is indicated by the white bar. In spleen **[B]** and lymph nodes **[C]**, the white bar indicates the prebleed 2 days prior to boosting and the black bar indicates the day 56 post-boost time point.

Statistical significance was determined by 2-way ANOVA with Holm-Sidak correction for multiple comparisons. The following p-values were obtained: **[A]** Rapamycin: Prebleed vs. Day 15: $p<0.0001$, Day 15 vs. Day 56: $p<0.0001$; Sham: Prebleed vs. Day 15: $p=0.007$, Day 15 vs. Day 56: $p=0.0099$; Day 15: prime only vs rapamycin: $p<0.0001$, prime only vs. sham: $p=0.0084$, rapamycin vs. sham: $p=0.0459$ **[B]** Rapamycin: Prebleed vs. Day 56: $p=0.0179$; Day 56: rapamycin vs. prime only: $p=0.0056$ **[C]** Rapamycin: prebleed vs. day 56: $p=0.0226$; Sham: prebleed vs. day 56: $p=0.0029$; Day 56: $p=0.0071$.

Significant differences are indicated by * for p-values ≤ 0.05-0.01, ** p-values < 0.01-0.001, *** p-values ≤ 0.001-0.0001, **** p-values < 0.0001. Lines show the comparison groups.

DISCUSSION

mTOR was elegantly demonstrated to play a critical role in memory $CD8^+$ T cell differentiation. Araki et al. demonstrated that limiting mTOR activity at different phases of the $CD8^+$ T cell response enhanced the induction of memory cells [154]. Specifically, low doses of rapamycin given during the T cell expansion phase to inhibit mTOR activity increased numbers of memory cell precursors by increasing expression of Bcl-2, an anti-apoptotic protein, ultimately leading to their increased survival during the contraction phase. Consistent with this, low dose rapamycin treatment was demonstrated to dramatically decrease apoptosis following immunization with a recombinant poxvirus [188]. Additionally, Araki et al. demonstrated that low doses of rapamycin given during the contraction phase accelerated differentiation into central memory. These results suggest that rapamycin may be a beneficial vaccine adjuvant to enhance memory differentiation.

The current study was performed to test the potential of mTOR inhibition to increase central memory development of transgene product-specific $CD8^+$ T cells induced by an Ad vector-based vaccine. The results presented here are partially in contrast with those described above. As expected, treatment with low doses of rapamycin during the early expansion phase following Ad immunization resulted in higher transgene product-specific $CD8^+$ T cell numbers at the peak of the response, but the effect was transient. Additionally, low dose rapamycin treatments given later in the response failed to enhance transgene product-specific $CD8^+$ T cell differentiation into central memory. These differences could possibly be due to the differences in timing of rapamycin treatment with the kinetics of the induced $CD8^+$ T cells. In the Araki et al study early rapamycin treatments coincided with the entire T cell expansion phase and ended at the peak response and later rapamycin treatments coincided with the entire contraction phase beginning at the peak response. However, the early rapamycin treatments given in the study presented here only coincided with about half of the expansion phase and the later treatments covered the late expansion and early contraction phases.

The differences observed in these studies could also be due to the nature of the viral models each used. The Araki et al. study infected mice with lymphocytic choriomeningitis virus (LCMV). As an acutely infecting virus, this pathogen is cleared completely from the host within 8 days [139]. TCR/CD28 signaling subsides as the virus is cleared and mTOR activity subsequently subsides, allowing responding T cells to become more quiescent and differentiate. On the other hand, adenoviruses, whether naturally acquired [65] or rendered replication-defective [123], establish persistent infection in activated T cells. Studies using Ad vectors carrying transgenes under the control of strong and ubiquitous promoters have revealed that Ad vectors remain transcriptionally active at low levels [123]. The continued presence of transgene product in turn maintains a pool of activated effector and effector memory transgene product-specific $CD8^+$ T cells and delays their differentiation into central memory cells. It is unknown how persistent antigen produced by adenovirus transduced T cells maintains activation of other T cells. Following vaccination, Ad vectors induce transgene product-specific $CD8^+$ T cells primarily through cross-presentation of transgene product by antigen presenting cells (APC) [189] rather than directly infecting them. During Ad persistence, $CD8^+$ T cells could be stimulated directly by the T cells harboring persistent vector or by cross-presentation of transgene product when transduced cells eventually become apoptotic. Regardless, as TCR stimulation continues mTOR would be expected to be active to some degree.

Much of our knowledge of the role mTOR plays in $CD8^+$ T cell differentiation comes from *in vitro* studies and mouse models with various members of the PI3K/Akt/mTOR pathway knocked out. Only a few studies have examined this pathway in the context of acute viral infections. Even less is known about the role of mTOR in $CD8^+$ T cells during persistent infections. It appears that mTOR phosphorylation gradually declines during persistent infection with LCMV clone 13 but, importantly, phosphorylation is not ablated [190], which could reflect continued TCR stimulation. Transplant recipients persistently infected with CMV who were treated with the rapamycin analog everolimus showed a specific increase in the magnitude of CMV-specific $CD8^+$ effector and effector memory T cells without affecting their quality and polyfunctionality [191], consistent with what was presented here. A recent study in which rapamycin

was administered for 35 days following vaccination with Ad revealed that the effector memory population of transgene product-specific $CD8^+$ T cells was enhanced in this model [192]. This response was magnified and central memory development was enhanced only when additional co-stimulation was provided through OX40 agonism. The results presented here are not in complete agreement with their report, which could be due to differences in the study design, in particular the vector dose. Using a dose 100 –fold lower than was used in the study presented in this chapter, rapamycin treatment alone increased the formation of MPECs. It could be argued that increase in memory differentiation was due to lower antigenic load present during the priming that prevented the establishment of a persisting reservoir. Indeed, in a later experiment they use the same immunization dose used here and the combined treatment did not increase central memory development. However, both doses of Ad vector and each treatment regimen selectively increased the proportion of effector memory cells. The results presented here (**Figure 3.1**) indicate that rapamycin treatment increases, albeit transiently, the absolute number of effector and effector memory cells without shifting the subset distribution. During the periods of rapamycin treatment, limiting mTOR activity may have favored the formation of memory cells, as a transient and subtle increase in $CD127^+$ cells was observed following early rapamycin treatment. However, this was expected to be transient once rapamycin treatment was discontinued because continued stimulation from persistent antigen could recall transgene product-specific $CD8^+$ T cells. This would ultimately increase the overall size of the response without changing the makeup of the pool. Consistent with the idea that persistent transgene expression prevents rapamycin treatment from enhancing central memory development, extinguishing transgene expression from an Ad vector during the combined rapamycin and OX40 treatment enhanced central memory development [192].

In conclusion, the studies presented here demonstrate that rapamycin treatment following immunization with a vector that is known to persist at low levels does not enhance $CD8^+$ T cell differentiation into central memory but increases the number of activated effector cells. Further elucidation of the role that mTOR plays in regulating T cell metabolism during chronic infections is necessary.

MATERIALS AND METHODS

Mice, immunizations, and rapamycin treatments

Groups of BALB/c mice were immunized intramuscularly (IM) with 10^{10} vp of the AdHu5-HIVgag vector diluted in 100 µL of sterile PBS. In one series of experiments, groups of mice received daily intraperitoneal (IP) injections of 75 µg/kg rapamycin (Sigma-Aldrich, St. Louis, MD) diluted in 0.1% DMSO in sterile PBS for 10 days following immunization [154]. In a second series of experiments, groups of mice received daily IP injections of 75 µg/kg rapamycin from day 10 after immunization until day 30 after immunization. In both series of experiments, control mice received daily IP injections of 10 µL/g 0.1% DMSO in PBS for the indicated length of time. In one experiment, both groups of mice (control- and rapamycin-treated) received a second immunization with 10^{10} vp AdC7-HIVgag 12 weeks after the primary immunization with the AdHu5 vector. A group of naïve mice were immunized concurrently with 10^{10} vp of AdC7-HIVgag as a control.

Tetramer staining

Tetramer staining was preformed by staining cells in PBS with an APC-labeled tetramer against the immunodominant MHC class I H-2K^d restricted epitope of Gag (AMQMLKETI). Additionally, cells were stained with PerCP-Cy5.5-labeled anti-CD8, PE-labeled anti-KLRG1 (Southern Biotech, Birmingham, AL), anti-CD62L (BD Biosciences, Franklin Lakes, NJ), Alexa700-labeled anti-CD44, anti-CD127 (eBioscience, San Diego CA), PE-Cy7-labeled anti-CD44 (eBioscience), and PacBlue-labeled anti-CD62L, anti-CD127 (eBioscience). Unless otherwise indicated, antibodies are from Biolegend (San Diego, CA). Antibodies labeled with identical fluorophores were used in separate samples. All samples included a dye that labels dead cells. Staining was preformed for 30 min at 4ºC. Cells were fixed with BD fixative after staining.

Intracellular cytokine staining (ICS)

In order to detect a Gag-specific $CD8^+$ T cell response, PBMCs and splenocytes were stimulated in the presence of Golgi Plug (BD Biosciences) for 5 hours at 37 °C with 1.25 µg/mL of Gag peptide, AMQMLKETI, or with 1.25 µg/mL of a non-specific peptide, WIZX-2 from rabies virus, to measure background stimulation. Peptides were prepared in DMEM containing 2% mixed lymphocyte culture media (MLC). Following stimulation and surface staining, Cytofix/Cytoperm (BD Biosciences) was used to permeabilize the cells, which were subsequently stained intracellularly with PacBlue-labeled anti-IFNγ, FITC-labeled anti-TNFα (BD Bioscience), Alexa700-labeled anti-IL-2 (BD Bioscience); splenocytes were additionally stained with APC-labeled anti-MIP-1α (R&D Systems; Minneapolis, MN). Staining at both steps was performed as described in the previous section.

Data acquisition and analysis

All samples were collected on a BD-LSR II and analyzed using FlowJo software. For tetramer staining, numbers of Gag-specific $CD8^+$ T cells were determined as follows. Acquired lymphoid cells were first gated to remove doublets and dead cells, then were gated on $CD8^+$ T cells. The remaining cells were plotted as tetramer (tet) compared to CD44. Numbers were determined by normalizing the numbers of double positive (tet^+CD44^+) cells to total live cells. Data are shown as tet^+CD8^+ T cells/10^6 PBMCs, splenocytes, or lymphocytes, depending on the compartment presented. Additionally, tet^+CD44^+ cells were phenotyped for the markers described. A gate on the $CD44^{lo}$ $CD8^+$ T cells served an internal, naïve control for phenotyping. For analysis of ICS, live $CD8^+$ T cells were gated as described above, then cells positive for each cytokine were gated. Boolean gates were generated to determine cytokine profile in each sample. Numbers of cells acquired for each cytokine and combination of cytokines were first normalized to total live cells per 10^6 PBMCs or splenocytes. The background obtained by stimulation with negative peptide was then subtracted from the samples stimulated with the positive peptide. Data are represented as $cytokine^+CD8^+/10^6$ PBMC or splenocytes, depending on compartment presented.

Statistical analysis

Each experiment was preformed with groups of 5 mice, unless otherwise indicated, and repeated 3 times. Statistical significance was determined using either multiple t-tests with Holm-Sidak correction for multiple comparisons or 2-way ANOVA with Holm-Sidak correction for multiple comparisons.

CHAPTER 4

ANTIGEN-EXPERIENCED $CD8^+$ T CELLS MAINTAIN THE $CD8^+$ T CELL RESPONSE FOLLOWING ADENOVIRUS IMMUNIZATION

ABSTRACT

Persistent adenoviral vectors induce transgene-product $CD8^+$ T cells responses that fail to contract and are phenotypically heterogeneous. Studies of other persistent viruses have demonstrated that asynchronous priming of naïve $CD8^+$ T cells throughout infection is a mechanism by which $CD8^+$ T cell pools can be maintained and remain functional during persistent infection. Alternatively, functional antigen-experienced $CD8^+$ T cells may respond to persistent antigen and thus replenish the response. Here we designed a series of adoptive transfer experiments to distinguish between these two possibilities. Our results indicate that naïve $CD8^+$ T cells are primarily not responsible for maintaining the transgene product-specific $CD8^+$ T cell response. Instead it is likely that persisting transgene product recalls antigen-experienced cells back into the response.

INTRODUCTION

Vectors based on adenovirus (Ad) are being extensively developed as vaccine platforms against numerous diseases. These highly immunogenic vectors have received such attention in part due to their ability to induce potent $CD8^+$ T cell responses. $CD8^+$ T cells are important mediators of immune responses and are indispensible in the control of viral infections. The $CD8^+$ T cell response following infection with a pathogen that is cleared from the host, termed an acute infection, is composed of three distinct stages [110]. The first phase is termed the expansion phase and occurs following antigenic encounter and activation. During this stage, a $CD8^+$ T cell undergoes vast and rapid clonal expansion. Such rapid expansion requires that the cells alter key metabolic pathways, including the PI3K-Akt-mTOR pathway, to promote the synthesis of raw materials needed to make new cells [105]. Armed with antiviral cytokines, such as IFN-γ, and cytolytic effector molecules, these newly generated cells traffic to inflamed tissues in the periphery to carry out their task of targeting and killing infected cells. After the pathogen is cleared from the host, the $CD8^+$ T cell response reaches a maximal peak that delineates the next stage of the response, contraction. At the peak of this response, the $CD8^+$ T cell pool is largely made up of short-lived effector cells (SLEC) but some memory precursor effector cells (MPEC) can be identified [114,121]. During the contraction phase, SLEC will die through apoptosis, resulting in a 90-95% reduction of the peak population. The final phase of the primary $CD8^+$ T cell response is memory differentiation. The MPEC that survived the contraction phase contribute to this population, which can be composed of effector memory and central memory cells that preferentially home to the periphery and lymph nodes, respectively. These cells further differentiate and are maintained through self-renewal in the absence of antigen.

However, not all pathogens are acutely infecting and instead establish persistent infections that are not cleared from the host. Much of our knowledge of the $CD8^+$ T cell response during persistent infection comes from models of highly pathogenic, chronically infecting mouse lymphocytic choriomeningitis virus (LCMV) clone 13. These studies demonstrate that responding $CD8^+$ T cells are significantly impaired and undergo functional exhaustion or are deleted from the

T cell repertoire [138,193]. Functional exhaustion is characterized by the hierarchical loss of T cell functions [110]. As the cells become progressively more exhausted, the ability to produce IL-2 is the first to be lost followed by TNF-α and then IFN-γ. Additionally, they gradually lose their ability to kill target cells and cannot be recalled robustly following secondary antigen encounter.

Adenoviruses fall into the group pathogens that establish persistent infections. Adenoviruses establish a reservoir in the lymphatic tissues and the genome is especially enriched in T cells [65,194]. While the viral genome can be isolated tissues following their surgical removal, infectious virus cannot be recovered from culturing the tissues [2,58]. However, *in vitro* stimulation with mitogens causes virus reactivation and replication [61]. As such, it was determined that Ad establishes a latent infection with intermittent periods of reactivation.

Adenoviral vectors also persist *in vivo.* Following intramuscular vaccination, the genome is enriched in activated $CD8^+$ T cells [123]. Importantly, low levels of transgene expression can be detected for a year after immunization [123]. Many have demonstrated that following immunization the transgene product-specific $CD8^+$ T cell response fails to contract [140,195]. Additionally, the $CD8^+$ T cell population that survives past the peak response to transition into the memory phase consists effector and effector memory cells. These qualities of the $CD8^+$ T cell response are consistent with those from other persistent viral infection models [152]. Indeed there has been a report that suggests the Ad-induced $CD8^+$ T cell response becomes exhausted over time [196]. However, exhaustion and functional impairment are directly linked to the antigen load that persists during chronic infection [137,196,197]. The LCMV clone 13 model, from which we have derived much information about T cell exhaustion, establishes a persistent infection characterized by high levels of viremia [198], which progressively pushes the anti-viral $CD8^+$ T cell response toward extreme functional impairment [193,197,198]. In contrast, adenovirus establishes a latent infection with periods of reactivation. Replication-deficient vectors follow a similar pattern. Transgene expression can be detected long after immunization, although it is not consistently expressed [123]. Therefore, the induced antigen-specific $CD8^+$ T cell responses are not constantly exposed to high levels of antigen and likely form functional memory responses that may be boosted upon antigen re-encounter. Indeed, transgene product-specific $CD8^+$ T cells gradually

accumulate in the lymph nodes and reacquire both IL7R-α (CD127) and CD62L many weeks after immunization. Further, Ad-induced $CD8^+$ T cells are polyfunctional and undergo robust recall responses following secondary exposure to antigen [97,123,130,195].

While persistent transgene expression is responsible for maintaining the transgene product-specific $CD8^+$ T cell response following Ad immunization, it is unknown how it does so. There are two models that may explain how the memory population may be maintained during latency. The first is that naïve virus-specific $CD8^+$ T cells are continuously recruited into the response by viral antigens expressed during persistence, thus replenishing the population as memory cells decay. This asynchronous priming results in a highly heterogeneous virus-specific $CD8^+$ T cell population with variable CD62L expression [199]. Such variability is generated because the individual cells composing the overall population would be primed in different contexts depending on when priming occurred during the persistent infection. This also would cause functional variability within the population. $CD8^+$ T cells primed during the acute phase of the infection can gradually progress toward exhaustion while those primed past the acute phase are more functional [200]. Asynchronously primed $CD8^+$ T cell responses are common in persistent infection models, including polyoma virus [201], γ-herpesviruses [202], and to some extent CMV [203]. Alternatively, the transgene product-specific $CD8^+$ response induced following Ad immunization could be maintained by existing memory cells that are recalled when re-stimulated with persistently expressed transgene product. This study was designed to distinguish between these two models. The results presented here suggest that naïve $CD8^+$ T cells are primarily not responsible for the maintenance of the $CD8^+$ T cell pool following vaccination.

RESULTS

Antigen-specific $CD8^+$ T cells continue to proliferate well after immunization

The transgene product-specific $CD8^+$ T cell response following immunization fails to contract. In order to determine if the cells that remain continue to proliferate, a bromodeoxyuridine (BrdU) incorporation assay was performed. Briefly, C57BL/6 mice were immunized with 10^{11} vp of

an E1-deleted adenoviral vector based on chimpanzee serotype 68 expressing influenza nucleoprotein fused to GFP by SIINFEKL, the MHC class I $H2k^b$ restricted immunodominant epitope of ovalbumin (AdC68-NPOVAGFP). Mice were euthanized ten days, one month, and five months after immunization. 72 hours prior to euthanasia, mice were pulsed intraperitoneally (IP) with 2 mg/mL BrdU and the drinking water was supplemented every 24 hours with 0.8 mg/mL BrdU. Upon euthanasia, lymphocytes were isolated from blood, spleen, and pooled popliteal and inguinal lymph nodes. OVA-specific $CD8^+$ T cells were measured using a MHC class I tetramer against SIINFEKL. **Figure 4.1** shows the frequency of OVA-specific $CD8^+$ T cells that incorporated BrdU during the three days of treatment, as well as the frequencies of antigen-experienced $CD8^+$ T cells ($CD44^{hi}$) and naïve $CD8^+$ T cells ($CD44^{lo}$) that incorporated BrdU. During the expansion phase following immunization dramatic incorporation of BrdU in the OVA-specific $CD8^+$ T cells was observed in all tissues. Additionally, high frequencies of other antigen experienced $CD8^+$ T cells ($CD44^{hi}$) had incorporated BrdU. This was likely because there are other antigens besides SIINFEKL present in the vaccine that triggered a T cell response. Taken together, the high rates of BrdU incorporation reflect the massive amount of proliferation these cells undergo following their induction. By normalizing the percentage of BrdU incorporation to that of the $CD44^{hi}$ cells, it can be seen that the OVA-specific $CD8^+$ T cells proliferate more robustly than the general $CD44^{hi}$ population. One month after immunization, BrdU incorporation was reduced in all tissues but was still elevated. The frequency of OVA-specific $CD8^+$ T cells that had incorporated BrdU at this time typically ranged between 10-15%, except in the lymph nodes, where about 50% continued to incorporate BrdU (**Figure 4.1C**). In all tissues only 10% of the $CD44^{hi}$ cells incorporated BrdU. Five months after immunization, BrdU incorporation was further reduced in all tissues but continued to be detected in the lymph nodes, where about 10% of OVA-specific $CD8^+$ T cells incorporated BrdU (**Figure 4.1C**). While the frequency of incorporation was not particularly high, the OVA-specific cells still proliferated about 3.5 times more than $CD44^{hi}$ cells. Taken together these results suggest that following induction with an Ad-based vaccine, transgene product-specific $CD8^+$ T cells proliferate robustly and this proliferation continues for at least five months after immunization, particularly in the lymph nodes.

FIGURE 4.1. Transgene product-specific $CD8^+$ T cells continue to proliferate months after induction.

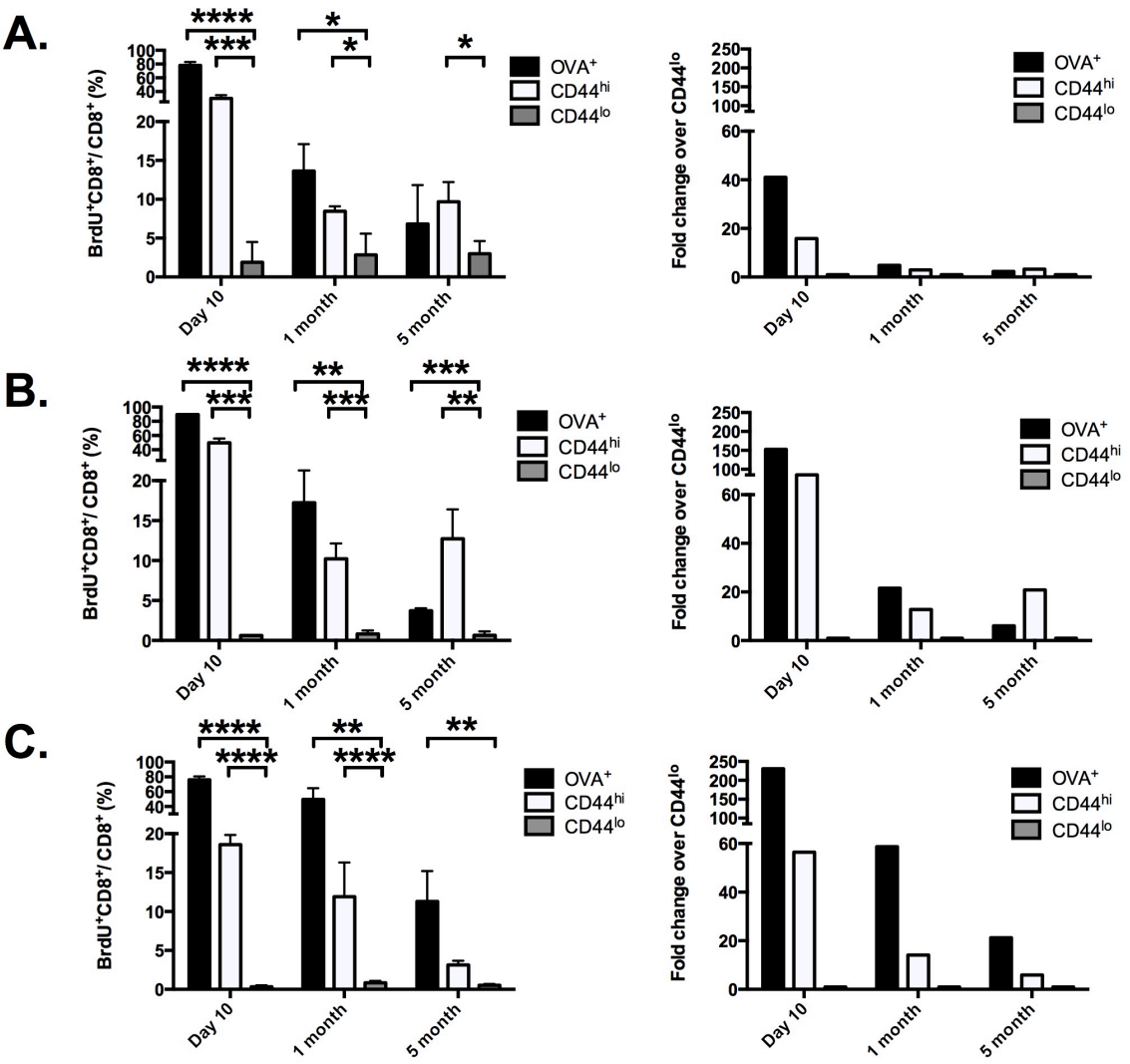

Shows Bromodeoxyuridine (BrdU) incorporation by $CD8^+$ T cells isolated from blood **[A]**, spleen **[B]**, and lymph nodes **[C]**. Briefly, C57BL/6 mice were immunized with 10^{11} vp of AdC68-NPOVAGFP and euthanized at the indicated times. 72 hours prior to euthanasia, mice were pulsed with 2mg/mL BrdU and drinking water was supplemented with 0.8 mg/mL BrdU. Frequencies of OVA-specific $CD8^+$ T cells that had incorporated BrdU were determined from individual mice by staining with an OVA-specific tetramer. As controls, BrdU incorporation was analyzed on antigen-experienced ($CD44^{hi}$) cells and naïve ($CD44^{lo}$) cells. Data are represented as mean frequency (%) ± standard deviation (SD) of $BrdU^+CD8^+$ per $CD8^+$. The second column of charts show the data represented as fold change in relation to $CD44^{lo}$ BrdU incorporation. Frequencies were compared to $CD44^{lo}$ population and were compared using multiple t-tests by Holm-Sidak method. The following p values were obtained: **[A]** Day 10: OVA: $p<0.0001$, $CD44^{hi}$: $p=0.0007$; 1 month: OVA: $p=0.0135$, $CD44^{hi}$: $p=0.0262$; 5 month: $CD44^{hi}$: $p=0.0185$; **[B]** Day 10: OVA: $p<0.0001$, $CD44^{hi}$: $p=0.0001$; 1 month: OVA: $p=0.002$, $CD44^{hi}$: $p=0.001$; 5 month: OVA: $p=0.0008$, $CD44^{hi}$: $p=0.0048$; **[C]** Day 10: OVA:$p<0.0001$, $CD44^{hi}$: $p<0.0001$; 1 month: OVA: $p=0.0049$, $CD44^{hi}$: $p<0.0001$; 5 month: OVA: $p=0.0089$. Significant differences are indicated by * for p-values ≤ 0.05-0.01, ** p-values < 0.01-0.001, *** p-values ≤ 0.001-0.0001, **** p-values < 0.0001. Lines show the comparison groups.

Naïve cells fail to respond to low-levels of persistent antigen following adenoviral immunization

Studies of other persistent infections have revealed that the $CD8^+$ T cell pool that persists during infection is made up of asynchronously primed naïve T cells [201,204]. In order to determine if naïve T cells proliferate in response to low-levels of transgene that persist following immunization, 3.14×10^6 naïve $Thy1.1^+$ $CD8^+$ T cells were isolated from the spleen and adoptively transferred into congenic $Thy1.2^+$ C57BL/6 mice that had been immunized 3 weeks earlier with either 10^{11} vp AdC68-NPOVAeGFP or 10^{11} vp AdC7-HIVgag, as a negative control. Mice were bled at the indicated times and the number of transferred OVA-specific $CD8^+$ T cells was determined by staining with a MHC class I tetramer specific to SIINFEKL and an antibody to Thy1.1 to distinguish donor from host cells. As shown in **Figure 4.2A**, in general naïve cells did not expand following transfer into immunized mice. In a notable exception, naïve cells transferred into one mouse not only engrafted but also robustly expanded and persisted for many months after transfer (**Figure 4.2B**).

Such disparate results between the one animal and the others may indicate that insufficient naïve precursors specific to OVA were transferred into the four mice in which naïve $CD8^+$ T cells did not expand. The precursor frequency of naïve $CD8^+$ T cells specific to a given antigen is rare. Estimates vary from epitope to epitope but generally range from as low as 1 precursor per million naïve $CD8^+$ T cells to ~80 precursors per million naïve $CD8^+$ T cells [205,206]. The frequency of $CD8^+$ T cells specific to SIINFEKL (OVA) bound to $H2k^b$ was estimated to be approximately 1 cell for every 150,000 $CD8^+$ T cells, which translates into approximately 130 cells within the total $CD8^+$ T cell population from the lymph nodes and the spleen [207]. Therefore, it is possible that the number of naïve OVA-specific $CD8^+$ T cells transferred ranged from three cells, on the lower end of the spectrum, to twenty cells at the higher end of the spectrum per mouse. As the size of the precursor population affects the magnitude of the primary response [207,208] and because it was possible that OVA-specific $CD8^+$ T cell precursors were not transferred, it was important to determine if sufficient numbers of naïve OVA-specific $CD8^+$ T cells were transferred.

To this end, 3.14 x 10^6 naïve Thy1.1$^+$ CD8$^+$ T cells were transferred via tail vein injection into naïve Thy1.2$^+$ C57BL/6 mice. After 18 hours, mice were immunized with either 10^{11} vp AdC68-NPOVAGFP or 10^{11} vp AdC68-rab.gp, as a negative control. The donor OVA-specific response was measured in the blood two weeks later. The donor OVA-specific CD8$^+$ T cells expanded very robustly following immunization (**Figure 4.2C**). This observation indicates that sufficient numbers of naïve precursors were transferred in order to observe a measurable response. Therefore, these results suggest that the antigenic load that persists three weeks after immunization with an adenovirus-based vaccine in general does not suffice to prime a *de novo* CD8$^+$ T cell response.

FIGURE 4.2. Naïve transgene product-specific CD8$^+$ T cells generally do not respond to persistent transgene product.

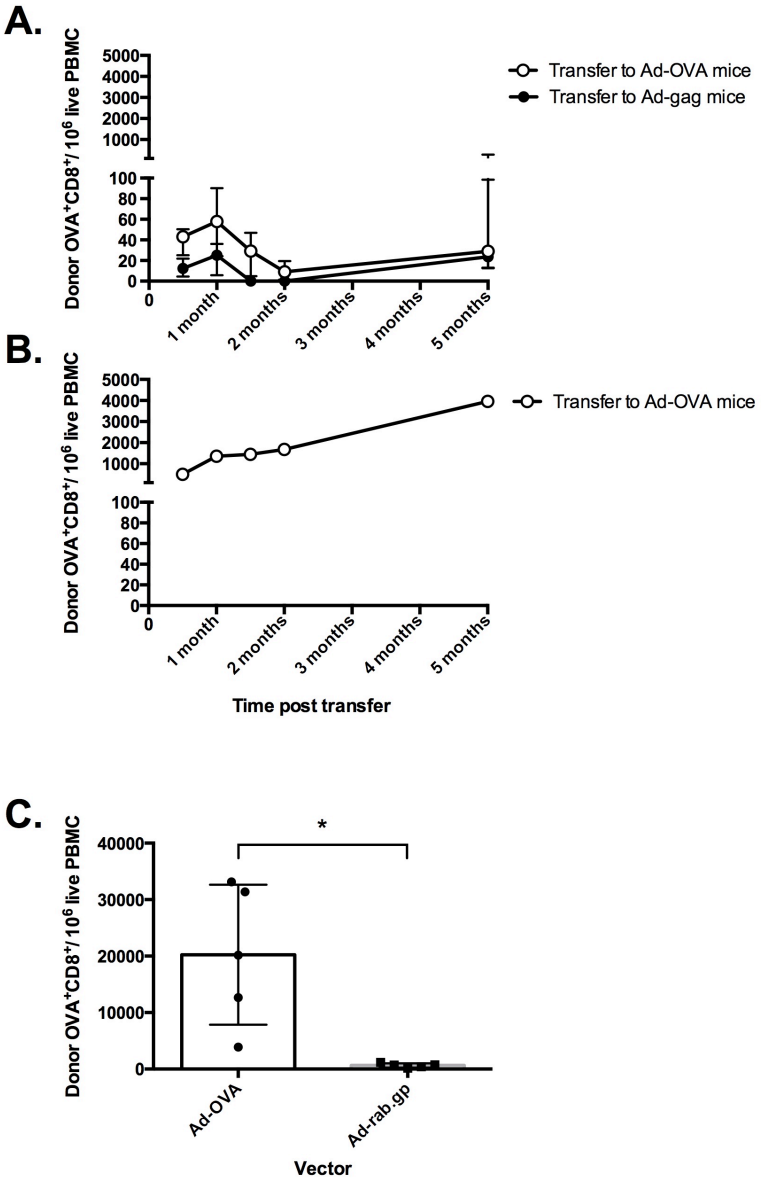

Groups of Thy1.2$^+$ C57BL/6 mice were immunized with 10^{11} vp AdC68-NPOVAGFP or 10^{11} vp AdC7-HIVgag, as a negative control. Three weeks later, 3.14 x 10^6 naïve congenic (Thy1.1$^+$) CD8$^+$ T cells were adoptively transferred via tail vein injection into each group. Mice were bled at the indicated time points for **[A]** and **[B].** Figure **[B]** shows a single mouse with exceptionally numbers of high donor cells. Frequencies of donor-specific (Thy1.1$^+$) OVA-specific CD8$^+$ T cells were determined by staining with an OVA-specific tetramer. Data for **[A]** and **[B]** are represented as mean numbers of Thy1.1$^+$ OVA$^+$ CD8$^+$ T cells per 10^6 live PBMCs. Lines in **[A]** represent SD. **[C]** shows that sufficient naïve precursors specific to OVA were transferred in **[A]** and **[B].** Briefly, groups of Thy1.1$^+$ C57BL/6 mice were adoptively transferred with 3.4 x 10^6 naïve congenic (Thy1.2$^+$) CD8$^+$ T cells. 18 hours later, each group was immunized with 10^{11} vp of AdC68-NPOVAGFP or 10^{11} vp AdC68-rab.gp. Mice were bled 2 weeks later and OVA-specific CD8$^+$ T cells were determined. Data shown for each plot is represented as mean $\pm$ SD. Significance was determined by unpaired t-test resulting in a p-value of 0.0241.

Antigen experienced cells continue to expand in response to low-level of persistent transgene product

The antigenic load that persists three weeks following immunization with an adenoviral vector is not enough to prime a *de novo* $CD8^+$ T cell response. Therefore, it is likely that antigen-experienced cells are recalled when they encounter persistent antigen. To further investigate if antigen-experienced cells respond to the low levels of persistent antigen, we transferred antigen-experienced $CD8^+$ T cells using the same protocol as described above. Briefly, C57BL/6 $Thy1.1^+$ mice were immunized IP with 10^7 PFU of vaccinia virus expressing the NPOVAGFP transgene (vac-OVA). These mice were euthanized one week after immunization, which coincides with the peak of the OVA-specific $CD8^+$ T cell response. At the time of euthanasia, splenocytes were isolated, $CD8^+$ T cells were negatively selected and then 3.14 x 10^6 cells were transferred via tail vein injection into congenic ($Thy1.2^+$) C57BL/6 mice that were immunized three weeks earlier with 10^{11} vp AdC68-NPOVAGFP or, as a negative control, 10^{11} vp AdC7-HIVgag. Mice were bled at the indicated times and the donor ($Thy1.1^+$) OVA-specific $CD8^+$ transferred T cell response was measured.

Figure 4.3 shows the OVA-specific $CD8^+$ T cell responses of donor $CD8^+$ T cells that were transferred 1 week after their induction with vac-OVA. OVA-specific $CD8^+$ T cells transferred into Ad-gag mice engrafted and persisted through the course of the experiment without any measurable expansion. However, the opposite was observed following transfer into Ad-OVA immunized mice. Over the course of eight weeks, the transferred cells steadily expanded, reaching approximately 300 cells per 10^6 live PBMCs (**Figure 4.3A**). Several months after transfer, the donor cell numbers showed variation. Numbers from 3 mice were largely stable but remained elevated. However, donor OVA-specific $CD8^+$ T cells in two Ad-OVA immunized mice continued to proliferate extensively until about 8 months after transfer. These results indicate that antigen-experienced transgene product-specific $CD8^+$ T cells can be maintained and further respond to low-levels of persistent transgene expression for many months.

Low levels of persistent antigen maintains an effector-like phenotype

In order to measure the consequences of long-term stimulation with a low-level antigen on the fate of the transferred cells, expression of CD62L and CD127 were measured on OVA-specific $CD8^+$ T cells circulating in blood eight weeks following transfer into Ad-OVA or Ad-gag immunized mice. OVA-specific $CD8^+$ T cells transferred into Ad-gag immunized mice were $CD62L^{hi}$ and had CD127 expression that was comparable to naïve cells (**Figure 4.4A**), indicating that these cells had rested down and transitioned into memory. On the other hand, OVA-specific $CD8^+$ T cells transferred into the Ad-OVA mice were predominantly $CD62L^{lo}$ with CD127 expression also comparable to naïve cells (**Figure 4.4A**). KLRG1 was included at a later time point to measure for stimulation history. At the peak response eight months after transfer, the transferred OVA-specific $CD8^+$ T cells largely remained $CD62L^{lo}$. However, they had higher levels of CD127 than naïve cells. Taken together, these three markers indicate that these cells are maintained in an effector memory phenotype. Supporting the notion that the expansion observed (**Figure 4.3A**) is due to continuous antigenic stimulation, the transferred OVA-specific $CD8^+$ T cells were predominantly $KLRG1^{hi}$, which reflects stimulation history and may indicate that these cells are reaching a point after which they may no longer continue to divide.

$CD8^+$ T cells responding to chronic infections are at risk of losing effector functions. This is characterized by progressive loss of ability to produce multiple cytokines. IL-2 production is the most sensitive to chronic stimulation and, as such, is the first cytokine to be lost. This is followed by loss of TNF-α production and, upon exhaustion, IFN-γ production is also lost [209]. Persistent transgene product expression appears to lead to the continued stimulation of antigen-experienced transgene product-specific $CD8^+$ T cells (**Figure 4.3**). There has been some debate over whether or not adenovirus vaccination drives responding $CD8^+$ T cells toward some degree of exhaustion [140,196]. Therefore, in order to test the functionality of antigen-experienced cells in the presence of low levels of persistent transgene product, intracellular cytokine staining was performed. Briefly, $Thy1.1^+$ C57BL/6 mice were immunized IM with 10^{11} vp AdC68-NPOVAGFP or 10^{11} vp AdC7-HIVgag, as a negative control. Three weeks later, $CD8^+$ T cells from congenic $Thy1.2^+$ C567BL/6 mice were adoptively transferred into them. One week prior to transfer, donor

mice had been vaccinated with 10^7 PFU vac-OVA and the following day they had been injected with 5 x 10^6 splenocytes from transgenic OT-1 C57BL/6 Thy1.2$^+$ mice. CD8$^+$ T cells from OT-1 mice are specific to the SIINFEKL epitope encoded in the Ad-OVA vector. Therefore, they were transferred to increase the frequency of responding OVA-specific CD8$^+$ T cells in order to enable better detection during intracellular cytokine staining. Mice were bled at the indicated time points and *in vitro* re-stimulation was performed to detect donor OVA-specific CD8$^+$ T cell production of IFN-γ, TNF-α, and IL-2.

Transfer of OVA-specific CD8$^+$ T cells into Ad-OVA immunized mice results in a number of OVA-specific CD8$^+$ T that produce cytokines upon re-stimulation that remain fairly stable over time (**Figure 4.5A**), although there was some fluctuation in the response at certain time points. This fluctuation may be due to an internal boosting effect from the persistent antigen that is not consistently expressed [123]. Additionally, the cells could be producing cytokines other than those measured in this assay. The CD8$^+$ T cells transferred into Ad-gag immunized mice did not produce cytokines following restimulation. This could be due to their egress from the blood as they transitioned into memory. The profile of the OVA-specific CD8$^+$ cytokine secreting T cells was fairly stable as well. Two weeks after transfer, the cytokine secreting cells were largely composed of cells that produce IFN-γ alone or in combination with TNF-α following re-stimulation, which is consistent with highly activated effector cells (**Figure 4.5B**). Although the total number of cytokine secreting cells was reduced six months following transfer (**Figure 4.5C**), the profile was similar to that of the cytokine producing cells at two weeks following transfer. However, the response was clearly dominated by cells that produce IFN-γ alone following re-stimulation. While the antigenic load clearly supports effector and effector memory cells (**Figures 4.4, 4.5B, 4.5C**), these cells do not appear to be greatly losing effector functions.

FIGURE 4.3. Antigen-experienced CD8$^+$ T cells respond and expand in response to persistent antigen.

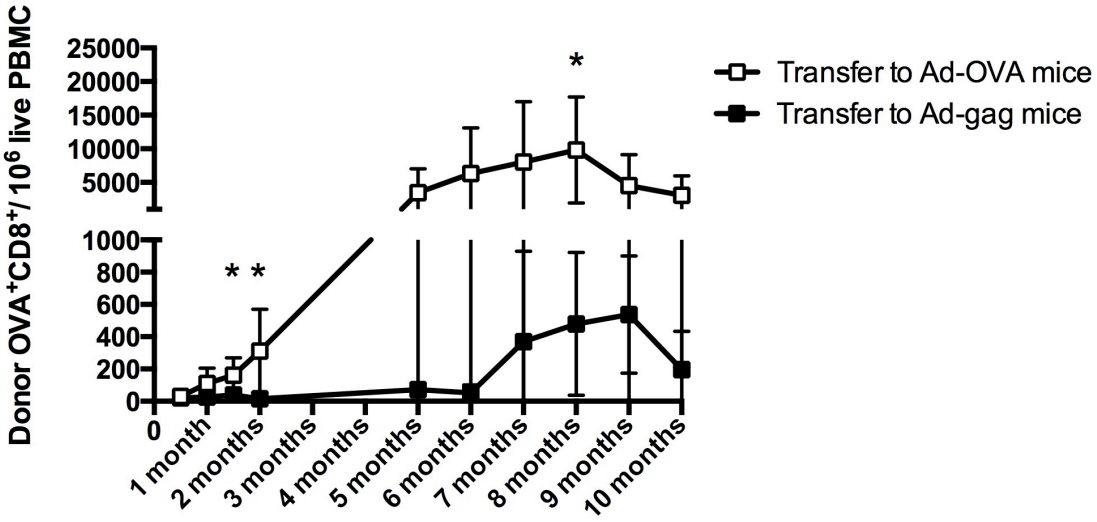

Groups of Thy1.2$^+$ C57BL/6 mice were immunized with 10^{11} vp AdC68-NPOVAGFP or 10^{11} vp AdC7-HIVgag, as a negative control. Three weeks later, 3.14 x 10^6 congenic (Thy1.1$^+$) CD8$^+$ T cells were adoptively transferred via tail vein injection into each group. Transferred cells were isolated from mice immunized 1 week earlier with 10^7 PFU vaccinia virus expressing NPOVAGFP (vac-OVA). Mice were bled at the indicated time points. Frequencies of donor-specific (Thy1.1$^+$) OVA-specific CD8$^+$ T cells were determined by staining with an OVA-specific tetramer. Data are represented as mean numbers ± SD of Thy1.1+ OVA$^+$ CD8$^+$ T cells per 10^6 live PBMCs. The bar indicates the mean of the group. Differences between numbers of OVA-specific CD8$^+$ T cells transferred into Ad-OVA and Ad-gag mice were determined at each time point using multiple t-tests with Sidak-Bonferroni correction. The following p-values were obtained: **[A]**: 6 weeks: p=0.0372, 8 weeks: p=0.0336 **[B]**: 8 months: p=0.0295.

FIGURE 4.4. Antigen-specific CD8$^+$ T cells maintain an effector memory phenotype regardless of presence of persistent antigen.

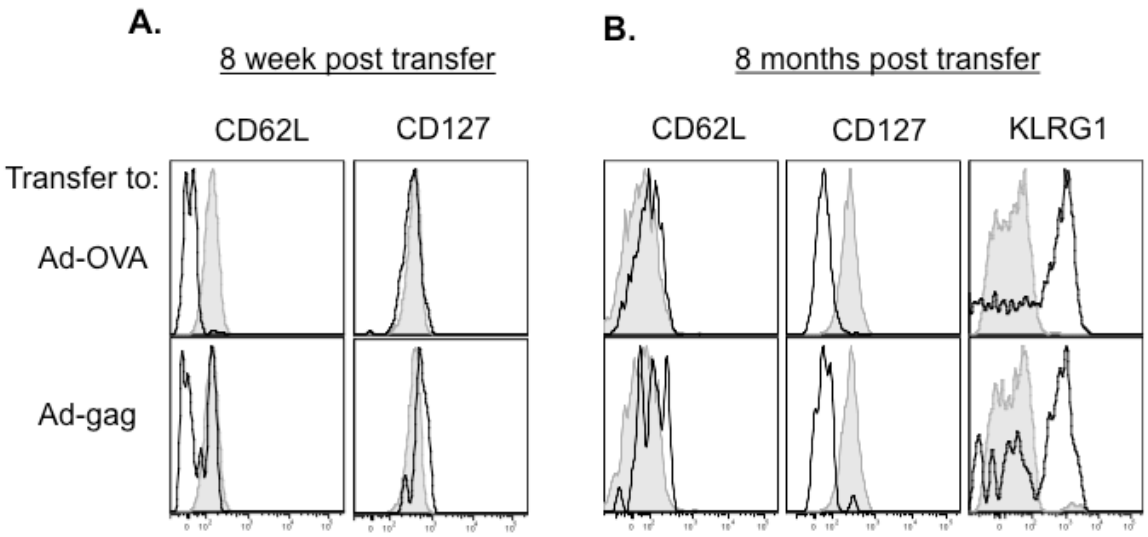

Expression of CD62L and CD127 was measured on donor (Thy1.1$^+$) OVA-specific CD8$^+$ T cells 8 weeks **[A]** and 8 months **[B]** after transfer into mice immunized with 10^{11} vp AdC68-NPOVAGFP (top row of graphs) or AdC7-gag (bottom row of graphs). KLRG1 was included at 8 months after transfer. Grey histograms represent staining for naïve host CD8$^+$ T cells. Open histograms represent concatenated data from 5 mice for each group.

FIGURE 4.5. Antigen-experienced CD8$^+$ T cells do not lose function over time in response to persistent antigen.

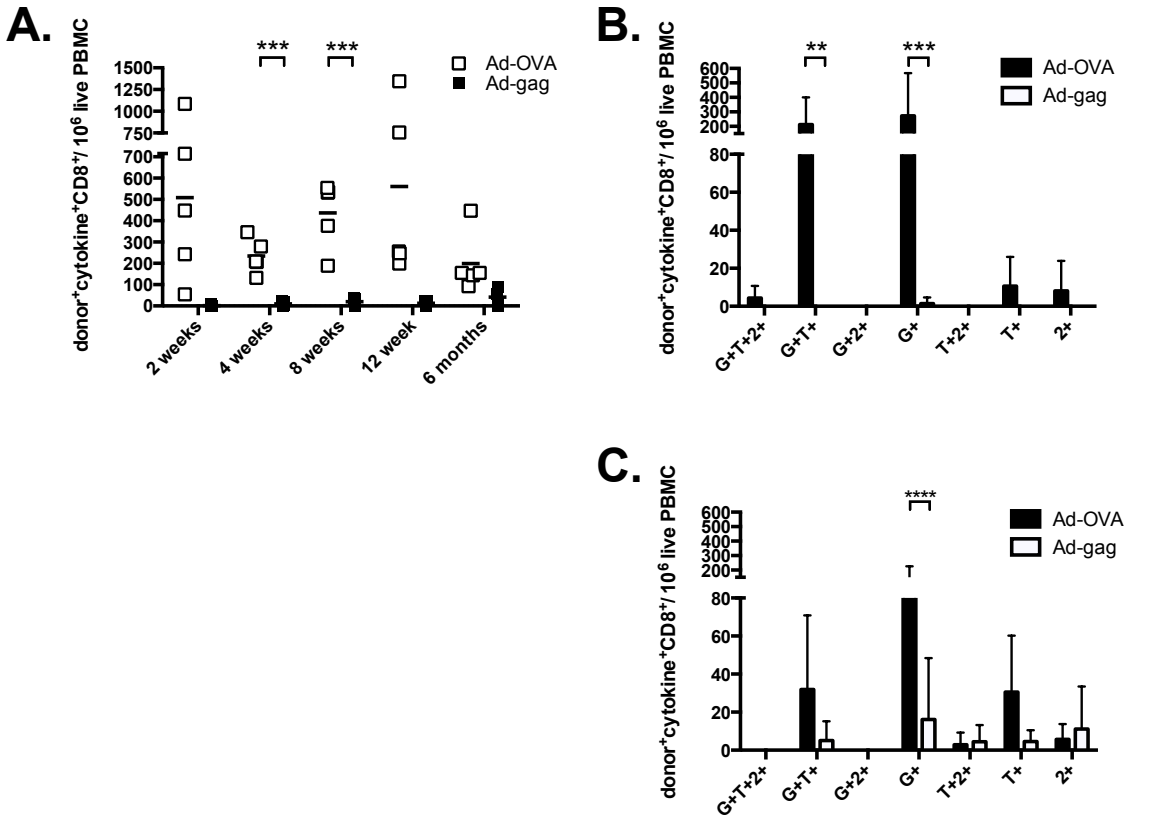

Shows the kinetics of total cytokine-producing donor cells **[A]** and the cytokine profile 12 weeks following immunization Groups of Thy1.1$^+$ C57BL/6 mice were immunized with 10^{11} vp AdC68-NPOVAGFP or 10^{11} vp AdC7-HIVgag, as a negative control. Three weeks later, 3.14 x 10^6 congenic (Thy1.2$^+$) CD8$^+$ T cells were adoptively transferred into each group. Congenic mice were transferred with 5 x 10^6 OT-1 cells and immunized with 10^7 PFU vac-OVA 1 week prior to transfer into Thy1.1$^+$ mice. Mice were bled at the indicated time points and PBMCs were stimulated with either SIINFEKL peptide or the equivalent amount of an irrelevant peptide to measure background stimulation. **[A]** Shows the number of cytokine producing cells following the subtraction of background stimulation. The profiles of donor CD8$^+$ cells producing cytokine combinations are shown for 2 weeks after transfer **[B]** and 6 months after transfer **[C]** and were determined by summation of Boolean gates for each cytokine. Data in each figure is represented as the number of donor (Thy1.2$^+$) CD8$^+$ producing cytokines per 10^6 live PBMC**.** Standard deviation is included for **[B]** and **[C]**. In **[A]**, the bar represents the mean. Significance between rapamycin- and sham–treated groups was determined for each time point using multiple t-tests with Holm-Sidak correction for multiple comparisons for **[A]** and 2way ANOVA with Holm-Sidak correction for multiple comparisons for **[B]** and **[C]**. The following p-values were obtained: **[A]** 4 weeks: p=0.0003, 6 weeks: p=0.0003; **[B]** G+T+: p=0.0048; G+: p=0.0002 **[C]** G+:p<0.0001

DISCUSSION

The experiments presented in this chapter were designed to address how the $CD8^+$ T cell pool that fails to contract following immunization with an Ad-based vaccine is maintained. Two possible scenarios can be envisioned. Naïve $CD8^+$ T cells could be recruited continuously into the response as they encounter their cognate antigen during Ad persistence. These cells would ultimately replace the terminally differentiated cells as they decay, thereby maintaining a stable response. Alternatively, $CD8^+$ T cells primed early in the response that differentiated into central memory cells could be restimulated as they encounter antigen during Ad persistence and thus replenish the on-going $CD8^+$ T cell response. The data presented here largely support the latter scenario.

Asynchronous priming of naïve $CD8^+$ T cells is a strategy commonly employed to maintain stable memory T cell numbers during various persistent infections, including mouse polyoma virus and CMV. Antigen-specific $CD8^+$ T cells that respond and persist during these infections are characterized by a large degree of heterogeneity in their expression of such markers as CD62L, CD127, and CD27 [201,204]. As transgene product-specific $CD8^+$ T cells elicited by Ad vector vaccination are also highly heterogeneous [123,140,195], it stood to reason that this heterogeneity could reflect that the transgene product-specific $CD8^+$ T cells are in various stages of differentiation due to priming with their antigen at different times during the response. However, when naïve cells were transferred into Ad immunized mice after clearance of most of the acutely transduced cells, the overall pattern was that the cells did not expand in response to transgene product. This suggests that naïve $CD8^+$ T cells are not recruited to maintain the elevated transgene product-specific $CD8^+$ T cell response. Indeed, while adult mice immunized with an Ad-based vaccine 8 weeks after being thymectomized mount slightly lower transgene product-specific $CD8^+$ T cell responses, the kinetics of the response are not altered and the cells do not have a more distinct contraction as would be expected if naïve cells were responsible for maintaining the $CD8^+$ T cell pool [140]. Interestingly though, transferred naïve $CD8^+$ T cells in one animal showed robust expansion and persisted for many months. Statistically, this was

considered an outlier. However, the results may be biologically relevant, perhaps indicating that at the time of transfer the Ad genome was more transcriptionally active, and thus producing more transgene product, in that mouse than in the others.

While these data do suggest that naïve $CD8^+$ T cells are primarily not responsible for maintaining the elevated $CD8^+$ T cell response, it is important to recognize the limitations of my approach. Despite demonstrating that enough transgene product-specific $CD8^+$ T cell precursors were transferred (**Figure 4.1B**), the recipient mice may not have permitted their engraftment. The recipient mice could not be T cell depleted prior to transfer as this would have removed the cells that harbor persisting Ad vector genomes and thus may not have had available niches in which the congenic naïve cells could engraft. Other groups have demonstrated a role for naïve $CD8^+$ T cells in responding to persistent infection by creating partial hematopoietic chimeric mice [201,202,204]. To accomplish this, persistently infected mice were treated with a low dose of busulfan, a non-immunosuppressive myeloablative agent, and then partially reconstituted with naïve, congenic bone marrow. This creates a population of stem cells to give rise to naïve $CD8^+$ T cells. While it has been reported that busulfan does not disturb virus-specific $CD8^+$ T cell responses [201], it would be critical to determine that the adenovirus reservoir is not affected and it persists in the lymphatics. It has been demonstrated that bone marrow is a reservoir for central memory $CD8^+$ T cells [210]. Whether or not these bone marrow-derived cells harbor persistent adenovirus has yet to be confirmed.

To test if antigen-experienced transgene product-specific $CD8^+$ T cells maintain the $CD8^+$ T cell pool, splenic OVA-specific $CD8^+$ effector T cells were transferred into Ad immunized mice. Vast and continuous accumulation of donor OVA-specific $CD8^+$ T cells was observed. This largely indicates that antigen-experienced cells are responsible for the maintenance of the $CD8^+$ T cell pool following vaccination with an Ad-based vaccine. However, these experiments do not reveal the nature of the antigen-experienced cell responsible. We would expect that the population of OVA-specific $CD8^+$ T cells present in the donor spleen seven days after immunization with vac-OVA would be heterogeneous, containing both short-lived effector cells and memory precursor cells. Therefore, we cannot rule out the possibility that a small number of memory cells were

transferred. In general, we would expect that those cell types would be responsible as terminally differentiated antigen-specific $CD8^+$ T cells have a limited capacity for proliferation and would be expected to decay over time. Further experiments would be warranted to determine the cell type involved in this expansion.

The cells that continued to accumulate in this transfer model had at 8 months after transfer an effector memory phenotype and expressed high levels of KLRG1, a marker that reflects the history of antigen stimulation. Therefore, the high expression of KLRG1 on these cells likely reflects that they continue to encounter their antigen. As such it would be important to assess if the donor derived antigen-specific $CD8^+$ T cell response requires antigen in order to persist. In some models of chronically infecting viruses, especially LCMV clone 13, virus-specific $CD8^+$ T cells become addicted to antigen. Once antigen is removed from the system, or the $CD8^+$T cells are transferred to a naïve environment, the cells die because they minimally express receptors for IL-7 and IL-15, which drive the homeostatic turnover over memory cells, thereby promoting their survival [99]. However, LCMV clone 13 is not equivalent to adenovirus. There is some evidence to suggest that transgene product-specific memory $CD8^+$ T cells induced following Ad immunization do not require antigen to be maintained. Utilizing Ad vectors encoding a SIINFEKL expression cassette that could be temporally regulated using the Tet-OFF system, the Bramson group demonstrated that the primary SIINFEKL-specific $CD8^+$ T cell response only requires SIINFEKL expression for the first two months following immunization, after which they become antigen-independent [211]. However, whether these cells remain antigen-independent many months following immunization remains to be elucidated. Therefore, it would be critically important to assess at a longer interval after Ad immunization the antigen-specific $CD8^+$ T cells' responsiveness to IL-7 and IL-15 as a measure of their capacity for homeostatic self-renewal and dependency on antigen.

The continuous accumulation observed in some mice resembles a phenomenon termed memory inflation, which is used to describe the accumulation of $CD8^+$ T cells responding to certain epitopes following cytomegalovirus infection. $CD8^+$ T cells that respond to inflationary epitopes have an effector memory phenotype and are highly functional, thus capable of both

producing cytokines following restimulation and lysing target cells [204]. This phenomenon occurs in the absence of viral replication, CMV vectors limited to a single cycle of replication continue to induce $CD8^+$ T cell inflation[212]. Indeed, memory inflation has recently been described following immunization with a β-galactosidase expressing adenovirus [213]. Antigen-specific $CD8^+$ T cell inflation occurs in response to immunodominant epitopes that due to their high affinity outcompete lower affinity peptides for MHC class I binding [214]. The immunodominant MHC class I-restricted epitope of ovalbumin, SIINFEKL, is a high affinity epitope that causes inflation in the context of a CMV vector [215]. It is therefore likely, that we observed a similar effect in the study presented here. Inflation following Ad immunization was followed for two epitopes from β-galactosidase [213], one was inflationary and the other was not. As such different epitopes processed from the same protein have different capacities to induce inflation. As the SIINFEKL epitope included in the Ad vectors used here was part of a larger transgene, the $CD8^+$ T cell response to additional epitopes in the transgene should be monitored for their inflationary ability. This could have important implications in the design of transgenes used in adenoviral vaccines to elicit protective immune responses against many pathogens, particularly those which a large pool of effector memory $CD8^+$ T cells are required for protection.

Given that antigen-experienced transgene product specific $CD8^+$ T cells appear primarily responsible for the maintenance of their memory pool following Ad immunization, it would be likely that these cells periodically reencounter transgene product, which promotes their continued expansion. Interestingly this indicates that the cells harboring persistent adenovirus vector, whose transgene's expression is controlled by a constitutively active promoter, are not destroyed by the on-going transgene product-specific $CD8^+$ T cell response. The mechanism by which this occurs is unclear. Gene products from the E3 domain are responsible for immunomodulation, including blocking MHC-I antigen presentation and mediating resistance to T cell cytolysis and cytokines that promote cell death, such as TNF-α [79,81,83]. However, later generation Ad vectors, including those used in this study, are deleted in this domain but still retain the ability to persist *in vivo* [123]. Alternatively, the persistence of an antigen depot in activated T cells could demonstrate that these cells are resistant to $CD8^+$ T cell-mediated lysis.

MATERIALS AND METHODS

Vectors and immunizations

All experiments were performed with E1-deleted adenovirus vectors based on chimpanzee serotype 68 (AdC68) or chimpanzee serotype 7 (AdC7). Mice were injected IM with 10^{11} viral particles (vp) of either a vector encoding influenza nucleoprotein fused to green fluorescent protein and the immunodominant MHC class I restricted epitope of ovalbumin (SIINFEKL) (AdC68-NPOVAGFP), a vector encoding the rabies virus glycoprotein (AdC68-rab.gp), or a vector encoding gag of HIV-1 (AdC7-HIVgag). Additional experiments used a vaccinia virus vector encoding the NPOVAGFP fusion protein (vac-OVA). Vectors for immunization were diluted to the appropriate concentration in sterile PBS (Cellgro; Manassas, VA). Mice were immunized intramuscularly (IM) with 50 µL of diluted vector in each hind limb, for a total of 100 µL per mouse. Where indicated, mice were immunized intraperitoneally (IP) with 200 µL of diluted vector.

Mice

Female 4 to 6 week old mice Thy1.2$^+$ C57BL/6 mice were purchased from the National Cancer Institute (Frederick, MD). Thy1.1$^+$ C57BL/6 mice were purchased from Jackson Laboratories (Bar Harbor, ME). Mice were housed in the vivarium at the Wistar Institute (Philadelphia, PA). All experiments and procedures were performed in accordance with approved animal protocols. C57BL/6 OT-1$^+$ breeding pairs were purchased from Jackson Laboratories and were then bred at Wistar following approved breeding protocols.

Lymphocyte isolation

Blood was collected via submandibular bleeding into 1 mL of 4% sodium citrate. 1 mL of L-15 (Cellgro) was added after collection. Peripheral blood mononuclear cells (PBMC) were isolated by Histopaque-1083 (Sigma-Aldrich; St. Louis, MO) gradient purification. PBMC were

collected and washed in L-15 containing 1% fetal bovine serum (FBS) (Gemini Bio Products; West Sacramento, CA). Red blood cells were lysed for 5 minutes at room temperature using RBC lysis buffer (eBioscience; San Diego, CA).

Spleens were homogenized against a 70 μm filter screen and collected in pre-warmed L-15 containing 1% FBS. Cells were pelleted at 1500 rpm for 5 minutes. Pellets were resuspended in RBC lysis buffer for 5 minutes at room temperature to lyse red blood cells.

Popliteal and inguinal lymph nodes were collected from both hind limbs and homogenized against a 70 μm filter screen. Lymphocytes were collected in L-15 containing 1% FBS and washed once with the same media. Lymphocytes isolated from peritoneal lavage were collected by flushing the peritoneal cavity with 10 mL L-15 containing 1% FBS and washing once.

BrdU Assay

C57BL/6 mice were immunized with 10^{11} vp AdC68-NPOVAGFP. Mice were euthanized 10 days, 1 month, or 5 months after immunization. Three days prior to euthanasia, mice were injected IP with 2 mg bromodeoxyuridine (BrdU) (Sigma-Aldrich) dissolved in 200 μL PBS. Additionally, drinking water was supplemented with 0.8 mg/mL BrdU and 1% sucrose (Sigma-Aldrich). Water was changed and fresh solution was added each day prior to euthanasia.

Blood, spleens, and popliteal and inguinal lymph nodes were isolated and prepared as described above. Cells were stained and permeabilized using BrdU Flow kit (BD Pharmingen; Franklin Lakes, NJ) following the manufacturer's protocol. Briefly, the cell surface was first stained with PerCP-Cy5.5-labeled anti-CD8 (BD Pharminogen), PE-Cy7-labeled anti-CD44 (BD Pharminogen), APC-labeled tetramer against the immunodominant MHC class I restricted epitope of Ovalbumin (SIINFEKL) (courtesy of Dr. E John Wherry), and Live/Dead fixable aqua dye (Life Technologies, Carlsbad, CA) for 30 minutes at 4°C. Following a PBS wash, samples were permeabilized with Cytofix/cytoperm (BD Biosciences; Franklin Lakes, NJ) for 30 minutes at 4°C then washed with 1X Perm/Wash (BD Biosciences). Cells were permeabilized further with Cytoperm Permeabilization Buffer Plus (BD Biosciences) for 10 minutes on ice and then washed as before. Samples were re-fixed by treating with 100 μL Cytofix/cytoperm and washed. To

expose BrdU for staining, samples were treated with 100 µL of 300 µg/mL DNase solution (BD Pharmingen) for 1 hour at 37°C and washed with 1X Perm/Wash. Samples were then stained for 20 minutes at room temperature with FITC-labeled anti-BrdU (BD Pharminogen) diluted 1:50 in 1X Perm/wash and then washed.

Adoptive Transfers

$CD8^+$ T cells used in transfer experiments were harvested from C57BL/6 $Thy1.1^+$ mice. Where indicated, naïve cells were isolated and transferred or cells were isolated from mice that had been immunized intraperitoneally (IP) 7 days earlier with 10^7 plaque-forming units (PFU) vac-OVA. On the day of transfer, these mice were euthanized and splenocytes were isolated. $CD8^+$ T cells were isolated by negative selection using EasySep Mouse $CD8^+$ T Cell Enrichment Kit (Stemcell Technologies; Vancouver, BC) following the manufacturer's protocol.

Isolated $CD8^+$ T cells were then transferred intravenously (IV) to recipient C57BL/6 ($Thy1.2^+$) via tail vein at a concentration of 3.14×10^6 cells per mouse. Recipient mice had been immunized 3 weeks earlier with 10^{11} vp of either AdC68-NPOVAGFP or AdC7-HIVgag.gp, as a negative control.

Intracellular Cytokine Staining (ICS)

Lymphocytes were plated on a 96-well plate in 200 µL of DMEM supplemented with 2% Mixed Lymphocyte Culture medium. Lymphocytes were stimulated in the presence of Golgi Plug (BD Biosciences) either with a positive peptide, SIINFEKL, or with a negative peptide, WIZX-2 from rabies virus. Each was used at 2.5 µg/mL. Stimulation was performed for 5 hours at 37°C in 10% CO_2. Following stimulation, lymphocytes were stained at 4°C for 30 minutes with fluorochrome-labeled antibodies against CD8, CD44, Thy1.1 or Thy1.2 to distinguish donor cells, and with Live/Dead Fixable Aqua dye to exclude dead cells from analysis. Cells were washed once and then permeabilized with 100 µL Cytofix/Cytoperm for 30 minutes at 4°C. Cells were then washed with 1X Perm/Wash and additionally stained for 30 minutes at 4°C with fluorochrome-labeled antibodies against IFN-γ, TNF-α, and IL-2 diluted 1:100 in 1X Perm/Wash.

Following staining, cells were washed and fixed with BD Fixative (BD Biosciences). Samples were stored at 4°C until analysis.

Cells were analyzed with a BD LSR-II flow cytometer (BD Biosciences) and post acquisition analysis was performed with FlowJo v.9.4 software (TreeStar, Ashland, OR). Samples were first gated to identify lymphocytes based on forward scatter area (FSC-A) and side scatter (SSC). Doublets were then removed using a plot of forward scatter height (FSC-H) vs. FSC-A. Live lymphocytes were then gated based on exclusion of Live/Dead stain. Donor $CD8^+$ T cells were identified by plotted Thy1.1/1.2$^+$ events vs. $CD8^+$ events. $CD8^+$ T cells were then gated on each intracellular cytokine. Boolean gates were then created to identify all possible cytokine combinations, equaling 2^n combinations, where *n* is equal to the number of individual cytokines measured.

CHAPTER 5

THE EFFECT OF ADENOVIRUS-SPECIFIC ANTIBODIES ON ADENOVIRAL VECTOR-INDUCED TRANSGENE PRODUCT-SPECIFIC T CELL RESPONSES

ABSTRACT

In this study we tested the effect of neutralizing antibodies to different serotypes of E1-deleted adenovirus (Ad) vectors on the immunogenicity of the homologous adenovirus vector or a vector derived from a heterologous serotype. Our results show that, as expected, even low titers of passively transferred neutralizing antibodies significantly reduce the homologous vectors' ability to elicit transgene-specific $CD8^+$ T cell responses. In addition antibodies changed the fate of transgene product-specific $CD8^+$ T cells by promoting their transition into the central memory cell pool, which resulted in markedly enhanced expansion of transgene product-specific $CD8^+$ T cells following a boost with a heterologous Ad vector. Non-neutralizing antibodies induced to one adenoviral serotype had no effect on the magnitude of transgene product-specific $CD8^+$ T cells induced by a distinct vector nor did such antibodies promote induction of more resting memory $CD8^+$ T cells. These results show that antibodies to an adenovirus vaccine carrier not only affect the magnitude but also the flavor of a vector-induced $CD8^+$ T cell response.

Adapted from: The effect of adenovirus-specific antibodies on adenoviral vector-induced transgene product-specific T cell responses. JC Small*, LH. Haut*, A Bian, HCJ Ertl. *Journal of Leukocyte Biology.* In press.

INTRODUCTION

E1-deleted adenovirus (Ad) vectors derived from human serotype 5 (AdHu5) are highly immunogenic, inducing potent B and T cell responses against its viral components and products of transgenes encoded from its genome. As such, these vectors are being developed as vaccine platforms against a wide array of pathogens. However, a concern with the use of AdHu5 vectors is that humans are commonly infected with the virus during childhood and therefore have pre-existing immunity against the vector. Animal studies demonstrated that virus-neutralizing antibodies (VNAs) against AdHu5 reduce transduction of target cells [92] by blocking its interaction with the coxsackie and adenovirus receptor (CAR) [91] thereby reducing transgene expression, ultimately dampening the vector's immunogenicity [93,216,217]. However, AdHu5 is more immunogenic than other vaccine platforms [217]. As such, an AdHu5-based vaccine encoding a transgene made up of HIV-1 clade B *gag/pol/nef* was developed to induce HIV-specific T cell responses with the goal of reducing viral load in infected individuals. Pre-clinically, the vector protected nonhuman primates challenged with the SIV-HIV chimera SHIV-89.6P [218] and early phase trials demonstrated the vaccine's immunogenicity in humans [219]. The phase IIB, or STEP, trial was designed to test the efficacy of this vaccine in individuals at high risk for HIV-1 acquisition and was tested in individuals who were both AdHu5 seronegative and seropositive. The trial was halted early after interim analysis revealed that the vaccine was not efficacious. More worrying though was that further analysis also demonstrated a significantly increased risk of HIV acquisition among men who were both AdHu5 seropositive and uncircumcised at the time of immunization [220], although this risk appears to become less pronounced with time [221]. While most vaccinees mounted immune responses to the HIV-1 antigens encoded in the vector, the responses were not very strong and T cell responses were also narrowly focused on one to three epitopes. Nevertheless, the reduced immunogenicity in seropositive participants could not explain their increased risk of HIV infection. A subsequent trial, HVTN505, was designed to test an HIV-1 vaccine regimen using a DNA vaccine prime followed by an AdHu5 boost in AdHu5 seronegative individuals. Again, the trial was halted because it failed to show efficacy and observed a non-

significant trend towards higher infection rates in vaccine recipients compared to placebo recipients [222]. Although a number of theories were formulated and tested to explain the increased acquisition rates in the STEP trial [223,224] the reasons for the apparent increased susceptibility to HIV-1 infection in AdHu5 vaccine recipients remain elusive.

To overcome the problem of pre-existing immunity, novel recombinant Ad vectors are being evaluated. Several groups are developing vectors based on alternative human serotypes such as HAdV-26 (AdHu26) [225] or HAdV-35 [226]. While these so-called "rare" human serotypes are potently immunogenic, humans are still exposed to these viruses and, depending on the geographic region, they either lack VNAs to these serotypes or they carry low titers [227]. Of note, regions where the development of an HIV vaccine is critical to public health tend to have seroprevalence rates to AdHu26 that are comparable to those AdHu5 [228]. Therefore, these vectors may face the same challenges as vectors derived from AdHu5. Alternatively, vectors derived from non-human adenovirus serotypes, such as those from chimpanzees (SAdV, also termed AdC), are also being explored [229,230]. As these viruses do not circulate in humans, prevalence rates to such viruses are even lower than those to alternative human serotypes [231,232]. It remains an open question if these two groups of alternative Ad vectors will outperform AdHu5-based vaccines in clinical trials or elicit the previously observed increased risk of HIV-1 infection in vaccine recipients.

Here we tested if VNAs against distinct serotypes of E1-deleted Ad vectors differentially affect the immunogenicity of the homologous vector. Although Ad-specific VNAs are serotype-specific and mainly directed to the hypervariable loops of hexon [13], non-neutralizing antibodies to more conserved regions of the viral surface proteins, such as fiber and the hexon stalk, cross-react between different human and simian serotypes [92]. Therefore, the effect of passive transfer of Ad-specific antibodies on the immune response induced by vaccination with an Ad vector derived from a heterologous serotype was also assessed. These results confirm that even low titers of adoptively transferred antibodies can significantly reduce the vectors' ability to elicit transgene product-specific $CD8^+$ T cell responses and there was no definite difference between

the different serotypes. Interestingly, passive transfer of Ad VNAs changed the fate of transgene product-specific $CD8^+$ T cells by promoting their transition into the central memory compartment, resulting in their enhanced expansion following a boost with a heterologous Ad vector. Ad VNAs induced to one serotype had no effect on the magnitude of transgene product-specific $CD8^+$ T cells induced by an Ad vector of a different serotype nor did such antibodies promote induction of more resting memory $CD8^+$ T cells. These results show that antibodies to an Ad vaccine carrier not only affect the magnitude but also the differentiation of an Ad vector-induced $CD8^+$ T cell response.

RESULTS

In order to determine if pre-existing vector-specific neutralizing antibodies differentially affected immune responses to transgene products encoded in Ad-based vaccines, serotype-specific hyperimmune sera were generated against three distinct Ad species. Vectors based on AdHu5, a common family C serotype, AdHu26, a family D serotype, and AdC6, a chimpanzee-derived serotype from family E, were used to repeatedly immunize BALB/c mice to generate hyperimmune sera. Sera were collected and tested for neutralization of the homologous virus. After determining the vector-specific neutralizing antibody titer, each sera was transferred intraperitoneally (IP) to groups of naïve BALB/c mice such that five days after transfer the groups had circulating vector-specific VNA titers of 1:1000, 1:100, or 1:10. As a control, a group of mice was treated with naïve BALB/c serum given at the equivalent volume to that used for the highest dose of hyperimmune serum (1:1000). The day following confirmation of circulating vector-specific VNAs mice were immunized with 10^{10} viral particles (vp) of an HIV-1 Gag-expressing Ad vector based on the identical serotype used for induction of serum the mice received. Ten days, three weeks, and eight weeks later mice were bled and peripheral blood mononuclear cells (PBMCs) were tested for Gag-specific $CD8^+$ T cell responses by staining with a tetramer specific to the immunodominant, H-2^d-restricted immunodominant epitope of Gag (AMQMLKETI) (**Figure 5.1A-C**). Vaccination affected overall numbers of circulating $CD8^+$ T cells; therefore, $tetramer^+$

cells were normalized to 10^6 live PBMCs. Gag-specific $CD8^+$ T cell responses elicited by each vector peaked three weeks after immunization and were sustained thereafter, although the responses induced by AdHu26-gag underwent more pronounced contraction compared to those induced by AdHu5-gag and AdC6-gag. Mice with circulating AdHu5-specific VNAs as low as 1:10 titer had significantly reduced Gag-specific $CD8^+$ T cell responses ten days after immunization with AdHu5-gag. This reduction became more pronounced at later time points, particularly in those mice with the highest titer of AdHu5-specific VNAs. Similarly, circulating AdHu26-specific VNA titers of 1:100 and 1:1000 caused significant reduction of Gag-specific $CD8^+$ T cells ten days after immunization with AdHu26-gag. By three weeks after immunization, even the lowest dose of AdHu26-specific VNAs caused pronounced decreases in the response, which were maintained eight weeks after immunization. Gag-specific $CD8^+$ T cells were reduced in those mice bearing AdC6-specific VNAs at the time of immunization with AdC6-gag, although at the earliest time point only mice with the highest titers had significant reduction.

To determine if immunization in the presence of vector-specific VNAs reduced Gag-specific $CD8^+$ T cell responses in compartments other than blood, lymphocytes from spleens and genital tract were isolated 8 weeks after immunization. Results from both tissues largely mirror those seen in the blood. In spleens (**Figure 5.1D-F**), AdHu5-gag and AdC6-gag induced robust Gag-specific $CD8^+$ T cell responses that were significantly reduced in mice primed in the presence of vector-specific VNAs, regardless of dose. In contrast, AdHu26-gag induced a poor Gag-specific $CD8^+$ T cell response that was only reduced in mice with the highest dose of AdHu26-specific VNAs. At the genital tract (**Figure 5.1G-I**), Gag-specific $CD8^+$ T cell responses induced by AdHu5-gag and AdC6-gag were comparable in control mice and, as expected, VNAs present at the time of immunization reduced those responses. In contrast, AdHu26-gag induced a poor Gag-specific $CD8^+$ T cell response at the genital tract in control mice but that was increased in mice that had a circulating titer of AdHu26-specific VNAs of 1:10. Treatment with the higher VNA doses resumed the pattern of reduction in responses.

To determine if transfer of Ad-specific VNAs altered $CD4^+$ T cell responses, PBMCs and splenocytes were tested at eight weeks after immunization. We observed variation in the antigen-

experienced ($CD44^+$) $CD4^+$ T cell responses in the blood following immunization with the different vectors. In comparison to $CD4^+$ T cell numbers found in blood of naïve mice, immunization with AdHu5 in the absence of vector-specific VNAs significantly increased $CD4^+$ T cell responses (**Figure 5.2A**). However, priming in the presence of AdHu5-specific VNAs, failed to increase $CD4^+$ T cell responses, which remained comparable to those seen in naïve mice. The exception to this was mice primed in the presence of the highest VNA dose, where $CD4^+$ T cell responses became elevated above baseline. In contrast, vaccination with AdHu26 significantly reduced $CD4^+$ T cell responses in all groups but for mice primed in the presence of the lowest dose of AdHu26-specific VNAs. While immunization with AdC6 did not change the $CD4^+$ T cell numbers in the blood, priming in the presence of AdC6-specific VNA, regardless of dose, reduced $CD4^+$ T cell responses. $CD4^+$ T cell responses in the spleen were largely unchanged following immunization with either AdHu5 or AdC6 (**Figure 5.2B**). Splenic $CD4^+$ T cells in AdC6-immunized mice were below those seen in naïve mice regardless of transfer of AdC6-specific antibodies.

Results from the STEP trial revealed that individuals previously exposed to AdHu5 with moderate to high levels of circulating AdHu5-specific VNAs at the time of immunization with the AdHu5-based vaccine had slightly higher rates of HIV-1 infection than those in the placebo arm of the trial. This seemingly enhanced susceptibility was unexpected and its underlying causes remain elusive. However, one possible explanation is that vaccination of those individuals increased numbers of activated $CD4^+$ T cells, and thus, targets of HIV-1 infection at mucosal surfaces. To this end, numbers of activated ($CD44^+$) $CD4^+$ T cells were analyzed in the genital tract in naïve mice and vaccinated mice treated with all serum doses (**Figure 5.2C**). Relative numbers of activated $CD4^+$ T cells in the genital tract were not dramatically changed following vaccination, although relative numbers seemed to increase following vaccination with AdHu5 but decreased slightly upon AdHu26 vaccination. Variation in numbers was observed for immune serum recipients, although there was no consistent trend between vectors, other than that the highest dose of serum did not increase the numbers of activated $CD4^+$ T cells. Regardless, the observed differences were modest and comparable to those observed in control mice.

Adenoviruses and vectors based on them are known to persist in immunologic tissues, particularly in activated T cells [123]. During persistence, the Ad genome remains transcriptionally active, albeit at low levels, and thus maintains high frequencies of effector T cells exhibiting delayed kinetics in their transition into the central memory pool [123]. As circulating vector-specific VNAs reduced frequencies of transgene product-specific $CD8^+$ T cells, it stands that their memory phenotype may be altered as well. Therefore, Gag-specific $CD8^+$ T cells induced in this experiment were analyzed for expression of CD62L, which can be used to distinguish effector and memory T cells based on either low or high expression, respectively. Immunization with either Ad vector in the presence of pre-existing vector-specific VNAs increased the frequencies of Gag-specific $CD8^+$ T cells with a $CD62L^{hi}$ phenotype (**Figure 5.3A-C**). This effect was observed as early as ten days after vaccination with AdHu5-gag and AdHu26-gag in the blood of mice with the highest titer of circulating vector-specific VNAs, and became more pronounced at eight weeks after vaccination in both blood and spleens. Increased CD62L expression was only observed at eight weeks following vaccination with AdC6-gag but was significantly increased in all groups of mice that had received AdC6-specific immune serum. Interestingly, increased frequencies in $CD62L^{hi}$ Gag-specific $CD8^+$ T cells were not observed in the spleens of these mice other than those that had received the low titer of AdC6-specific VNAs at the time of immunization.

FIGURE 5.1. Passive transfer of Ad-immune serum reduces transgene product-specific CD8$^+$ T cells to Ad vector immunization.

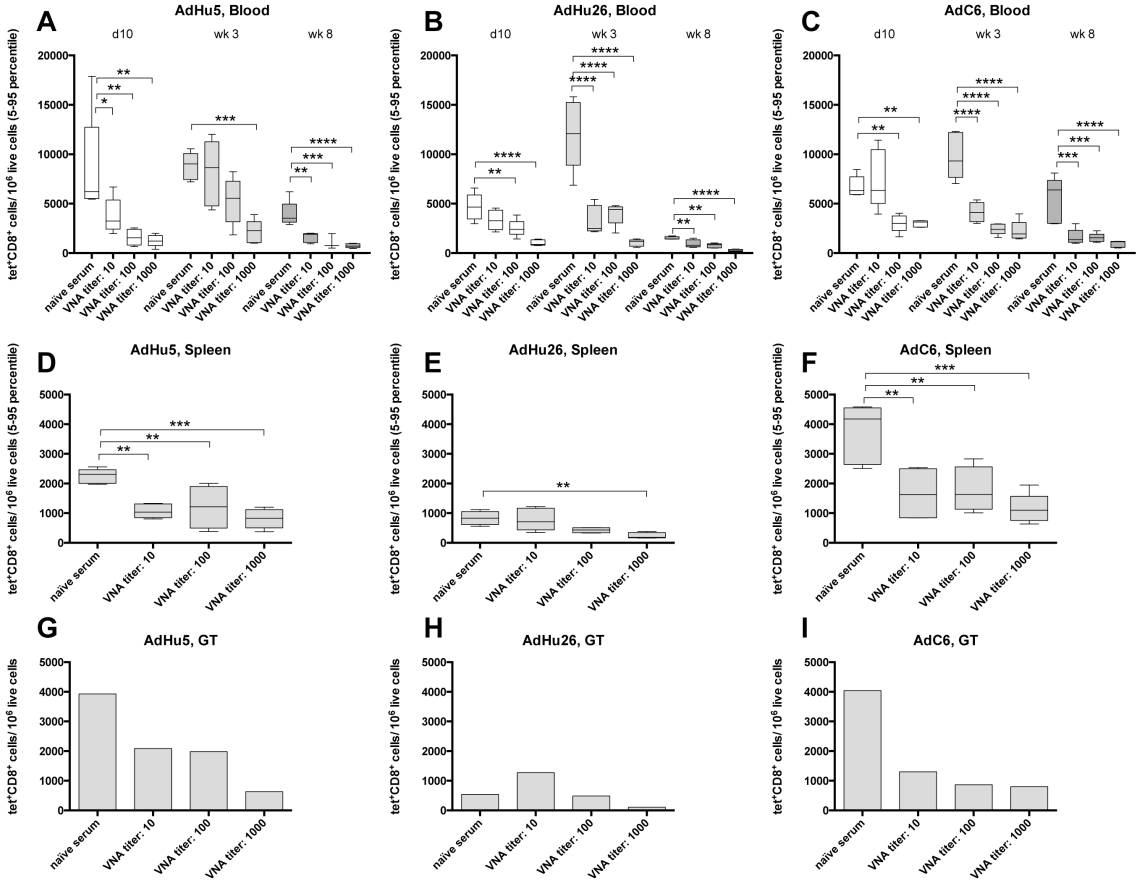

Groups of female BALB/c mice (5 per group) were injected with pooled serum from donor mice that had been immunized twice with an Ad vector expressing the rabies virus glycoprotein. Doses of serum were adjusted so that titers of Ad-specific VNAs measured from recipient mice 24 hours later equaled 1:10, 1:100 or 1:1000. Control mice received a volume of serum from naïve donor mice that equaled the highest volume of the immune serum. Mice were injected after serum transfer with 10^{10} vp of the Ad vector that was homologous to the Ad used to induce the transferred serum. Ad vectors expressed HIVgag. Significant differences are indicated by * for p-values ≤ 0.05-0.01, ** p-values < 0.01-0.001, *** p-values ≤ 0.001-0.0001, **** p-values < 0.0001. Lines show the comparison groups.

[A-C] Mice were bled on day 10 (white bars), 3 (light grey bars) and 8 weeks (dark grey bars) later and frequencies of gag-specific CD8$^+$ T cells were determined from individual mice by staining with a specific tetramer. Data are expressed as average numbers of tetramer (tet)$^+$CD8$^+$ cells per 10^6 live PBMCs ± standard deviations (SD). Differences between numbers of immune versus naïve serum were determined by one-way ANOVA with Dunnett correction for type 1 errors. The following p-values were obtained: **[A]** AdHu5: d10: 1:10 p=0.044, 1:100 p=0.0037, 1:1000 p=0.0025; wk 3: 1:1000 p=0.0006; wk 8: 1:10 p=0.0012, 1:100 p=0.0007, 1:1000 p<0.0001; **[B]** AdHu26: d10: 1:100 p=0.007, 1:1000 p<0.0001; wk 3: all serum dilutions p<0.0001, wk 8: 1:10 p=0.0012, 1:100 p=0.0013, 1:1000 p<0.0001; **[C]** AdC6: d10 1:100 p=0.0073, 1:1000 p=0.0068, wk 3: 1:10 p<0.0001, 1:100 p<0.0001, 1:1000 p<0.0001; wk 8: 1:10 p=0.0006, 1:100 p=0.0004, 1:1000 p<0.0001.

[D-F] Splenocytes were tested 8 weeks after immunization. The following p-values were obtained: (by one-way ANOVA with Dunnett correction for type 1 errors.): **[D]** AdHu5: d10: 1:10 p=0.001, 1:100 p=0.0044, 1:1000 p=0.0002, **[E]** AdHu26: 1:1000 p=0.0061, **[F]** AdC6: 1:10 p=0.0057, 1:100 p=0.0086, 1:1000 p=0.0006.

FIGURE LEGEND CONTINUED ON PAGE 113

FIGURE 5.2. CD4$^+$ T cell responses in blood and spleen and recruitment to the genital tract.

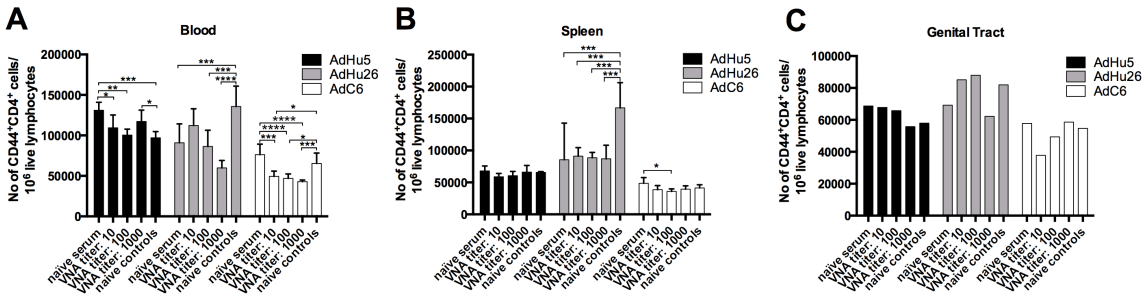

The graphs show relative numbers of CD44$^+$CD3$^+$CD8$^-$ cells isolated 8 weeks after immunization from blood **[A]**, the spleen **[B]**, and the pooled genital tracts **[C]** of the same mice shown in Figure 5.1. CD4$^+$ cells were identified upon staining for CD8 and CD3 as cells that were CD3$^+$CD8$^-$. Graphs shows numbers of cells over 10^6 live cells ± standard deviations (SD). Significant differences between the number of lymphocytes from (I) naive serum vs. immune serum and (II) number of lymphocytes from naïve mice vs. immunized mice were determined by one-way ANOVA with Dunnet correction for type 1 errors. The following p-values were obtained: **[A] (I)** AdHu5: 1:10 p = 0.025, 1:100 p = 0.0015; AdC6: 1:10 p = 0.0002, 1:100 p < 0.0001, 1:1000 p < 0.0001; **(II)** AdHu5: naïve serum: p = 0.0005, 1:1000 p = 0.0387; AdHu26: naïve serum: p = 0.0082, 1:100 p = 0.0038, 1:1000 p < 0.0001; AdC6: 1:10 p = 0.0378, 1:100 p = 0.0148, 1:1000 p = 0.0030 **[B] (I)** AdC6: 1:100 p = 0.0143. **(II)** AdHu26: naïve serum: p = 0.0035, 1:10 p = 0.0064, 1:100 p = 0.0049, 1:1000 p = 0.0041.

Significant differences are indicated by * for p-values ≤ 0.05-0.01, ** p-values < 0.01-0.001, *** p-values ≤ 0.001-0.0001, **** p-values < 0.0001. Lines show the comparison groups.

CONTINUED FROM PAGE 112:

[G-E] The graphs show results of genital tract samples pooled from 5 mice as relative numbers of Gag-specific CD8$^+$ T cells over 10^6 live lymphocytes.

FIGURE 5.3. Pre-existing Ad-specific VNAs increase frequencies of transgene product-specific CD62L^{+}CD8^{+} T cells.

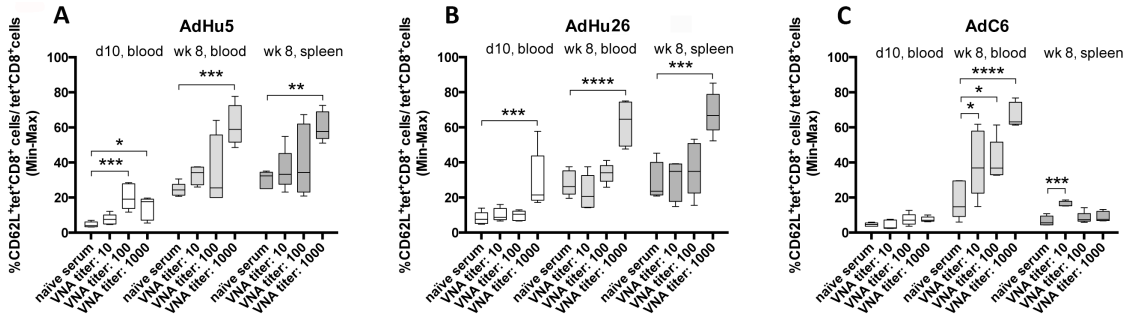

Blood-derived Gag-specific CD8^{+} T cells, identified by stains for CD3, CD8 and the Gag-specific tetramer from groups of 5 mice serum treated and immunized as in Figure 5.1 were tested for expression of CD62L 10 days (white bars) and 8 weeks (light grey bars) after immunization. Splenocytes (dark grey bars) were tested at 8 weeks after immunization with 10^{10} vp of either AdHu5-gag **[A]**, AdHu26-gag **[B]**, or AdC6-gag **[C]**. Differences between frequencies in serum recipients vs. controls were determined by one-way ANOVA with Dunnett correction for type 1 errors. The following p-values were obtained for blood: **[A]** AdHu5: d 10: 1:100 p = 0.0005, 1:1000 p = 0.027, wk 8: 1:1000 p = 0.0014; **[B]** AdHu26: d 10: 1:1000 p = 0.0046, wk 8: 1:1000 p<0.0001; **[C]** AdC6: wk 8: 1:10 p = 0.045, 1:100 p = 0.032, 1:1000 p <0.0001 and spleens: **[A]** AdHu5 1:1000 p = 0.0044, **[B]** AdHu26 1:1000 p = 0.0008, **[C]** AdC6 1:10 p = 0.0001.

Significant differences are indicated by * for p-values ≤ 0.05-0.01, ** p-values < 0.01-0.001, *** p-values ≤ 0.001-0.0001, **** p-values < 0.0001. Lines show the comparison groups.

Antigenic load during T cell priming is a determining factor in memory $CD8^+$ T cell development [122]. Therefore, the increased frequencies of Gag-specific $CD8^+$ T cells highly expressing CD62L could reflect that the vector-specific VNAs neutralized the vector and thus reduced the antigenic load available for induction of $CD8^+$ T cell responses. If the vector-specific VNAs reduced the amount of antigen available for priming, mice immunized with fewer viral particles would be expected to have the same increased frequencies of $CD62L^{hi}$ Gag-specific $CD8^+$ T cells. To this end, groups of mice were immunized with AdHu5gag at doses 100- (10^8 vp) and 10-fold (10^9 vp) lower than used in the previous experiments. As expected, five and eight weeks after immunization the magnitude of Gag-specific $CD8^+$ T cells in the blood was significantly reduced when lower doses of vector were used (**Figure 5.4A**). Nevertheless, the frequency of $CD62L^{hi}$ Gag-specific $CD8^+$ T cells was not increased with any dose of vector (**Figure 5.4B**), suggesting that a mechanism other than reduction of vector load at priming is at play.

A second possible mechanism is that the vector-specific VNAs altered the Ad vectors' ability to transduce the lymphocytes that would serve as the viral reservoir during persistence. To address this, groups of C57BL/6 mice were treated with naïve serum or a dose AdHu5-specific hyperimmune serum resulting in a circulating titer of 1:340. Mice were immunized 24 hours later with 10^{10} vp of an AdHu5-based vaccine that expressed a influenza nucleoprotein fused to GFP by the immunodominant epitope of ovalbumin (NPOVAGFP). A naïve group of mice were included as a negative control. Five weeks after immunization, mice were sacrificed and genomic DNA was isolated from splenocytes. The DNA (20 ng) was then tested for the AdHu5 vector genome using highly sensitive nested PCR against AdHu5 hexon (**Figure 5.5**). As expected, the genome was not detected in the naïve mice but was detected in three out of five mice that were immunized following transfer of naïve serum. The AdHu5 genome could only be faintly detected in one of three mice that had been treated with AdHu5-specific VNAs, largely suggesting the VNAs altered the vector's persistence, which would allow for increased transition into central memory.

FIGURE 5.4. Low doses of Ad vector fail to promote increases of transgene product-specific CD62L$^+$CD8$^+$ T cells.

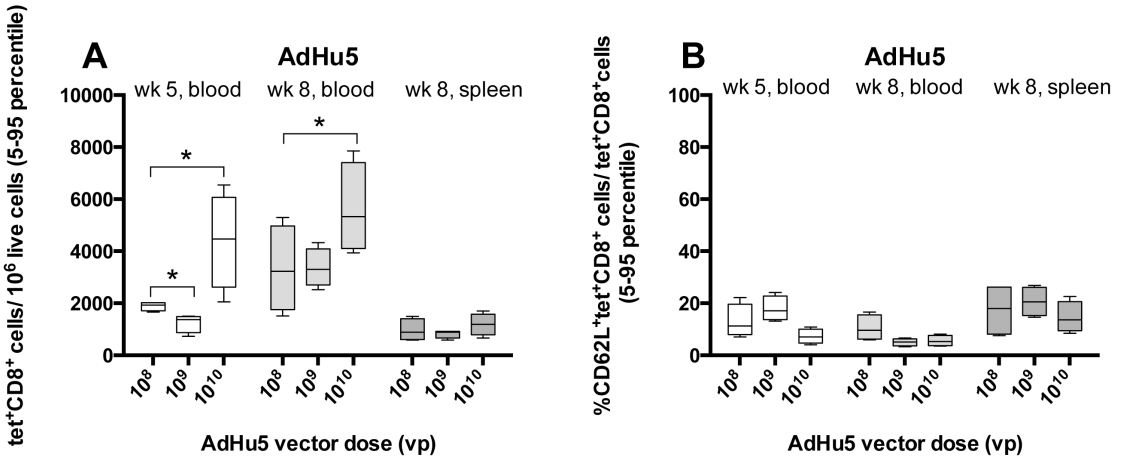

Groups of 4 mice were vaccinated with 10^8, 10^9 or 10^{10} vp of AdHu5-gag vector. **[A]** PBMCs were tested 5 (white bars) and 8 (light grey bars) weeks later, splenocytes were tested 8 weeks later (dark grey bars) for numbers of Gag-tet$^+$CD8$^+$ T cells over 10^6 live lymphoid cells. Data were analyzed by ANOVA with uncorrected Fischer's LSD. Lines show the comparison groups. The following differences were significant in blood: wk 5: 10^8 vs. 10^9 vp p = 0.012, 10^9 vs. 10^{10} vp p = 0.047; wk 8: 10^8 vs. 10^{10} vp p = 0.033. **[B]** Tet$^+$CD8$^+$ T cells were tested for expression of CD62L and the right graph shows % CD62L$^+$Gag-specific CD8$^+$ T cells over all Gag-specific CD8$^+$ T cells. There were no differences in percentages of CD62L$^+$ cells.

Significant differences are indicated by * for p-values ≤ 0.05-0.01, ** p-values < 0.01-0.001, *** p-values ≤ 0.001-0.0001, **** p-values < 0.0001. Lines show the comparison groups.

FIGURE 5.5. Pre-existing Ad-specific VNAs reduce persistence of Ad vector genome.

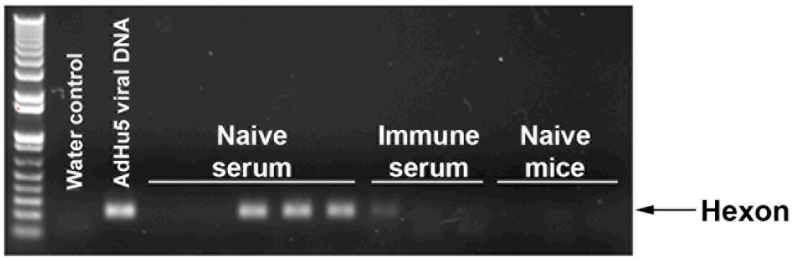

Mice received naïve serum (n=5) or AdHu5 immune serum at a dose between the middle and high titers from previous experiments (1:320) (n=3) and were immunized 24 hours later with 10^{10} vp AdHu5-NPOVAGFP vector. A control group (n=3) was unimmunized. Splenocytes were tested 5 weeks later for AdHu5 hexon DNA by nested PCR and real-time nested PCR. Amplicons from non-quantitative nested PCR (250 bp) were analyzed on 1% TAE gel.

To further characterize the Gag-specific $CD8^+$ T cells induced in the presence of the high titer of AdHu5-specific VNAs, additional differentiation markers were analyzed, including killer cell lectin-like receptor subfamily G member 1 (KLRG1), a marker of terminal differentiation that has been shown to reflect a $CD8^+$ T cell's stimulation history in that its expression is increased on cells that repeatedly encounter their antigen [124,148], CCR7, a chemokine receptor that regulates T cell migration to the lymphoid tissues and whose co-expression with CD62L on T lymphocytes is used to differentiate between effector memory (low expression) and central memory (high expression) [103,233], and CD127, the IL-7 receptor which is required for formation of memory [234]. As in the previous set of experiments, mice treated with the high dose of AdHu5-specific VNAs had higher frequencies of circulating $CD62L^+$ Gag-specific $CD8^+$ T cells eight weeks after immunization with AdHu5-gag. Consistent with the idea that the VNAs reduced vector persistence, the frequencies of $KLRG1^+$ Gag-specific $CD8^+$ T cells were significantly lower in mice that had been primed in the presence of AdHu5-specific VNAs (**Figure 5.6A**). Trends toward higher frequencies of $CCR7^+$ and $CD127^+$ Gag-specific $CD8^+$ T cells were observed but did not reach statistical significance.

A hallmark characteristic of memory $CD8^+$ T cells is that they have a very high proliferative capacity. As such, they vastly expand during recall responses. Therefore, in order to functionally confirm that the VNAs led to better induction of $CD8^+$ T cell memory, each group of mice received a second immunization with a heterologous Ad vector. Eight weeks after priming with AdHu5-gag, all groups of mice were boosted with 10^{10} vp AdC7-gag. A group of naïve mice was primed as a control. Gag-specific $CD8^+$ T cell responses were analyzed in the blood ten days later (**Figure 5.6B**). As expected, the numbers of responding cells vastly expanded in all mice, regardless of VNAs at the time priming. Although boosting resulted in higher numbers of Gag-specific $CD8^+$ T cells in mice primed in the absence of VNAs, it is worth noting that these mice had significantly higher frequencies at the time of the boost. As such, comparison of the relative increases of Gag-specific $CD8^+$ T cells between the two groups of mice revealed that the cells isolated from mice with circulating VNAs at the time of the prime expanded more robustly (35-fold) than those mice treated with naïve serum (14-fold). The frequencies of $CD62L^+$ Gag-specific

$CD8^+$ T cells were notably lower than before the prime and were comparable between both groups of mice; whereas $CCR7^+$ and $CD127^+$ frequencies were unchanged (**Figure 5.6C**). The frequencies of Gag-specific $CD8^+$ T cells that were $KLRG1^+$ were increased in both groups after the boost, as expected, but the pattern observed before the boost remained: fewer $KLRG1^+$ Gag-specific $CD8^+$ T cells were detected in mice who bore pre-existing AdHu5-specific VNAs at the time priming (**Figure 5.6C**).

Expression of certain markers on Gag-specific $CD8^+$ T cells at 8 weeks after the prime correlated very significantly with the fold increases in numbers of specific cells due to their expansion following the boost. Even though the slightly higher frequencies of $CD127^+$ Gag-specific $CD8^+$ observed in the mice primed in the presence of pre-existing VNAs was not significant, the frequency of $CD127^+$ cells measured just before boosting was directly correlated to Gag-specific $CD8^+$ T cell expansion after boosting (**Figure 5.6D**). As expected, the frequency of $KLRG1^+$ Gag-specific $CD8^+$ T cells 8 weeks after priming was inversely correlated to their expansion after the boost (**Figure 5.6E**). Correlations to $CD62L^+$ cells, on the other hand, were not significant (not shown). As a whole, these data indicate that priming in the presence of vector-specific neutralizing antibodies (NAb) enhances transition into memory and, thus, leads to more robust recall responses.

Serotype-specific neutralizing antibodies are primarily directed against the hypervariable loops on hexon [13], although other capsid components, such as penton and fiber, can also be targets [235]. Other, more conserved capsid elements, such as the hexon stalk, are targets for antibodies that cross-react between two distinct serotypes. Therefore, the induction and fate of transgene product-specific $CD8^+$ T cells were analyzed in mice that were primed with a heterologous vector in the presence of Ad vector-specific hyperimmune serum. First, each hyperimmune serum used in the experiments described above was assessed for reactivity with vectors derived from AdHu5, AdHu26, AdC6, and chimpanzee serotype 7 (AdC7) using ELISAs (**Figure 5.7A**). Although each serum preferentially reacted with the homologous vector used for induction, cross-reactivity between the different serotypes was observed. AdHu26 did not significantly bind antibodies from AdHu5 and AdC6 hyperimmune serum. While AdHu5 virus

cross-reacted with AdHu26 and AdC6 sera, the highest levels of cross reactivity were observed for the chimpanzee vectors, especially for AdC7 which very significantly bound antibodies from all three hyperimmune sera.

AdHu26 has a high seroprevalence rate in developing nations [228] and transfer of AdHu26-specific VNAs strongly reduced induction of transgene product-specific $CD8^+$ T cell responses following AdHu26-gag vaccination (**Figure 5.1**), causing a pronounced increase in Gag-specific $CD62L^+CD8^+$ T cells as early as 3 weeks after vaccination (**Figure 5.3**). Additionally as AdHu26 sera showed strong cross-reactivity with AdC7 vector (**Figure 5.7A**), the hyperimmune serum was chosen to continue investigation into the role, if any, cross-reactive antibodies play in modulating $CD8^+$ T cell responses to heterologous Ad vectors. The AdHu26 sera's capacity to neutralize AdC7 was next measured (**Figure 5.7B**). A virus neutralizing antibody assay was performed using naïve BALB/c and the AdHu26 hyperimmune serum to test the neutralization of AdC7 expressing GFP (AdC7-GFP). As a positive control for neutralization, AdHu26-GFP was included. The neutralization titer was determined as the dilution at which the serum neutralized 90% GFP expression. A titer of 10 or below was considered non-neutralizing. As expected, naïve serum neutralized neither AdHu26-GFP nor AdC7-GFP. Additionally, AdHu26 hyperimmune serum had an extremely high titer of AdHu26-specific neutralizing NAbs that neutralized AdHu26-GFP at the 1:40960 dilution. However, this serum did not neutralize AdC7-GFP.

In order to determine if immunization in the presence of heterologous vector-specific antibodies affected transgene product-specific $CD8^+$ T cell responses, AdHu26 hyperimmune serum was transferred to BALB/c mice such that the mice had a circulating AdHu26-specific VNA titer of 1:1000 six days later at the time of immunization. Control mice received naïve serum. Mice were immunized with 10^{10} AdC7-gag. Gag-specific $CD8^+$ T cell responses were measured ten days and four weeks later in the blood and eight weeks later in the spleen. Gag-specific $CD8^+$ T cell responses were comparable between both the control mice and the mice that had received AdHu26-hyperimmune serum (**Figure 5.7C**), indicating that AdHu26-specific antibodies failed to neutralize AdC7 vector *in vivo.* CD62L, CCR7, KLRG1, and CD127 expression on Gag-specific

$CD8^+$ T cells in blood were measured four weeks after vaccination. Expression of all four markers was comparable between both groups (**Figure 5.7D**), indicating that priming in the presence of heterologous vector-specific antibodies did not alter differentiation of transgene product-specific $CD8^+$ T cells. Taken together these data indicate that vector-specific neutralizing antibodies are responsible for the observed phenomena in these studies.

FIGURE 5.6. Ad-specific VNAs present at the time of priming promote recall responses.

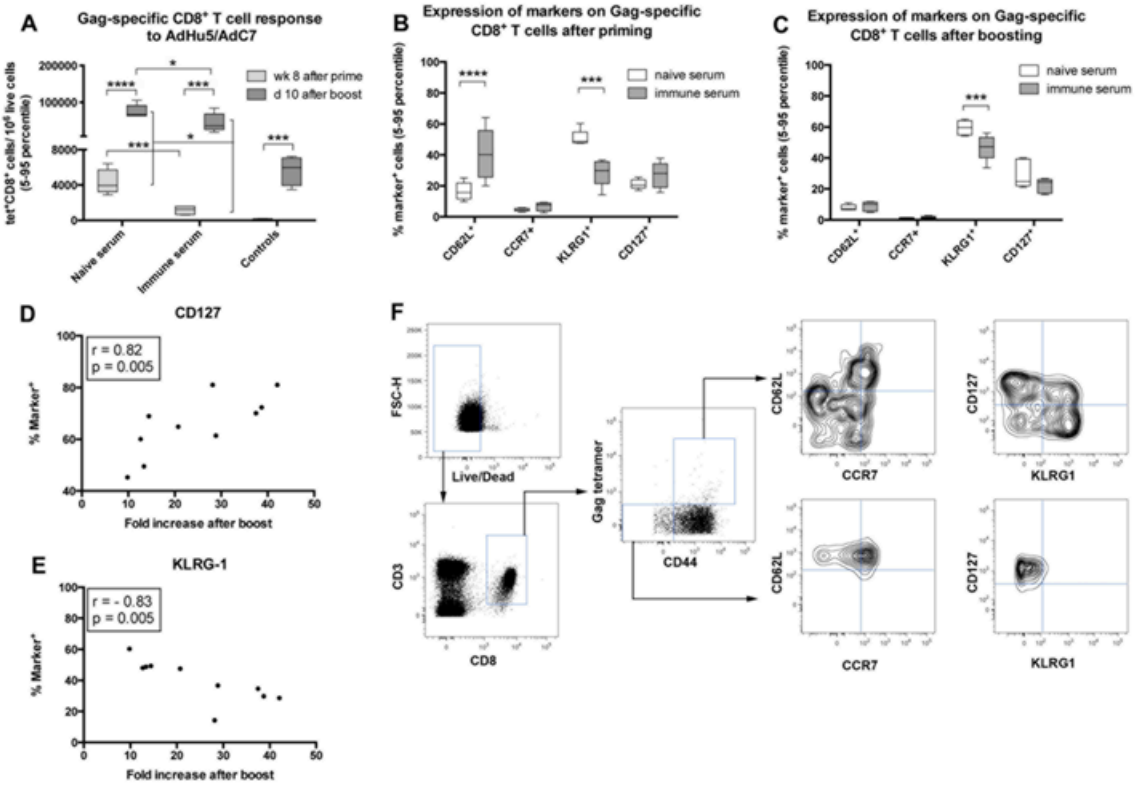

[A] A group of 5 BALB/c mice were transferred with an AdHu5 immune serum given at a dose that resulted in a 1:1000 titers of VNAs in the recipient mice. Another group of 5 mice received the same volume of serum from naïve mice. Both groups were vaccinated with 10^{10} vp of AdHu5-gag after serum transfer. A third group of 5 mice was left untreated (Controls). Eight weeks later mice were bled and Gag-specific $CD8^+$ T cells were measured (light grey bars). All mice were vaccinated the following day with 10^{10} vp of AdC7-gag vector. Gag-specific $CD8^+$ T cell responses were measured from blood 10 days later (dark grey bars). Graphs show number of Gag-specific $CD8^+$ T cells identified by staining with the tetramer over 10^6 live lymphoid cells as bars (min to max) ± SD. Differences between the two groups of serum recipients were determined by t-tests. The following p values were obtained comparing recipients of immune vs naïve serum: after priming p = 0.0044. Differences of the same cohort comparing data after priming to those after the boost gave the following p-values: naïve serum recipients p < 0.0001, immune serum recipients p = 0.0043. Fold increases of numbers of Gag-specific $CD8^+$ T cells were calculated (number after the boost divided by numbers before the boost). Differences between the two groups were significant: p = 0.011. Controls (no priming, AdHu5 at the time of boost) p = 0.0001.

[B] Graphs show percentage of Gag-specific $CD8^+$ T cells tested 8 weeks after immunization for expression of CD62L, CCR7, KLRG1 and CD127. Differences were determined by multiple t-test with Sidak-Holm correction. The following significant p-values were obtained: CD62L p< 0.0001, KLRG1 p = 0.00012.

[C] Graph shows percentages of Gag-specific $CD8^+$ T cells positive for the indicated markers over all $CD8^+$ T cells at 10 days after the boost for mice that receive immune or naïve serum before priming. Differences were calculated by multiple t-test with Sidak-Holm correction. Only KLRG1 was differentially expressed (p = 0.0004). Significant differences are indicated by * for p-values ≤ 0.05-0.01, ** p-values < 0.01-0.001, *** p-values ≤ 0.001-0.0001, **** p-values < 0.0001. Lines show the comparison groups.

[D] and **[E]** show correlations between fold increases after the boost and % of Gag-specific $CD8^+$ T cells positive for CD127 or KRLG-1 respectively. R and p-values are shown within the graphs.

FIGURE LEGEND CONTINUED ON PAGE 123

FIGURE 5.7. Effect of pre-existing Ad-specific antibodies on transgene product-specific CD8$^+$ T cells to a heterologous Ad vector.

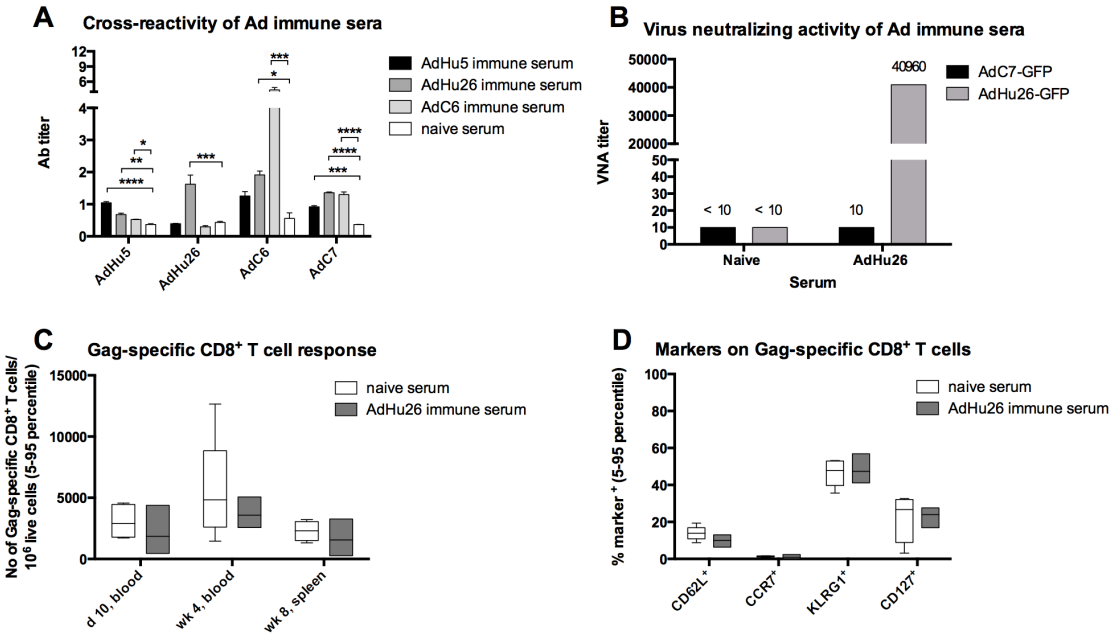

[A] Graph shows binding of the transferred sera to different Ad serotypes as shown in the legend within the figure. Titers were calculated by determining the area under the curve of adsorbance data obtained by serially diluted sera. ELISAs were conducted in duplicate wells and results shows mean ± SD. Differences in titer of immune sera to naïve sera were calculated by ANOVA with Dunnett correction. The following sera showed significant reactivity with the following vectors: AdHu5 serum: on AdHu5 vector $p < 0.00001$, on AdC7 vector $p = 0.0006$; AdHu26 serum on AdHu5 vector $p = 0.0013$, on AdHu26 vector $p = 0.0008$, on AdC6 vector $p = 0.0132$; on AdC7 vector $p < 0.0001$; AdC6 serum on AdHu5 vector $p = 0.016$, on AdC6 vector $p = 0.0003$; on AdC7 vector $p < 0.0001$.

[B] Graph shows analysis of naive BALB/c sera and AdHu26 hyperimmune sera for neutralization of AdHu26 or AdC7. Sera were tested for virus-neutralizing antibodies (VNA) against AdC7-GFP and AdHu26-GFP using VNA assay. Titers of 10 and below were considered non-neutralizing.

[C-D] Groups of 5 mice were injected with a dose of AdHu26-immune serum that resulted in a VNA titer of 1:1000 or an equal dose of serum from naïve mice. Mice were then immunized with AdC7gag. **[C]** shows Gag-specific CD8$^+$ T cell responses tested from blood 10 days and 4 weeks later and spleens 8 weeks later.

[D] shows frequencies of Gag-specific CD8$^+$ T cells that were positive for the indicated markers.

Significant differences are indicated by * for p-values ≤ 0.05-0.01, ** p-values < 0.01-0.001, *** p-values ≤ 0.001-0.0001, **** p-values < 0.0001. Lines show the comparison groups.

CONTINUED FROM PAGE 122:

[F] shows the gating strategy of a representative sample. After lymphocytes were identified based on FSC and SSC, doublets were excluded (not shown). Live cells were identified based on exclusion of live/dead stain. CD8$^+$ T cells were gated (CD3$^+$CD8$^+$). The subsequent gates were designed to isolate Gag-specific CD8$^+$ T cells (tetramer$^+$CD44$^+$) and naïve cells (tetramer$^+$CD44^{low}) as an internal control. Each population was then gated on CD62L and CCR7 or CD127 and KLRG1 based on naïve cells' expression of each.

DISCUSSION

Ad vectors are very attractive vaccine platforms thanks to their robust induction of B and T cell responses. However a major obstacle to use of these vectors is that virus-neutralizing antibodies (VNAs) to them are common. Historically, AdHu5 has been one of the most commonly studied vectors for this purpose. However, infection with AdHu5 often occurs during childhood, and, as such, pre-existing immunity to this virus is extremely common. Prior studies have demonstrated that the seroprevalence of AdHu5-specific neutralizing antibodies among adults in developed nations, including the United States and those constituting Europe, is typically between 30-60% [228,231,236], although serum immunoglobulin against Ad may be found in all individuals [237]. These seroprevalance rates are dramatically increased in developing nations. Studies suggest that prevalence rates of neutralizing antibodies against AdHu5 are between 70-80% in Brazil [228,232], between 75-100% in the Asian nations of Thailand [228,231] and India [238], and between 80-100% in sub-Saharan nations [228,231,236]. In all regions, about 30% or more of adults have moderate to high titers of AdHu5-specific VNAs [232]. As these neutralizing antibodies can dampen the vector's immunogenicity, this high seroprevalance of AdHu5-specific neutralizing antibodies poses a challenge to the development of AdHu5-based vaccines to protect against pathogens that plague the developing world.

A common strategy to circumvent the problem of pre-existing immunity to common Ad serotypes is development of vectors based on uncommon Ad serotypes. So-called "rare" human serotypes, such as AdHu26, circulate less frequently in humans. This "rare" designation is largely based on seroprevalence rates found in the developed world. Indeed, AdHu26 neutralizing antibodies are found in approximately 20% of adults in the United States and only 2% carry a titer of 1:200 or greater [228]. However, AdHu26 is not particularly rare in developing nations. Approximately 65-85% of adults in sub-Saharan Africa are seropositive for neutralizing antibodies against AdHu26. Prevalence of individuals carrying titers of 1:200 or greater seems to vary in this region but ranged from 0-22% [228]. Elsewhere, including South America and Asia, AdHu26-specific neutralizing antibody seroprevalance rates range from about 40-70% [228,232], with 32-37%

of adults carrying high titers [228]. Based on the seroprevalence rates, it would be expected that immunogenicity of an AdHu26-based vaccine would also be compromised. Therefore, others have focused on the development of vectors based on non-human adenovirus serotypes that do not circulate in humans, particularly those isolated from chimpanzees, e.g. AdC6. Pre-existing immunity to AdC6 is very rare in the United States and Thailand [229,231]. Seroprevalance climbs to nearly 20% of adults in certain regions of sub-Saharan Africa [231], which was speculated to be due to the chimpanzee populations endemic to those regions. Native populations of New World monkeys genetically unrelated to chimpanzees may be responsible for the similar seroprevalance rate found in adults living in the Brazilian rainforest [232].

This high incidence of pre-existing immunity to Ad has prompted extensive work looking at how pre-existing immunity to adenovirus affects induction of T cell responses following vaccination with an Ad-based vaccine. Models focusing on pre-exposing mice [92] and NHP [216,217] to adenovirus prior to vaccination have revealed that transgene product-specific $CD8^+$ T cell responses are reduced in these animals. Pre-exposure to Ad induces both cellular and humoral immunity directed against the vector. Neutralizing antibodies are generally directed against the hypervariable loops of hexon [13,235], although NAb against fiber and penton are also detected [235]. Ad-specific T cells have also been described [237]. While pre-exposure models at least in part mirror naturally acquired Ad infections in humans, these studies do not differentiate between the individual roles that the cellular and humoral components play in the reduction of responses. As such, both arms of the adaptive immune system have been implicated [93]. A recent study in which B cell-deficient mice were pre-exposed to Ad before vaccination revealed that induction of transgene product-specific $CD8^+$ T cells was unaffected by pre-exposure [239], suggesting that vector neutralizing antibodies are primarily responsible for this reduction. Thus, the study presented here was performed in order to assess how pre-existing Ad-specific neutralizing antibodies present at the time of immunization affect induction and differentiation of transgene product-specific $CD8^+$ T cells generated by vectors based on distinct Ad serotypes. The experiments presented here clearly demonstrate that pre-existing vector neutralizing antibodies present at the time of immunization, regardless of serotype, dramatically inhibit transgene

product-specific $CD8^+$ T cell responses in the blood, spleen, and genital tract. However, the results presented above demonstrate that priming of the $CD8^+$ T cell response still occurs in a manner that is indirectly related to the titer of vector-specific NAbs present at priming. This likely indicates that not all vector particles are neutralized and that some remain to infect target cells and prime T cell responses.

The vectors presented in this study each represent different *Adenoviridae* families, as such, they may have differences in their biology, including their ability to bind to receptors and co-receptors, their inflammatory potential that induces innate responses and their tropism, which all could affect their capacity to induce transgene product-specific $CD8^+$ T cells in the face of pre-existing VNAs. Although each vector was sensitive to neutralization by homologous vector-specific VNAs, differences in the kinetics of transgene product-specific $CD8^+$ T cell induction were observed. VNAs present at the time of immunization with either vector reduced induction of Gag-specific responses at the earliest time point measured. However, immunization with AdHu5-gag in the presence of VNAs induced robust peak responses that were only significantly reduced in mice treated with the highest dose of serum. These results are consistent with another report that demonstrated using an AdHu5 pre-exposure model, which induced titers of AdHu5-specific VNAs in mice ranging from 1:40-1:80 [240], that although circulating transgene product-specific $CD8^+$ T cell responses were reduced in the presence of vector specific immunity, they still induced peak responses. Gag-specific $CD8^+$ T cells induced in the presence of vector-specific VNAs by AdHu26-gag and AdC6-gag did not show this peak response and instead remained low through the experiment.

Ad vectors persist at low levels in a transcriptionally active state in activated T cells and maintain a pool of activated effector transgene product-specific $CD8^+$ T cells that have delayed kinetics in their transition into the central memory pool [123]. Unexpectedly, vector-specific neutralizing antibodies present at high titers at the time of immunization promoted transgene product-specific $CD8^+$ T cells' transition into the memory pool, as evidenced by increased CD62L expression and very robust recall responses. It is well known that $CD8^+$ T cell responses and fate decisions are influenced by conditions present early in their activation. One such condition is the

amount and duration of antigenic stimulation. High levels of antigen and longer TCR engagement tend to favor differentiation towards effector populations, while limiting amounts of antigen available for priming favors development of the central memory population [122]. Therefore, it was possible that increased CD62L expression observed on Gag-specific $CD8^+$ T cells primed in the presence of vector-specific NAb was caused by the reduction of antigen available due to neutralization of the vector. However, this result was not recapitulated by simply decreasing the vector dosage 100-fold. While it is possible that the vector dose was not decreased enough in order to observe increased CD62L expression, further dosage reduction would likely compromise a measurable response.

Alternatively, pre-existing immunity could alter the innate immune response induced by the Ad vector. Inflammation during T cell priming provides the danger signal to the T cell and dramatically impacts $CD8^+$ T cell differentiation. High inflammation favors development of more terminally differentiated effector cells [114] while reduction of inflammation enhances development of more plastic central memory cells [241]. These developmental decisions are mediated at the transcriptional level during T cell priming. The level of inflammatory cytokines directly affects the level of T-bet expression in a dose-dependent manner [182] ultimately shifting the balance of expression between T-bet and Eomesodermin. In a follow up to the STEP trial, a systems biology approach using gene mapping revealed that AdHu5 seropositive individuals had dampened inflammatory responses following vaccination with Merck's Ad5-based vaccine [242]. Therefore, Ad-specific VNAs in the study presented here may have reduced inflammation at the time of priming and thus promoted differentiation towards memory. $CD4^+$ T cell help during the primary response is required for induction of $CD8^+$ T cell memory responses, although this is dependent on the infectious agent. $CD4^+$ T cell help promotes the activation and maturation of dendritic cells, thus increasing their expression of CD80 and CD86, to provide costimulation to T cells through CD28, and of proinflammatory cytokines, especially IL-12 [243]. It is therefore possible that $CD4^+$ T cell help played a role in changing the priming environment in the context of pre-existing vector-specific neutralizing antibodies. The study presented here does not rule out this possibility and this could be addressed by repeating these studies in $CD4^+$ T cell-deficient or MHC-II-deficient

mice. Although an important caveat is that studies using CD4-deficient and -depleted mice have demonstrated that generation of proper $CD8^+$ T cell responses following adenovirus immunization requires $CD4^+$ T cell help [244].

These NAb-virus immune complexes could in turn affect the natural tropism of the virus. The majority of adenoviruses enter cells by binding the coxsackie adenovirus receptor (CAR) however coating in antibodies could retarget the virus to cells bearing Fc-receptors. *In vitro* studies have revealed that these immune complexes are potentially capable of infecting and expressing transgenes in cells that express FcγR [245]. T cells, which are capable of expressing Fc receptors either endogenously following activation [223] or by acquiring them via trogocytosis from APCs [246,247], serve as the reservoir for adenovirus during its persistence [65,123]. However, instead of enhancing transduction of T cells, the Ad-specific VNAs seem to reduce the vector reservoir within them. In fact, we were not able to detect Ad vector genome in two out of three samples of splenic lymphocytes from animals primed in the presence of vector specific-VNAs, but Ad genome was detected in three out of five animals primed in the absence of vector specific-VNAs. We performed the same nested PCR on splenocytes isolated from mice used in the boost experiment shown in **Figure 5.5.** We were able to detect AdHu5 genome in 5 out of 5 mice primed in the absence of AdHu5-specific VNAs but were unable to detect AdHu5 genome in 4 of 5 mice primed in the presence of AdHu5-specific VNAs (data not shown). Although these two experiments are not quantitative they nevertheless suggest that pre-existing neutralizing antibodies may interfere with the establishment of a persisting viral reservoir. This in turn may have influenced the long-term development of central memory Gag-specific $CD8^+$ T cells by reducing the persisting transgene product. KLRG1 expression reflects a T cell's antigenic stimulation history as it is more highly expressed with subsequent rounds of antigen exposure [124,148]. Frequencies of $KLRG1^{hi}$ Gag-specific $CD8^+$ T cells were reduced in mice primed in the presence of vector-specific NAbs. Therefore, this could indicate that there was less persistent antigen available to stimulate the transgene product-specific $CD8^+$ T cells.

These results have important implications for the use of Ad vectors as vaccine carriers as they clearly demonstrate that although the primary response is attenuated in the presence of vector-specific immunity, this does not preclude a robust secondary response.

MATERIALS AND METHODS

Generation of immune sera

Groups of 20 BALB/c mice were immunized IM with 10^{11} vp of AdHu5-, AdHu26-, or AdC6-rab.gp and boosted IM 6 weeks later with 10^{11} vp of the identical vector used for priming. Mice were bled 4 weeks after the boost to confirm titers of Ad-specific VNAs. Mice immunized with AdHu5-rab.gp and AdHu26-rab.gp were euthanized 5 weeks after the boost, serum was collected and VNA titers were determined to be 1:13,000 and 1:40,000, respectively. Mice immunized with AdC6-rab.gp were boosted a second time and euthanized 6 weeks later. The serum VNA titer was determined to be 1:20,000.

Titration of Ad-specific VNAs

Sera were incubated at 56°C for 30 minutes. 100 µl of serial, two-fold dilutions, starting at 1:20, were incubated with a GFP-expressing Ad matching the serotype used for immunization for 1 hour at 37°C. The virus-serum mixtures were added to HEK 293 cells in 96-well plates and incubated overnight at 37°C. The cells were analyzed for GFP expression 24 hours later. The VNA titer was determined by the highest dilution with less than 50% GFP-positive cells when compared to control wells.

Administration of immune sera and immunization of mice

Immune sera were passively transferred into mice to achieve VNA titers of 1:1000, 1:100 and 1:10. Sera were diluted in sterile PBS to a volume of 200 µl per mouse and were administered IP. One group of mice received naïve BALB/c serum diluted to the highest dose of immune serum. Mice were bled to confirm appropriate VNA titers 5 days after transfer and immunized the following day IM with 10^{10} vp of the indicated vector diluted in 100 µl of sterile PBS.

Enzyme-linked immunoadsorbent assay (ELISA)

ELISA plates were coated with 10^8 vp/well of AdHu5-HIVgag, AdHu26-HIVgag, AdC6-HIVgag, or AdC7-HIVgag in 100 µl of coating buffer [2 carbonate-bicarbonate capsules (Sigma-Aldrich) dissolved in 100 mL H_2O] and incubated overnight at 4°C. Plates were washed with 0.05% Tween (Biorad; Hercules, CA) in PBS (PBS-T) and blocked overnight at 4°C with 3% BSA (Sigma-Aldrich) in PBS-T (blocking buffer). After PBS-T wash, two-fold serial dilutions of AdHu5, AdHu26, and AdC6 immune sera starting at 1:200 were incubated on coated plates for 2 hours at room temperature. Plates were washed with PBS-T and alkaline phosphatase (AP)-conjugated anti-mouse IgG (Sigma-Aldrich) diluted to 1:30,000 was applied to plates for 1 hour at room temperature. At the end of the incubation, plates were washed, developed (2 tabs phosphatase substrate (Sigma-Aldrich) dissolved in 10 mL diethanolamine buffer (KPL; Gaithersburg, Maryland) and read 30 minutes later at 405 nm. All samples were run in duplicates.

Tetramer staining

Lymphocytes were stained with an APC-labeled tetramer against the immunodominant MHC class I restricted epitope of HIV-1 Gag (AMQMLKETI). Additionally, cells were stained with antibodies to CD3, CD8, CD44, KLRG1 (Southern Biotech, Birmingham, AL), CD62L (BD Pharmingen, San Jose, CA), CD127, CCR7 (eBioscience, San Diego,CA). Unless otherwise indicated, antibodies were from Biolegend (San Diego, CA). A stain for dead cells was included in the panel.

Data acquisition and analysis for tetramer stains

Samples were run on a BD-LSR II and analyzed by FlowJo software. After lymphoid cell acquisition, doublets and dead cells were removed and samples were gated on $CD3^+CD8^+$ T cells. Remaining cells were plotted as tetramer against CD44. Data is shown as tet^+CD8^+ T cells/10^6 live lymphoid cells. Additionally, tet^+CD44^+ cells were phenotyped for the markers described above. A gate on the $CD44^{lo}$ $CD8^+$ T cells served an internal, naïve control for

phenotyping. In the genital tract, lymphocytes were additionally gated on $CD3^+CD8^-$ T cells to assess the $CD4^+$ T cell population.

Nested polymerase chain reaction

C57Bl/6 mice were treated with naïve serum or AdHu5 hyperimmune serum at a VNA titer greater than 1:100. Mice were immunized IM 24 hours later with 10^{10} vp of AdHu5-NPOVAGFP. Mice were euthanized and splenocytes were harvested 4 weeks later. Genomic DNA was isolated using DNeasy Tissue kit (Qiagen; Valencia, CA). 20 ng of genomic DNA from each sample were used to first amplify AdHu5 hexon by polymerase chain reaction (PCR) using 5' primer: 5'-ATCATGCAGCTGGGAGAGTC-3' and 3' primer: 5'-ACACCTCCCAGTGGAAAGCA-3'. The PCR consisted of 30 cycles of 95°C for 30 seconds, 55°C for 30 seconds, and 72°C for 30 seconds. The resulting PCR fragment was 650 bp. The amplicon from the first PCR was diluted 1:50 and 1 µL was used as template for quantitative nested PCR. The 5' and 3' primers, 5'-GAC TCC TAA AGT GGT ATT GT-3' and 5'-GTC TTG CAA ATC TAC AAC AG-3', respectively, amplified a 250 bp fragment. The nested PCR consisted of 40 cycles of 95°C for 30 seconds, 56.8°C for 30 seconds, and 72°C for 30 seconds.

Statistical analysis

Significance of differences between 2 populations were calculated by t-tests with Sidak-Holm correction for type 1 errors in multiple tests. When normality of distribution could not be assumed, differences were analyzed by Mann-Whitney tests. Differences between multiple groups were tested by ANOVA with Dunnett correction for type 1 errors, Tukey's multiple comparison tests or with uncorrected Fischer's LSD as indicated in the figure legends. Correlations were conducted by Spearman with Bonferroni corrections for type 1 errors. Data were analyzed by GraphPad Prism 6.

CHAPTER 6

CONCLUSIONS

The contribution of central memory and effector memory $CD8^+$ T cells in controlling infection is dependent on a number of factors, most notably the infecting pathogen. Indeed numerous studies have demonstrated roles for each subset. Results from the LCMV clone 13 model have suggested that central memory $CD8^+$ T cells, with their capacity to generate large amounts of effector $CD8^+$ T cells upon secondary antigen encounters, are more suited to control infections once pathogens have spread systemically [107]. Evidence for this also comes from HIV vaccine models, which have suggested that more anamnestic responses are necessary to lower viral set point loads once the acute infection phase has passed [135]. On the other hand, numerous other studies suggested that effector memory $CD8^+$ T cells, with their more activated, cytotoxic nature and localization at the periphery, are necessary to halt pathogens as they invade. This subset of cells is attributed to mediating early control of a highly pathogenic SIV in an HIV vaccine model based on a CMV-based vaccine [134,135]. Studies of these subsets have led to the paradigm that effector memory cells are the first line of defense at the port of viral entry while central memory cells provide a second line of defense that provides backup in the event of a pathogen that overwhelms the first line of defense.

As adenoviruses continue to be pursued as vaccine carriers, understanding their interaction with the immune system and how memory responses are induced to their transgene products is of the utmost importance. Adenoviral vectors are desirable vaccine carriers because they induce potent and sustained $CD8^+$ T cell responses that are biased toward effector memory. In these chapters we demonstrate that antigen-experienced cells maintain the transgene product-specific $CD8^+$ T cell pool with little to no contribution from newly primed naïve $CD8^+$ T cells. These data may give us insight into how memory responses following adenoviral immunization fit current models of memory formation. One model states that memory responses are programmed during priming and the fate of a newly activated T cell is determined by the sum of the signals it receives at it is primed [114,115,248]. Alternatively, the linear differentiation model states that memory differentiation occurs along a continuum following the effector phase [107,111]. In the latter model,

cells that survive contraction will progressively dedifferentiate from effector cells to effector memory cells to central memory cells. An important point in this model is that this de-differentiation occurs in the absence of antigen [107], which largely suggests that in persistent infections, central memory cells will never form. However, our data seem to suggest that antigen-experienced cells maintain the $CD8^+$ T_{EM} pool induced by adenovirus immunization. If central memory cells are truly formed and recalled by persisting antigen, then this would suggest that they were programmed and not dedifferentiating from effectors. Therefore, memory formation following adenovirus immunization does not conform the linear differentiation model. In support of this, others have found that halting transcription from the adenoviral genome two months after priming does not cause a contraction to central memory [211], as would be expected if memory formation after infection with an adenovirus vector conformed to the linear differentiation model.

An optimal vaccine against a given pathogen will likely need to induce immune responses that mimic natural, protective immune responses induced by the pathogen itself. Ample evidence highlights that both $CD8^+$ T_{EM} and T_{CM} play a role in these protective immune responses [107,249]. A primary goal of this thesis was to create a tractable vaccine carrier that could induce a $CD8^+$ T cell response with a better balance between central memory and effector memory. A factor that has been found to influence the balance of $CD8^+$ T cell memory is antigen persistence. Since adenoviral vectors remain transcriptionally active during persistence we created vectors that would allow us to temporally regulate transgene transcription. Their unexpected recombination highlights the importance of considering stability when designing novel adenoviral vectors.

Novel approaches to gain transcriptional control over a transgene would have to be explored. Transgenic mouse models expressing site-specific recombinanses are readily available. Additionally, inducible promoters are commonly used to control gene expression experimentally. While these are viable approaches and allow us to further address how transgene expression influences T cell responses in in mouse models, a larger goal is to investigate how continued transgene expression influences immune responses in larger animal models, including non-human primates. An interesting approach may be to take advantage of a cellular pathway for regulating gene expression. Small, non-coding RNAs, including microRNAs (miRNA), bind to and

prevent translation of mature mRNA sequences. Their role in regulating myriad cellular processes is well documented and has been extended to the immune system. Indeed miRNAs have been discovered that are differentially expressed during the differentiation of $CD8^+$ T cells, and are therefore likely involved in determining the gene expression profiles of naïve, effector, and memory $CD8^+$ T cell subsets [250,251]. As adenoviral vector genomes are enriched and transcriptionally active in effector-like $CD8^+$ T cells, taking advantage of more highly expressed miRNA in those subsets may allow us to regulate when and where transgenes are expressed.

The metabolic processes involved in T cell fate decisions continue to be studied. mTOR has been identified as an important modulator of T cell responses that integrates the complex signals involved in T cell activation to coordinate the dramatic metabolic changes required for T cell differentiation [154,181]. Given this role, it has been suggested that drugs that target mTOR, specifically complex 1, could be used as novel vaccine adjuvants to enhance the magnitude and rate of central memory differentiation. However, results from this thesis suggest that rapamycin as a vaccine adjuvant may not be applicable to vaccine modalities that persist *in vivo*, as we failed to observe any significant enhancement in differentiation of $CD8^+$ T cells to central memory. The reason for this may simply be that as the vector persists, and continues to produce transgene product, low dosing of rapamycin may not be able to overcome ongoing T cell receptor-induced mTOR activation. As we gain deeper understanding of the metabolic pathways involved in regulating T cell fate decisions in settings in which viruses and other pathogens persist, pathways other than those influencing mTOR complex 1 will emerge that may allow us to manipulate memory differentiation. Indeed, a role for mTOR complex 2 in driving the rapid switch to glycolysis in reactivation of memory $CD8^+$ T cells has recently been described [252].

Preclinically, adenoviral vectors have performed well as vaccine carriers. However, results from clinical trials have thus far been disappointing, if not concerning. Testing of Merck's AdHu5-based HIV vaccine in the STEP trial was halted in 2007 due futility. Analysis revealed that T cell responses against the vaccine's antigens were induced, although they were not particularly strong and were limited in breadth. However, what was more troubling was that vaccinated men who were AdHu5 seropositive and uncircumcised at the time of vaccination were at increased risk

of becoming infected with HIV-1 compared to placebo recipients [220]. This risk was transient and has not been observed in other Ad-based HIV vaccine trials [253,254]. Regardless, in response to these alarming results, many continue to investigate the influence of pre-existing immunity to adenoviral vectors on the induction of *de novo* $CD8^+$ T cell responses. In an effort to characterize vectors from different subgroups of adenoviruses under consideration for vaccine development, we discovered that while pre-existing neutralizing antibodies specific to the adenovirus capsid dampen *de novo* $CD8^+$ T cell responses they also accelerate and enhance $CD8^+$ T cell central memory differentiation in mice. These results are counterintuitive in light of the STEP trial and raise an important question: how could an anamnestic, central memory-biased $CD8^+$ T cell response increase HIV-1 acquisition? This result is also seemingly in contrast with a mouse infection model that demonstrates that $CD8^+$ T cells primed in the context of both pre-existing cellular and humoral immunity to a vector mount rapid anamnestic transgene product-specific CD8+ T cell responses to effectively control an infection that is typically prevented by effector memory T cells [249]. Given the complexity of HIV and the speed with which it escapes immune control, our results may in fact reinforce the concept that a successful HIV-1 vaccine will need to induce a layered response of both B and T cells. T cells should include both potent effector memory cells that localize to the mucosa and a central memory cells to control virus once it becomes systemic. In support of this, while the CMV-based HIV-1 vaccine candidate that induces a strong effector memory T cell response but no anamnestic central memory T cells provides early protection from SIV infection in 50% of vaccinated monkeys, those with breakthrough infections develop high viral loads similar to unvaccinated control animals [134,135].

Although the reasons for the increased HIV acquisition observed in the STEP trial continue to elude us, pre-existing immunity to a vaccine carrier should be considered in the interest of safety when designing vaccines. Indeed, adenoviral vectors based on serotypes less common than AdHu5 are being tested in the clinic [225]. Our results here suggest that pre-existing immunity will likely impact these vectors as well. In fact, it is safe to assume pre-existing immunity may be detrimental regardless of the platform. Fortunately for the adenoviral platform,

development of alternative, non-human serotypes that do not circulate in humans is under way [94,96,225].

In testing candidate vaccines, we assess them in various animal models, including mice and monkeys, before testing can begin in humans. Millions of years of evolution have led to vastly different immune systems and responses to pathogens. Indeed this holds true for adenoviruses and immune responses against them. It has been demonstrated that ongoing anti-adenovirus immune responses to persistent adenoviruses in humans and monkeys are very different from each other. Adenovirus seems to undergo substantial chronic replication and is consistently shed in monkeys; in humans the virus is more latent and shedding in general is only observed for a few weeks following an acute infection [255]. This ultimately impacts immune responses, monkeys mount stronger systemic humoral responses and humans mount stronger cellular responses [255]. The impact this has on immunization with adenoviral vectors and the interpretation of results in animal models is an important future route.

It is with hope that the studies presented in this thesis continue to stimulate investigation into the optimization of adenovirus-based vaccines. Further understanding of factors that influence $CD8^+$ T cell memory development, particularly in settings involving persistent vaccine carriers, will enable development of vaccines that can be tailored to particular pathogens. Manipulation of factors involved in fate decisions in order to enhance vaccine development continues to be an exciting area of research.

CHAPTER 7

REFERENCES

1. Hllleman, M. R. & Werner, J. H. Recovery of New Agent from Patients with Acute Respiratory Illness. *Exp Biol Med (Maywood)* **85,** 183–188 (1954).

2. ROWE, W. P., HUEBNER, R. J. & GILMORE, L. K. Isolation of a cytopathogenic agent from human adenoids undergoing spontaneous degeneration in tissue culture. *Proc Soc Exp Biol Med* **84,** 570-573 (1953).

3. Rainbow, A. J. & Castillo, J. E. Homologous recombination of adenovirus DNA in mammalian cells: enhanced recombination following UV-irradiation of the virus. *Mutat. Res.* **274,** 201–210 (1992).

4. Young, C. S. & Fisher, P. B. Adenovirus recombination in normal and repair-deficient human fibroblasts. *Virology* **100,** 179–184 (1980).

5. Robinson, C. M. *et al.* Molecular evolution of human adenoviruses. *Sci Rep* **3,** 1812 (2013).

6. Dehghan, S. *et al.* Computational analysis of four human adenovirus type 4 genomes reveals molecular evolution through two interspecies recombination events. *Virology* **443,** 197–207 (2013).

7. Robinson, C. M. *et al.* Computational analysis and identification of an emergent human adenovirus pathogen implicated in a respiratory fatality. *Virology* **409,** 141–147 (2011).

8. Walsh, M. P. *et al.* Evidence of molecular evolution driven by recombination events influencing tropism in a novel human adenovirus that causes epidemic keratoconjunctivitis. *PLoS ONE* **4,** e5635 (2009).

9. Rux, J. J., Kuser, P. R. & Burnett, R. M. Structural and phylogenetic analysis of adenovirus hexons by use of high-resolution x-ray crystallographic, molecular modeling, and sequence-based methods. *J. Virol.* **77,** 9553–9566 (2003).

10. Duncan, M. *et al.* Adenoviruses isolated from wild gorillas are closely related to human species C viruses. *Virology* **444,** 119–123 (2013).

11. Colloca, S. *et al.* Vaccine vectors derived from a large collection of simian adenoviruses induce potent cellular immunity across multiple species. *Sci Transl Med* **4,** 115ra2–115ra2 (2012).

12. Lasaro, M. O. & Ertl, H. C. J. New insights on adenovirus as vaccine vectors. *Mol. Ther.* **17,** 1333–1339 (2009).

13. Sumida, S. M., Truitt, D. M. & Lemckert, A. Neutralizing antibodies to adenovirus serotype 5 vaccine vectors are directed primarily against the adenovirus hexon protein. *J Immunol* **174**, 7179-7185 (2005).

14. Shayakhmetov, D. M. & Lieber, A. Dependence of adenovirus infectivity on length of the fiber shaft domain. *J. Virol.* **9,** 1408-1412 (2000).

15. Wu, E., Pache, L., Seggern, Von, D. J. & Mullen, T. M. Flexibility of the adenovirus fiber is required for efficient receptor interaction. *J Virol* **77,** 7225-7235 (2003).

16. Philipson, L., Lonberg-Holm, K. & Pettersson, U. Virus-receptor interaction in an

adenovirus system. *J. Virol.* **2,** 1064–1075 (1968).

17. Henry, L. J., Xia, D., Wilke, M. E., Deisenhofer, J. & Gerard, R. D. Characterization of the knob domain of the adenovirus type 5 fiber protein expressed in Escherichia coli. *J. Virol.* **68,** 5239–5246 (1994).

18. Wu, L., Rosser, D. S., Schmidt, M. C. & Berk, A. A TATA box implicated in E1A transcriptional activation of a simple adenovirus 2 promoter. *Nature* **326,** 512–515 (1987).

19. Jones, N. & Shenk, T. An adenovirus type 5 early gene function regulates expression of other early viral genes. *Proc. Natl. Acad. Sci. U.S.A.* **76,** 3665–3669 (1979).

20. Culp, J. S. *et al.* The 289-amino acid E1A protein of adenovirus binds zinc in a region that is important for trans-activation. *Proc. Natl. Acad. Sci. U.S.A.* **85,** 6450–6454 (1988).

21. Murray, J. D., Bellett, A. & Braithwaite, A. W. Altered cell cycle progression and aberrant mitosis in adenovirus-infected rodent cells. *Journal of Cellular Physiology* **111,** 89-96 (1982).

22. Braithwaite, A. W. *et al.* Adenovirus-induced alterations of the cell growth cycle: a requirement for expression of E1A but not of E1B. *J. Virol.* **45,** 192–199 (1983).

23. Howe, J. A. & Bayley, S. T. Effects of Ad5 E1A mutant viruses on the cell cycle in relation to the binding of cellular proteins including the retinoblastoma protein and cyclin A. *Virology* **186,** 15–24 (1992).

24. Harford, C. G., Hamlin, A., Parker, E. & van Ravenswaay, T. ELECTRON MICROSCOPY OF HELA CELLS INFECTED WITH ADENOVIRUSES. *J Exp Med* **104,** 443–454 (1956).

25. Lonberg-Holm, K., Crowell, R. L. & Philipson, L. Unrelated animal viruses share receptors. *Nature* **259,** 679–681 (1976).

26. Bergelson, J. M. *et al.* Isolation of a common receptor for Coxsackie B viruses and adenoviruses 2 and 5. *Science* **275,** 1320–1323 (1997).

27. Cohen, C. J. *et al.* The coxsackievirus and adenovirus receptor is a transmembrane component of the tight junction. *Proc. Natl. Acad. Sci. U.S.A.* **98,** 15191–15196 (2001).

28. Roelvink, P. W. *et al.* The coxsackievirus-adenovirus receptor protein can function as a cellular attachment protein for adenovirus serotypes from subgroups A, C, D, E, and F. *J. Virol.* **72,** 7909–7915 (1998).

29. Walters, R. W. *et al.* Basolateral localization of fiber receptors limits adenovirus infection from the apical surface of airway epithelia. *J. Biol. Chem.* **274,** 10219–10226 (1999).

30. Walters, R. W. *et al.* Adenovirus Fiber Disrupts CAR-Mediated Intercellular Adhesion Allowing Virus Escape. *Cell* **110,** 789–799 (2002).

31. Defer, C., Belin, M. T., Caillet-Boudin, M. L. & Boulanger, P. Human adenovirus-host cell interactions: comparative study with members of subgroups B and C. *J. Virol.* **64,** 3661–3673 (1990).

32. Gaggar, A., Shayakhmetov, D. M. & Lieber, A. CD46 is a cellular receptor for group B adenoviruses. *Nat. Med.* **9,** 1408–1412 (2003).

33. Wang, H. *et al.* Desmoglein 2 is a receptor for adenovirus serotypes 3, 7, 11 and 14. *Nat. Med.* **17,** 96–104 (2011).

34. Short, J. J. *et al.* Adenovirus serotype 3 utilizes CD80 (B7.1) and CD86 (B7.2) as cellular attachment receptors. *Virology* **322,** 349–359 (2004).

35. Dechecchi, M. C., Melotti, P. & Bonizzato, A. Heparan sulfate glycosaminoglycans are receptors sufficient to mediate the initial binding of adenovirus types 2 and 5. *J Virol* **75,** 8772-8780 (2001).

36. Hong, S. S., Karayan, L., Tournier, J., Curiel, D. T. & Boulanger, P. A. Adenovirus type 5 fiber knob binds to MHC class I alpha2 domain at the surface of human epithelial and B lymphoblastoid cells. *EMBO J.* **16,** 2294–2306 (1997).

37. Davison, E., Kirby, I., Elliott, T. & Santis, G. The human HLA-A* 0201 allele, expressed in hamster cells, is not a high-affinity receptor for adenovirus type 5 fiber. *J. Virol.* **73,** 4513-4517 (1999).

38. Burmeister, W. P., Guilligay, D., Cusack, S., Wadell, G. & Arnberg, N. Crystal structure of species D adenovirus fiber knobs and their sialic acid binding sites. *J. Virol.* **78,** 7727–7736 (2004).

39. Leon, R. P., Hedlund, T., Meech, S. J. & Li, S. Adenoviral-mediated gene transfer in lymphocytes. *Proc Natl Acad Sci* **95,** 13159-13164 (1998).

40. Wickham, T. J., Mathias, P., Cheresh, D. A. & Nemerow, G. R. Integrins alpha v beta 3 and alpha v beta 5 promote adenovirus internalization but not virus attachment. *Cell* **73,** 309-319 (1993).

41. Bai, M., Harfe, B. & Freimuth, P. Mutations that alter an Arg-Gly-Asp (RGD) sequence in the adenovirus type 2 penton base protein abolish its cell-rounding activity and delay virus reproduction in flat cells. *J. Virol.* **67,** 5198–5205 (1993).

42. Chardonnet, Y. & Dales, S. Early events in the interaction of adenoviruses with HeLa cells. I. Penetration of type 5 and intracellular release of the DNA genome. *Virology* **40,** 462–477 (1970).

43. Patterson, S. & Russell, W. C. Ultrastructural and Immunofluorescence Studies of Early Events in Adenovirus-HeLa Cell Interactions. *J. Gen. Virol.* **64,** 1091–1099 (1983).

44. Leopold, P. L., Ferris, B., Grinberg, I. & Worgall, S. Fluorescent virions: dynamic tracking of the pathway of adenoviral gene transfer vectors in living cells. *Hum Gene Ther* **9,** 367-378 (1998).

45. Greber, U. F., Willetts, M., Webster, P. & Helenius, A. Stepwise dismantling of adenovirus 2 during entry into cells. *Cell* **75,** 477–486 (1993).

46. Kelkar, S. A., Pfister, K. K., Crystal, R. G. & Leopold, P. L. Cytoplasmic dynein mediates adenovirus binding to microtubules. *J. Virol.* **78,** 10122–10132 (2004).

47. Wisnivesky, J. P., Leopold, P. L. & Crystal, R. G. Specific binding of the adenovirus capsid to the nuclear envelope. *Hum. Gene Ther.* **10,** 2187–2195 (1999).

48. Fox, J. P. *et al.* The virus watch program: a continuing surveillance of viral infections in metropolitan New York families. VI. Observations of adenovirus infections: virus

excretion patterns, antibody response, efficiency of surveillance, patterns of infections, and relation to illness. *Am. J. Epidemiol.* **89,** 25–50 (1969).

49. Garnett, C. T. *et al.* Latent species C adenoviruses in human tonsil tissues. *J. Virol.* **83,** 2417–2428 (2009).

50. Fox, J. P., Hall, C. E. & Cooney, M. K. The Seattle Virus Watch. VII. Observations of adenovirus infections. *Am. J. Epidemiol.* **105,** 362–386 (1977).

51. Bates, P. R., Bailey, A. S., Wood, D. J., Morris, D. J. & Couriel, J. M. Comparative epidemiology of rotavirus, subgenus F (types 40 and 41) adenovirus and astrovirus gastroenteritis in children. *Journal of Medical Virology* **39,** 224–228 (1993).

52. Dingle, J. H. & Langmuir, A. D. Epidemiology of acute, respiratory disease in military recruits. *Am. Rev. Respir. Dis.* **97,** Suppl:1–65 (1968).

53. Kampmann, B. *et al.* Improved outcome for children with disseminated adenoviral infection following allogeneic stem cell transplantation. *Br. J. Haematol.* **130,** 595–603 (2005).

54. Durepaire, N. *et al.* Detection of adenovirus DNA by polymerase chain reaction in peripheral blood lymphocytes from HIV-infected patients and a control group: preliminary results. *J. Acquir. Immune Defic. Syndr. Hum. Retrovirol.* **14,** 189–190 (1997).

55. Yan, Z., Nguyen, S., Poles, M., Melamed, J. & Scholes, J. V. Adenovirus colitis in human immunodeficiency virus infection: an underdiagnosed entity. *Am. J. Surg. Pathol.* **22,** 1101–1106 (1998).

56. Curlin, M. E. *et al.* Frequent detection of human adenovirus from the lower gastrointestinal tract in men who have sex with men. *PLoS ONE* **5,** e11321 (2010).

57. Adrian, T., Schäfer, G., Cooney, M. K., Fox, J. P. & Wigand, R. Persistent enteral infections with adenovirus types 1 and 2 in infants: no evidence of reinfection. *Epidemiol. Infect.* **101,** 503–509 (1988).

58. EVANS, A. S. Latent adenovirus infections of the human respiratory tract. *Am J Hyg* **67,** 256–266 (1958).

59. Neumann, R., Genersch, E. & Eggers, H. J. Detection of adenovirus nucleic acid sequences in human tonsils in the absence of infectious virus. *Virus Res.* **7,** 93–97 (1987).

60. August, C. S., Merler, E., Lucas, D. O. & Janeway, C. A. The response in vitro of human lymphocytes to phytohemagglutinin and to antigens after fractionation on discontinuous density gradients of albumin. *Cellular Immunology* **1,** 603–618 (1970).

61. van der Veen, J. & Lambriex, M. Relationship of adenovirus to lymphocytes in naturally infected human tonsils and adenoids. *Infect. Immun.* **7,** 604–609 (1973).

62. Strohl, W. A. & Schlesinger, R. W. QUANTITATIVE STUDIES OF NATURAL AND EXPERIMENTAL ADENOVIRUS INFECTIONS OF HUMAN CELLS. I. CHARACTERISTICS OF VIRAL MULTIPLICATION IN FIBROBLASTS DERIVED BY LONG-TERM CULTURE FROM TONSILS. *Virology* **26,** 199–207 (1965).

63. Strohl, W. A. & Schlesinger, R. W. QUANTITATIVE STUDIES OF NATURAL AND

EXPERIMENTAL ADENOVIRUS INFECTIONS OF HUMAN CELLS. II. PRIMARY CULTURES AND THE POSSIBLE ROLE OF ASYNCHRONOUS VIRAL MULTIPLICATION IN THE MAINTENANCE OF INFECTION. *Virology* **26,** 208–220 (1965).

64. Nasz, I., Kulcsár, G., Dan, P. & Sallay, K. A Possible Pathogenic Role for Virus-Carrier Lymphocytes. *J Infect Dis.* **124,** 214–216 (1971).

65. Garnett, C. T., Erdman, D., Xu, W. & Gooding, L. R. Prevalence and quantitation of species C adenovirus DNA in human mucosal lymphocytes. *J. Virol.* **76,** 10608–10616 (2002).

66. Roy, S. *et al.* Adenoviruses in lymphocytes of the human gastro-intestinal tract. *PLoS ONE* **6,** e24859 (2011).

67. Huang, S., Endo, R. I. & Nemerow, G. R. Upregulation of integrins alpha v beta 3 and alpha v beta 5 on human monocytes and T lymphocytes facilitates adenovirus-mediated gene delivery. *J. Virol.* **69,** 2257–2263 (1995).

68. Wan, Y. Y. *et al.* Transgenic expression of the coxsackie/adenovirus receptor enables adenoviral-mediated gene delivery in naive T cells. *Proc. Natl. Acad. Sci. U.S.A.* **97,** 13784–13789 (2000).

69. Zhang, Y., Huang, W., Ornelles, D. A. & Gooding, L. R. Modeling adenovirus latency in human lymphocyte cell lines. *J. Virol.* **84,** 8799–8810 (2010).

70. Sengupta, S., Ulasov, I. V., Thaci, B., Ahmed, A. U. & Lesniak, M. S. Enhanced transduction and replication of RGD-fiber modified adenovirus in primary T cells. *PLoS ONE* **6,** e18091 (2011).

71. Schirm, S. & Doerfler, W. Expression of viral DNA in adenovirus type 12-transformed cells, in tumor cells, and in revertants. *J. Virol.* **39,** 694–702 (1981).

72. Kuwano, K. *et al.* Detection of group C adenovirus DNA in small-cell lung cancer with the nested polymerase chain reaction. *J. Cancer Res. Clin. Oncol.* **123,** 377–382 (1997).

73. Mackey, J. K., Rigden, P. M. & Green, M. Do highly oncogenic group A human adenoviruses cause human cancer? Analysis of human tumors for adenovirus 12 transforming DNA sequences. *Proc. Natl. Acad. Sci. U.S.A.* **73,** 4657–4661 (1976).

74. Kosulin, K., Hoffmann, F., Clauditz, T. S., Wilczak, W. & Dobner, T. Presence of adenovirus species C in infiltrating lymphocytes of human sarcoma. *PLoS ONE* **8,** e63646 (2013).

75. Harui, A., Suzuki, S., Kochanek, S. & Mitani, K. Frequency and stability of chromosomal integration of adenovirus vectors. *J. Virol.* **73,** 6141–6146 (1999).

76. Anderson, K. P. & Fennie, E. H. Adenovirus early region 1A modulation of interferon antiviral activity. *J. Virol.* **61,** 787–795 (1987).

77. Deryckere, F. & Burgert, H. G. Tumor necrosis factor alpha induces the adenovirus early 3 promoter by activation of NF-kappaB. *J. Biol. Chem.* **271,** 30249–30255 (1996).

78. Andersson, M., Pääbo, S., Nilsson, T. & Peterson, P. A. Impaired intracellular transport of class I MHC antigens as a possible means for adenoviruses to evade immune

surveillance. *Cell* **43,** 215–222 (1985).

79. Burgert, H. G. & Kvist, S. The E3/19K protein of adenovirus type 2 binds to the domains of histocompatibility antigens required for CTL recognition. *EMBO J.* **6,** 2019–2026 (1987).
80. Pääbo, S., Nilsson, T. & Peterson, P. A. Adenoviruses of subgenera B, C, D, and E modulate cell-surface expression of major histocompatibility complex class I antigens. *Proc. Natl. Acad. Sci. U.S.A.* **83,** 9665–9669 (1986).

81. Fu, J., Li, L. & Bouvier, M. Adenovirus E3-19K proteins of different serotypes and subgroups have similar, yet distinct, immunomodulatory functions toward major histocompatibility class I molecules. *J. Biol. Chem.* **286,** 17631–17639 (2011).

82. Hermiston, T. W., Hellwig, R., Hierholzer, J. C. & Wold, W. S. Sequence and functional analysis of the human adenovirus type 7 E3-gp19K protein from 17 clinical isolates. *Virology* **197,** 593–600 (1993).

83. McNees, A. L., Garnett, C. T. & Gooding, L. R. The adenovirus E3 RID complex protects some cultured human T and B lymphocytes from Fas-induced apoptosis. *J. Virol.* **76,** 9716–9723 (2002).

84. Zhou, D. *et al.* An efficient method of directly cloning chimpanzee adenovirus as a vaccine vector. *Nat Protoc* **5,** 1775–1785 (2010).

85. Dai, Y. *et al.* Cellular and humoral immune responses to adenoviral vectors containing factor IX gene: tolerization of factor IX and vector antigens allows for long-term expression. *Proc. Natl. Acad. Sci. U.S.A.* **92,** 1401–1405 (1995).

86. Yang, Y. *et al.* Cellular immunity to viral antigens limits E1-deleted adenoviruses for gene therapy. *Proc. Natl. Acad. Sci. U.S.A.* **91,** 4407–4411 (1994).

87. Kafri, T. *et al.* Cellular immune response to adenoviral vector infected cells does not require de novo viral gene expression: implications for gene therapy. *Proc. Natl. Acad. Sci. U.S.A.* **95,** 11377–11382 (1998).

88. Ouédraogo, A. *et al.* A phase 1b randomized, controlled, double-blinded dosage-escalation trial to evaluate the safety, reactogenicity and immunogenicity of an adenovirus type 35 based circumsporozoite malaria vaccine in Burkinabe healthy adults 18 to 45 years of age. *PLoS ONE* **8,** e78679 (2013).

89. Ledgerwood, J. E. *et al.* A replication defective recombinant Ad5 vaccine expressing Ebola virus GP is safe and immunogenic in healthy adults. *Vaccine* **29,** 304–313 (2010).

90. Barnes, E. *et al.* Novel adenovirus-based vaccines induce broad and sustained T cell responses to HCV in man. *Sci Transl Med* **4,** 115ra1–115ra1 (2012).

91. Vincent, T. *et al.* Rapid assessment of adenovirus serum neutralizing antibody titer based on quantitative, morphometric evaluation of capsid binding and intracellular trafficking: population analysis of adenovirus capsid association with cells is predictive of adenovirus infectivity. *J. Virol.* **75,** 1516–1521 (2001).

92. Xiang, Z. *et al.* Novel, chimpanzee serotype 68-based adenoviral vaccine carrier for induction of antibodies to a transgene product. *J. Virol.* **76,** 2667–2675 (2002).
93. Sumida, S. M., Truitt, D. M., Kishko, M. G. & Arthur, J. C. Neutralizing antibodies and CD8+ T lymphocytes both contribute to immunity to adenovirus serotype 5 vaccine

vectors. *J Virol* **78,** 2666-2673 (2004).

94. Vogels, R. *et al.* Replication-deficient human adenovirus type 35 vectors for gene transfer and vaccination: efficient human cell infection and bypass of preexisting adenovirus immunity. *J. Virol.* **77,** 8263–8271 (2003).

95. Liu, J. *et al.* Magnitude and phenotype of cellular immune responses elicited by recombinant adenovirus vectors and heterologous prime-boost regimens in rhesus monkeys. *J. Virol.* **82,** 4844–4852 (2008).

96. Tatsis, N. *et al.* Chimpanzee-origin adenovirus vectors as vaccine carriers. *Gene Ther.* **13,** 421–429 (2006).

97. Fitzgerald, J. C. *et al.* A simian replication-defective adenoviral recombinant vaccine to HIV-1 gag. *J. Immunol.* **170,** 1416–1422 (2003).

98. Plotkin, S. A. Vaccines: correlates of vaccine-induced immunity. *Clin. Infect. Dis.* **47,** 401–409 (2008).

99. Tan, J. T., Ernst, B., Kieper, W. C. & LeRoy, E. Interleukin (IL)-15 and IL-7 jointly regulate homeostatic proliferation of memory phenotype CD8+ cells but are not required for memory phenotype CD4+ cells. *J Exp Med* **195,** 1523-1532 (2002).

100. Schmidt, N. W. *et al.* Memory CD8 T cell responses exceeding a large but definable threshold provide long-term immunity to malaria. *Proc. Natl. Acad. Sci. U.S.A.* **105,** 14017–14022 (2008).

101. Badovinac, V. P., Messingham, K. A. N., Hamilton, S. E. & Harty, J. T. Regulation of CD8+ T cells undergoing primary and secondary responses to infection in the same host. *J. Immunol.* **170,** 4933–4942 (2003).

102. Fraser, K. A., Schenkel, J. M., Jameson, S. C., Vezys, V. & Masopust, D. Preexisting high frequencies of memory CD8+ T cells favor rapid memory differentiation and preservation of proliferative potential upon boosting. *Immunity* **39,** 171–183 (2013).

103. Sallusto, F., Lenig, D., Förster, R., Lipp, M. & Lanzavecchia, A. Two subsets of memory T lymphocytes with distinct homing potentials and effector functions. *Nature* **401,** 708–712 (1999).

104. Masopust, D., Vezys, V., Marzo, A. L. & Lefrançois, L. Preferential localization of effector memory cells in nonlymphoid tissue. *Science* **291,** 2413-2417 (2001).

105. Zeng, H. & Chi, H. mTOR and lymphocyte metabolism. *Curr. Opin. Immunol.* **25,** 347–355 (2013).

106. Harari, A., Bellutti Enders, F., Cellerai, C., Bart, P.-A. & Pantaleo, G. Distinct profiles of cytotoxic granules in memory CD8 T cells correlate with function, differentiation stage, and antigen exposure. *J. Virol.* **83,** 2862–2871 (2009).

107. Wherry, E. J. *et al.* Lineage relationship and protective immunity of memory CD8 T cell subsets. *Nat. Immunol.* **4,** 225–234 (2003).

108. Berard, M., Brandt, K., Bulfone-Paus, S. & Tough, D. F. IL-15 promotes the survival of naive and memory phenotype CD8+ T cells. *J. Immunol.* **170,** 5018–5026 (2003).

109. Stemberger, C. *et al.* A single naive CD8+ T cell precursor can develop into diverse

effector and memory subsets. *Immunity* **27,** 985–997 (2007).

110. Wherry, E. J. & Ahmed, R. Memory CD8 T-cell differentiation during viral infection. *J. Virol.* **78,** 5535–5545 (2004).

111. Kaech, S. M., Hemby, S., Kersh, E. & Ahmed, R. Molecular and functional profiling of memory CD8 T cell differentiation. *Cell* **111,** 837–851 (2002).

112. Opferman, J. T., Ober, B. T. & Ashton-Rickardt, P. G. Linear differentiation of cytotoxic effectors into memory T lymphocytes. *Science* **283,** 1745–1748 (1999).

113. Manjunath, N. *et al.* Effector differentiation is not prerequisite for generation of memory cytotoxic T lymphocytes. *J. Clin. Invest.* **108,** 871–878 (2001).

114. Joshi, N. S. *et al.* Inflammation directs memory precursor and short-lived effector CD8(+) T cell fates via the graded expression of T-bet transcription factor. *Immunity* **27,** 281–295 (2007).

115. Badovinac, V. P., Haring, J. S. & Harty, J. T. Initial T Cell Receptor Transgenic Cell Precursor Frequency Dictates Critical Aspects of the CD8+ T Cell Response to Infection. *Immunity* **26,** 827–841 (2007).

116. Obar, J. J., Khanna, K. M. & Lefrançois, L. Endogenous naive CD8+ T cell precursor frequency regulates primary and memory responses to infection. *Immunity* **28,** 859–869 (2008).

117. Bachmann, M. F. *et al.* Long-lived memory CD8+ T cells are programmed by prolonged antigen exposure and low levels of cellular activation. *Eur. J. Immunol.* **36,** 842–854 (2006).

118. Dong, H. *et al.* CD27 stimulation promotes the frequency of IL-7 receptor-expressing memory precursors and prevents IL-12-mediated loss of CD8(+) T cell memory in the absence of CD4(+) T cell help. *J. Immunol.* **188,** 3829–3838 (2012).

119. Huster, K. M. *et al.* Selective expression of IL-7 receptor on memory T cells identifies early CD40L-dependent generation of distinct CD8+ memory T cell subsets. *Proc. Natl. Acad. Sci. U.S.A.* **101,** 5610–5615 (2004).

120. Chang, J. T. *et al.* Asymmetric T lymphocyte division in the initiation of adaptive immune responses. *Science* **315,** 1687–1691 (2007).

121. Kaech, S. M. *et al.* Selective expression of the interleukin 7 receptor identifies effector CD8 T cells that give rise to long-lived memory cells. *Nat. Immunol.* **4,** 1191–1198 (2003).

122. Obar, J. J. & Lefrançois, L. Early signals during CD8+ T cell priming regulate the generation of central memory cells. *J Immunol* **185,** 263-272(2010).

123. Tatsis, N. *et al.* Adenoviral vectors persist in vivo and maintain activated CD8+ T cells: implications for their use as vaccines. *Blood* **110,** 1916–1923 (2007).

124. Masopust, D., Ha, S.-J., Vezys, V. & Ahmed, R. Stimulation history dictates memory CD8 T cell phenotype: implications for prime-boost vaccination. *J. Immunol.* **177,** 831–839 (2006).

125. Jabbari, A. & Harty, J. T. Secondary memory CD8+ T cells are more protective but slower to acquire a central-memory phenotype. *J Exp Med* **203,** 919–932 (2006).
126. Ochsenbein, A. F. *et al.* A comparison of T cell memory against the same antigen induced by virus versus intracellular bacteria. *Proc. Natl. Acad. Sci. U.S.A.* **96,** 9293–9298 (1999).

127. Bachmann, M. F. & Kündig, T. M. Protection against immunopathological consequences of a viral infection by activated but not resting cytotoxic T cells: T cell memory without 'memory T cells'? *Proc Natl Acad Sci* **94,** 640-645 (1997).

128. Haase, A. T. Perils at mucosal front lines for HIV and SIV and their hosts. *Nat. Rev. Immunol.* **5,** 783–792 (2005).

129. Berenzon, D. *et al.* Protracted protection to Plasmodium berghei malaria is linked to functionally and phenotypically heterogeneous liver memory CD8+ T cells. *J. Immunol.* **171,** 2024–2034 (2003).

130. Reyes-Sandoval, A. *et al.* CD8+ T effector memory cells protect against liver-stage malaria. *J. Immunol.* **187,** 1347–1357 (2011).

131. Hogan, R. J. *et al.* Activated antigen-specific CD8+ T cells persist in the lungs following recovery from respiratory virus infections. *J. Immunol.* **166,** 1813–1822 (2001).

132. Jones-Carson, J., McCollister, B. D., Clambey, E. T. & Vázquez-Torres, A. Systemic CD8 T-cell memory response to a Salmonella pathogenicity island 2 effector is restricted to Salmonella enterica encountered in the gastrointestinal mucosa. *Infect. Immun.* **75,** 2708–2716 (2007).

133. Girard, M. P. & Plotkin, S. A. HIV vaccine development at the turn of the 21st century. *Curr Opin HIV AIDS* **7,** 4–9 (2012).

134. Hansen, S. G. *et al.* Effector memory T cell responses are associated with protection of rhesus monkeys from mucosal simian immunodeficiency virus challenge. *Nat. Med.* **15,** 293–299 (2009).

135. Hansen, S. G. *et al.* Profound early control of highly pathogenic SIV by an effector memory T-cell vaccine. *Nature* **473,** 523–527 (2011).

136. Hatziioannou, T. & Evans, D. T. Animal models for HIV/AIDS research. *Nat. Rev. Microbiol.* **10,** 852–867 (2012).

137. Mueller, S. N. & Ahmed, R. High antigen levels are the cause of T cell exhaustion during chronic viral infection. *Proc Natl Acad Sci* **106,** 8623-8628 (2009).

138. Wherry, E. J. *et al.* Molecular signature of CD8+ T cell exhaustion during chronic viral infection. *Immunity* **27,** 670–684 (2007).

139. Wherry, E. J., Blattman, J. N., Murali-Krishna, K., van der Most, R. & Ahmed, R. Viral persistence alters CD8 T-cell immunodominance and tissue distribution and results in distinct stages of functional impairment. *J. Virol.* **77,** 4911–4927 (2003).

140. Yang, T.-C. *et al.* The CD8+ T cell population elicited by recombinant adenovirus displays a novel partially exhausted phenotype associated with prolonged antigen presentation that nonetheless provides long-term immunity. *J. Immunol.* **176,** 200–210 (2006).

141. Romero, P. *et al.* Four functionally distinct populations of human effector-memory CD8+ T lymphocytes. *J. Immunol.* **178,** 4112–4119 (2007).

142. Valenzuela, H. F. & Effros, R. B. Divergent telomerase and CD28 expression patterns in human CD4 and CD8 T cells following repeated encounters with the same antigenic stimulus. *Clin. Immunol.* **105,** 117–125 (2002).

143. Voehringer, D., Koschella, M. & Pircher, H. Lack of proliferative capacity of human effector and memory T cells expressing killer cell lectinlike receptor G1 (KLRG1). *Blood* **100,** 3698–3702 (2002).

144. Voehringer, D. *et al.* Viral infections induce abundant numbers of senescent CD8 T cells. *J. Immunol.* **167,** 4838–4843 (2001).

145. Tessmer, M. S. *et al.* KLRG1 binds cadherins and preferentially associates with SHIP-1. *Int. Immunol.* **19,** 391–400 (2007).

146. Gründemann, C. *et al.* Cutting edge: identification of E-cadherin as a ligand for the murine killer cell lectin-like receptor G1. *J. Immunol.* **176,** 1311–1315 (2006).

147. Thimme, R. *et al.* Increased expression of the NK cell receptor KLRG1 by virus-specific CD8 T cells during persistent antigen stimulation. *J. Virol.* **79,** 12112–12116 (2005).

148. Wirth, T. C. *et al.* Repetitive Antigen Stimulation Induces Stepwise Transcriptome Diversification but Preserves a Core Signature of Memory CD8+ T Cell Differentiation. *Immunity* **33,** 128-140 (2010).

149. Hogan, R. J. *et al.* Long-term maintenance of virus-specific effector memory CD8+ T cells in the lung airways depends on proliferation. *J. Immunol.* **169,** 4976–4981 (2002).

150. Kohlmeier, J. E. & Miller, S. C. Cutting edge: Antigen is not required for the activation and maintenance of virus-specific memory CD8+ T cells in the lung airways. *J Immunol* **178,** 4721-4725 (2007).

151. Ely, K. H., Cookenham, T., Roberts, A. D. & Woodland, D. L. Memory T cell populations in the lung airways are maintained by continual recruitment. *J. Immunol.* **176,** 537–543 (2006).

152. Bachmann, M. F., Wolint, P. & Schwarz, K. Functional properties and lineage relationship of CD8+ T cell subsets identified by expression of IL-7 receptor α and CD62L. *J Immunol* **175,** 4686-4696 (2005).

153. Casimiro, D. R. *et al.* Attenuation of simian immunodeficiency virus SIVmac239 infection by prophylactic immunization with dna and recombinant adenoviral vaccine vectors expressing Gag. *J. Virol.* **79,** 15547–15555 (2005).

154. Araki, K. *et al.* mTOR regulates memory CD8 T-cell differentiation. *Nature* **460,** 108–112 (2009).

155. Brody, S. L. & Crystal, R. G. Adenovirus-Mediated in Vivo Gene Transfer. *Ann N Y Acad Sci* ***716,*** 90-101(1994).

156. Catanzaro, A. T. *et al.* Phase 1 safety and immunogenicity evaluation of a multiclade HIV-1 candidate vaccine delivered by a replication-defective recombinant adenovirus

vector. *J Infect Dis.* **194,** 1638–1649 (2006).

157. Tatsis, N., Tesema, L., Robinson, E. R. & Giles-Davis, W. Chimpanzee-origin adenovirus vectors as vaccine carriers. *Gene Ther.* **13,** 421-429 (2006).

158. Zinn, K. R. *et al.* Gamma Camera Dual Imaging with a Somatostatin Receptor and Thymidine Kinase after Gene Transfer with a Bicistronic Adenovirus in Mice. *Radiology* **223,** 417–425 (2013).

159. Bett, A. J., Prevec, L. & Graham, F. L. Packaging capacity and stability of human adenovirus type 5 vectors. *J. Virol.* **67,** 5911-5921(1993).

160. Hayashi, S. & McMahon, A. P. Efficient recombination in diverse tissues by a tamoxifen-inducible form of Cre: a tool for temporally regulated gene activation/inactivation in the mouse. *Developmental biology* **244,** 305-318 (2002).

161. Qiu, H. *et al.* Adenovirus-Mediated Dual Gene Expression of Human Interleukin-10 and Hepatic Growth Factor Exerts Protective Effect Against CCl4-Induced Hepatocyte Injury in Rats. *Dig Dis Sci* **57,** 1857–1865 (2012).

162. Improved angiogenic response in pig heart following ischaemic injury using human skeletal myoblast simultaneously expressing VEGF165 and angiopoietin-1. *Eur J Heart Fail* **9,** 15–22 (2007).

163. Aurigemma, R., Zhu, Z. B., Curiel, D. T. & Alvarez, R. D. Circumventing recombination events encountered with production of a clinical-grade adenoviral vector with a double-expression cassette. *Mol Pharmacol* **5,** 1488-193 (2006).

164. Liu, X. R. *et al.* A new oncolytic adenoviral vector carrying dual tumour suppressor genes shows potent anti-tumour effect. *Journal of Cellular and Molecular Medicine* **16,** 1298–1309 (2012).

165. Liu, X. *et al.* Gene-viro-therapy targeting liver cancer by a dual-regulated oncolytic adenoviral vector harboring IL-24 and TRAIL. *Cancer Gene Therapy* **19,** 49–57 (2012).

166. Chai, L. *et al.* A novel conditionally replicating adenoviral vector with dual expression of IL-24 and arresten inserted in E1 and the region between E4 and fiber for improved melanoma therapy. *Cancer Gene Therapy* **4,** 247-254 (2012).

167. Goudsmit, J. & Havenga, M. High-level expression from two independent expression cassettes in replication-incompetent adenovirus type 35 vector. *J Gen Virol* **88**, 2915-2924 (2007).

168. Shin, S.-P. *et al.* Adenovirus Expressing Both Thymidine Kinase and Soluble PD1 Enhances Antitumor Immunity by Strengthening CD8 T-cell Response. *Molecular Therapy* **21,** 688–695 (2013).

169. Bramson, J., Hitt, M. & Gallichan, W. S. Construction of a double recombinant adenovirus vector expressing a heterodimeric cytokine: in vitro and in vivo production of biologically active interleukin-12. *Hum Gene Ther* **7,** 333-342 (1996).

170. Harms, J. S. & Splitter, G. A. Interferon-γ inhibits transgene expression driven by SV40 or CMV promoters but augments expression driven by the mammalian MHC I promoter. *Hum. Gene Ther.* **6,** 1291-1297 (1995).

171. Papadakis, E. D., Nicklin, S. A., Baker, A. H. & White, S. J. Promoters and Control Elements: Designing Expression Cassettes for Gene Therapy. *CGT* **4,** 89–113 (2004).

172. Niu, G. *et al.* Dual-expressing adenoviral vectors encoding the sodium iodide symporter for use in noninvasive radiological imaging of therapeutic gene transfer. *Nuclear Medicine and Biology* **33,** 391–398 (2006).

173. Youil, R., Toner, T. J., Su, Q. & Casimiro, D. Comparative analysis of the effects of packaging signal, transgene orientation, promoters, polyadenylation signals, and E3 region on growth properties of first-generation adenoviruses. *Hum Gene Ther* **14,** 1017-1034 (2003).

174. Addison, C. L., Hitt, M. & Kunsken, D. Comparison of the human versus murine cytomegalovirus immediate early gene promoters for transgene expression by adenoviral vectors. *J Gen Virol* **78,** 1653-1661 (1997).

175. Murakami, P., Pungor, E., Files, J. & Do, L. A single short stretch of homology between adenoviral vector and packaging cell line can give rise to cytopathic effect-inducing, helper-dependent E1-positive particles. *Hum Gene Ther* **13,** 909-920 (2002).

176. Yang, K. & Chi, H. mTOR and metabolic pathways in T cell quiescence and functional activation. *Semin. Immunol.* **24,** 421–428 (2012).

177. Yang, K., Neale, G., Green, D. R., He, W. & Chi, H. The tumor suppressor Tsc1 enforces quiescence of naive T cells to promote immune homeostasis and function. *Nat. Immunol.* **12,** 888–897 (2011).

178. Sinclair, L. V. *et al.* Phosphatidylinositol-3-OH kinase and nutrient-sensing mTOR pathways control T lymphocyte trafficking. *Nat. Immunol.* **9,** 513–521 (2008).

179. Rolf, J. *et al.* AMPKα1: a glucose sensor that controls CD8 T-cell memory. *Eur. J. Immunol.* **43,** 889–896 (2013).

180. Pearce, E. L. *et al.* Enhancing CD8 T-cell memory by modulating fatty acid metabolism. *Nature* **460,** 103–107 (2009).

181. Rao, R. R., Li, Q., Odunsi, K. & Shrikant, P. A. The mTOR kinase determines effector versus memory CD8+ T cell fate by regulating the expression of transcription factors T-bet and Eomesodermin. *Immunity* **32,** 67–78 (2010).

182. Joshi, N. S., Cui, W., Chandele, A., Lee, H. K. & Urso, D. R. Inflammation Directs Memory Precursor and Short-Lived Effector CD8+ T Cell Fates via the Graded Expression of T-bet Transcription Factor. *Immunity* **27,** 281-295 (2007).

183. Turner, A. P. *et al.* Sirolimus enhances the magnitude and quality of viral-specific CD8+ T-cell responses to vaccinia virus vaccination in rhesus macaques. *Am. J. Transplant.* **11,** 613–618 (2011).

184. Xiang, Z. Q., Yang, Y., Wilson, J. M. & Ertl, H. C. A replication-defective human adenovirus recombinant serves as a highly efficacious vaccine carrier. *Virology* **219,** 220–227 (1996).

185. Ahlers, J. D. & Belyakov, I. M. Memories that last forever: strategies for optimizing vaccine T-cell memory. *Blood* **115,** 1678–1689 (2010).

186. Kaech, S. M. & Cui, W. Transcriptional control of effector and memory CD8+ T cell differentiation. *Nat. Rev. Immunol.* **12,** 749–761 (2012).

187. Hand, T. W., Morre, M. & Kaech, S. M. Expression of IL-7 receptor alpha is necessary but not sufficient for the formation of memory CD8 T cells during viral infection. *Proc. Natl. Acad. Sci. U.S.A.* **104,** 11730–11735 (2007).

188. Li, Q. *et al.* Regulating mammalian target of rapamycin to tune vaccination-induced CD8(+) T cell responses for tumor immunity. *J. Immunol.* **188,** 3080–3087 (2012).

189. Prasad, S. A., Norbury, C. C., Chen, W., Bennink, J. R. & Yewdell, J. W. Cutting edge: recombinant adenoviruses induce CD8 T cell responses to an inserted protein whose expression is limited to nonimmune cells. *J. Immunol.* **166,** 4809–4812 (2001).

190. Sullivan, J. A., Kim, E. H., Plisch, E. H. & Suresh, M. FOXO3 regulates the CD8 T cell response to a chronic viral infection. *J. Virol.* **86,** 9025–9034 (2012).

191. Havenith, S. H. C. *et al.* Everolimus-treated renal transplant recipients have a more robust CMV-specific CD8+ T-cell response compared with cyclosporine- or mycophenolate-treated patients. *Transplantation* **95,** 184–191 (2013).

192. Bassett, J. D. *et al.* Combined mTOR inhibition and OX40 agonism enhances CD8(+) T cell memory and protective immunity produced by recombinant adenovirus vaccines. *Mol. Ther.* **20,** 860–869 (2012).

193. Angelosanto, J. M., Blackburn, S. D., Crawford, A. & Wherry, E. J. Progressive loss of memory T cell potential and commitment to exhaustion during chronic viral infection. *J. Virol.* **86,** 8161–8170 (2012).

194. Roy, S. *et al.* Isolation and characterization of adenoviruses persistently shed from the gastrointestinal tract of non-human primates. *PLoS Pathog.* **5,** e1000503 (2009).

195. Yang, T. C., Dayball, K., Wan, Y. H. & Bramson, J. Detailed analysis of the CD8+ T-cell response following adenovirus vaccination. *J. Virol.* **77,** 13407-13411 (2003).

196. Krebs, P., Scandella, E., Odermatt, B. & Ludewig, B. Rapid functional exhaustion and deletion of CTL following immunization with recombinant adenovirus. *J. Immunol.* **174,** 4559–4566 (2005).

197. Bucks, C. M., Norton, J. A. & Boesteanu, A. C. Chronic antigen stimulation alone is sufficient to drive CD8+ T cell exhaustion. *J Immunol* **182,** 6697-6708 (2009).

198. Pircher, H. Virus persistence in acutely infected immunocompetent mice by exhaustion of antiviral cytotoxic effector T cells. *Nature* **362,** 758-761(1993).

199. Kemball, C. C., Lee, E. & Vezys, V. Late priming and variability of epitope-specific CD8+ T cell responses during a persistent virus infection. *J Immunol* **174,** 7950-7960 (2005).

200. Wilson, J. J. *et al.* CD8 T cells recruited early in mouse polyomavirus infection undergo exhaustion. *J. Immunol.* **188,** 4340–4348 (2012).

201. Vezys, V. *et al.* Continuous recruitment of naive T cells contributes to heterogeneity of antiviral CD8 T cells during persistent infection. *J Exp Med* **203,** 2263–2269 (2006).

202. Freeman, M. L., Burkum, C. E., Jensen, M. K., Woodland, D. L. & Blackman, M. A. γ-Herpesvirus reactivation differentially stimulates epitope-specific CD8 T cell responses. *J. Immunol.* **188,** 3812–3819 (2012).

203. Snyder, C. M., Cho, K. S., Bonnett, E. L. & van Dommelen, S. Memory inflation during chronic viral infection is maintained by continuous production of short-lived, functional T cells. *Immunity* **29,** 650-659 (2008).

204. Karrer, U. *et al.* Memory inflation: continuous accumulation of antiviral CD8+ T cells over time. *J. Immunol.* **170,** 2022–2029 (2003).

205. Day, E. B., Charlton, K. L. & La Gruta, N. L. Effect of MHC class I diversification on influenza epitope-specific CD8+ T cell precursor frequency and subsequent effector function. *J Immunol* **186,** 6319-6328 (2011).

206. Kotturi, M. F., Scott, I., Wolfe, T. & Peters, B. Naive precursor frequencies and MHC binding rather than the degree of epitope diversity shape CD8+ T cell immunodominance. *J Immunol* **181,** 2124-2133 (2008).

207. Obar, J. J., Khanna, K. M. & Lefrançois, L. Endogenous Naive CD8+T Cell Precursor Frequency Regulates Primary and Memory Responses to Infection. *Immunity* **28,** 859-869 (2008).

208. Nicole L La Gruta, *et al*. Primary CTL response magnitude in mice is determined by the extent of naive T cell recruitment and subsequent clonal expansion. *J. Clin. Invest.* **120,** 1885–1894 (2010).

209. Wherry, E. J. & Ahmed, R. Memory CD8 T-cell differentiation during viral infection. *J. Virol.* **78,** 5535-5545 (2004).

210. Mazo, I. B., Honczarenko, M., Leung, H. & Cavanagh, L. L. Bone Marrow Is a Major Reservoir and Site of Recruitment for Central Memory CD8+ T Cells. *Immunity* **22,** 259-270 (2005).

211. Finn, J. D. *et al.* Persistence of transgene expression influences CD8+ T-cell expansion and maintenance following immunization with recombinant adenovirus. *J. Virol.* **83,** 12027–12036 (2009).

212. Snyder, C. M., Cho, K. S., Bonnett, E. L., Allan, J. E. & Hill, A. B. Sustained CD8+ T cell memory inflation after infection with a single-cycle cytomegalovirus. *PLoS Pathog.* **7,** e1002295 (2011).

213. Bolinger, B. *et al.* A new model for CD8+ T cell memory inflation based upon a recombinant adenoviral vector. *J. Immunol.* **190,** 4162–4174 (2013).

214. Sierro, S., Oxenius, A., Hengel, H. & Dumrese, T. Expansion of protective CD8+ T-cell responses driven by recombinant cytomegaloviruses. *J Virol* **78,** 2255-2264 (2004).

215. Farrington, L. A., Smith, T. A., Grey, F., Hill, A. B. & Snyder, C. M. Competition for antigen at the level of the APC is a major determinant of immunodominance during memory inflation in murine cytomegalovirus infection. *J. Immunol.* **190,** 3410–3416 (2013).

216. McCoy, K., Tatsis, N. & Korioth-Schmitz, B. Effect of preexisting immunity to adenovirus human serotype 5 antigens on the immune responses of nonhuman primates to vaccine regimens based on human- or chimpanzee-derived adenovirus vectors. *J Virol* **81,** 6594-6604 (2007).

217. Casimiro, D. R., Chen, L., Fu, T. M. & Evans, R. K. Comparative immunogenicity in rhesus monkeys of DNA plasmid, recombinant vaccinia virus, and replication-defective adenovirus vectors expressing a human immunodeficiency virus type 1 gag gene. *J Virol* **77,** 6305-6313 (2003).
218. Shiver, J. W. *et al.* Replication-incompetent adenoviral vaccine vector elicits effective anti-immunodeficiency-virus immunity. *Nature* **415,** 331–335 (2002).
219. Harro, C. D. *et al.* Safety and Immunogenicity of Adenovirus-Vectored Near-Consensus HIV Type 1 Clade B gag Vaccines in Healthy Adults. *AIDS Res Hum Retroviruses* **25,** 103–114 (2009).

220. Buchbinder, S. P., Mehrotra, D. V., Duerr, A. & Fitzgerald, D. W. Efficacy assessment of a cell-mediated immunity HIV-1 vaccine (the Step Study): a double-blind, randomised, placebo-controlled, test-of-concept trial. *The Lancet* **372,** 1881-1893 (2008).

221. Duerr, A. *et al.* Extended follow-up confirms early vaccine-enhanced risk of HIV acquisition and demonstrates waning effect over time among participants in a randomized trial of recombinant adenovirus HIV vaccine (Step Study). *J Infect Dis.* **206,** 258–266 (2012).

222. Cohen, Y. Z. & Dolin, R. Novel HIV vaccine strategies: overview and perspective. *Therapeutic Advances in Vaccines* **1,** 99-112 (2013).

223. Perreau, M., Pantaleo, G. & Kremer, E. J. Activation of a dendritic cell-T cell axis by Ad5 immune complexes creates an improved environment for replication of HIV in T cells. *J Exp Med* **205,** 2717–2725 (2008).

224. Harris, J., Meiser, A. & Papagatsias, T. Adenovirus vector vaccination induces expansion of memory CD4 T cells with a mucosal homing phenotype that are readily susceptible to HIV-1. *Proc N*atl *Acad Sci* **106,** 19940-19945 (2009).

225. Barouch, D. H. *et al.* Characterization of humoral and cellular immune responses elicited by a recombinant adenovirus serotype 26 HIV-1 Env vaccine in healthy adults (IPCAVD 001). *J Infect Dis.* **207,** 248–256 (2013).

226. Reddy, P. S., Ganesh, S., Limbach, M. P. & Brann, T. Development of adenovirus serotype 35 as a gene transfer vector. *Virology* **311,** 384-393 (2003).

227. Barouch, D. H., Kik, S. V., Weverling, G. J., Dilan, R. & King, S. L. International seroepidemiology of adenovirus serotypes 5, 26, 35, and 48 in pediatric and adult populations. *Vaccine* **29,** 5203-5209 (2011).

228. Mast, T. C. *et al.* International epidemiology of human pre-existing adenovirus (Ad) type-5, type-6, type-26 and type-36 neutralizing antibodies: Correlates of high Ad5 titers and implications for potential HIV vaccine trials. *Vaccine* **28,** 950–957 (2010).

229. Farina, S. F. *et al.* Replication-defective vector based on a chimpanzee adenovirus. *J. Virol.* **75,** 11603–11613 (2001).

230. Chen, H. *et al.* Adenovirus-based vaccines: comparison of vectors from three species of adenoviridae. *J. Virol.* **84,** 10522–10532 (2010).

231. Xiang, Z., Li, Y., Cun, A., Yang, W. & Ellenberg, S. Chimpanzee adenovirus antibodies in humans, sub-Saharan Africa. *Emerg Infect Dis* **12,** 1596-1599 (2006).

232. Ersching, J., Hernandez, M. & Cezarotto, F. S. Neutralizing antibodies to human and

simian adenoviruses in humans and New-World monkeys. *Virology* **407,** 1-6 (2010).

233. Sallusto, F., Langenkamp, A., Geginat, J. & Lanzavecchia, A. in *Lymphoid Organogenesis* **251,** 167–171 (2000).

234. Kaech, S. M., Tan, J. T., Wherry, E. J. & Konieczny, B. T. Selective expression of the interleukin 7 receptor identifies effector CD8 T cells that give rise to long-lived memory cells. *Nature Immunol* **4,** 1191-1198 (2003).

235. Bradley, R. R., Lynch, D. M., Iampietro, M. J., Borducchi, E. N. & Barouch, D. H. Adenovirus serotype 5 neutralizing antibodies target both hexon and fiber following vaccination and natural infection. *J. Virol.* **86,** 625–629 (2012).

236. Kostense, S., Koudstaal, W., Sprangers, M. & Weverling, G. J. Adenovirus types 5 and 35 seroprevalence in AIDS risk groups supports type 35 as a vaccine vector. *Aids* (2004).

237. Chirmule, N., Propert, K. J., Magosin, S. A. & Qian, Y. Immune responses to adenovirus and adeno-associated virus in humans. *Gene Ther* **6,** 1574-1583 (1999).

238. Pilankatta, R., Chawla, T., Khanna, N. & Swaminathan, S. The prevalence of antibodies to adenovirus serotype 5 in an adult Indian population and implications for adenovirus vector vaccines. *Journal of Medical Virology* **82,** 407–414 (2010).

239. Steffensen, M. A., Jensen, B., Holst, P. J. & Bassi, M. R. Pre-existing vector immunity does not prevent replication deficient adenovirus from inducing efficient CD8 T-cell memory and recall responses. *PLoS ONE* **7,** e34884 (2012).

240. Haut, L. H., Ratcliffe, S. & Pinto, A. R. Effect of Preexisting Immunity to Adenovirus on Transgene Product–Specific Genital T Cell Responses on Vaccination of Mice With a Homologous Vector. *J Infect Dis* **203,** 1073-1081 (2011).

241. Badovinac, V. P., Porter, B. B. & Harty, J. T. CD8+ T cell contraction is controlled by early inflammation. *Nat. Immunol.* **5,** 809-817 (2004).

242. Zak, D. E. & Andersen-Nissen, E. Merck Ad5/HIV induces broad innate immune activation that predicts CD8+ T-cell responses but is attenuated by preexisting Ad5 immunity. *Proc Natl Acad Sci* **109,** E3503-3512 (2012).

243. Wiesel, M. & Oxenius, A. From crucial to negligible: Functional CD8+ T-cell responses and their dependence on CD4+ T-cell help. *Eur. J. Immunol.* **42,** 1080-1088 (2012).

244. Yang, Y., Xiang, Z. & Ertl, H. C. Upregulation of class I major histocompatibility complex antigens by interferon gamma is necessary for T-cell-mediated elimination of recombinant adenovirus-infected hepatocytes in vivo. *Proc Natl Acad Sci* **92,** 7257-7261 (1995).

245. Leopold, P. L., Wendland, R. L. & Vincent, T. Neutralized adenovirus-immune complexes can mediate effective gene transfer via an Fc receptor-dependent infection pathway. *J Virol* **80,** 10237-10247 (2006).

246. Hudrisier, D., Clemenceau, B. & Balor, S. Ligand binding but undetected functional response of FcR after their capture by T cells via trogocytosis. *J Immunol* **183,** 6102-6113 (2009).

247. Lee, S. T. & Paraskevas, F. Macrophage—T cell interactions: I. The uptake by T cells of Fc receptors released from macrophages. *Cellular Immunology* **40,** 141-153 (1978).

248. D'Souza, W. N. & Hedrick, S. M. Cutting edge: latecomer CD8 T cells are imprinted with a unique differentiation program. *J. Immunol.* **177,** 777–781 (2006).

249. Martin, M. D., Wirth, T. C., Lauer, P., Harty, J. T. & Badovinac, V. P. The impact of pre-existing memory on differentiation of newly recruited naive CD8 T cells. *J. Immunol.* **187,** 2923–2931 (2011).

250. Salaun, B. *et al.* Differentiation associated regulation of microRNA expression in vivo in human CD8+ T cell subsets. *J Transl Med* **9,** 44 (2011).

251. Wu, H. *et al.* miRNA profiling of naïve, effector and memory CD8 T cells. *PLoS ONE* **2,** e1020 (2007).

252. Gubser, P. M. *et al.* Rapid effector function of memory CD8+ T cells requires an immediate-early glycolytic switch. *Nat. Immunol.* **14,** 1064–1072 (2013).

253. Gray, G. E. *et al.* Recombinant adenovirus type 5 HIV gag/pol/nef vaccine in South Africa: unblinded, long-term follow-up of the phase 2b HVTN 503/Phambili study. *The Lancet Infectious Diseases* **14,** 388–396 (2014).

254. Hammer, S. M. *et al.* Efficacy Trial of a DNA/rAd5 HIV-1 Preventive Vaccine. *N Engl J Med* **369,** 2083–2092 (2013).

255. Calcedo, R. *et al.* Host immune responses to chronic adenovirus infections in human and nonhuman primates. *J. Virol.* **83,** 2623–2631 (2009).